



DBUH-I₃ COMPLEX CATALYSED SYNTHESIS OF ARYLIDENE DERIVATIVES OF PYRAZOLE

R. Gawade,^{a,b} P. Jadhav,^b S. Shinde,^d and P. Kulkarni^{*a,c}

^aBaburaoji Gholap College Sangvi, Haveli, Pune 411027, Maharashtra, India

^bS. M. Joshi College Hadapsar, Haveli, Pune 411028, Maharashtra, India

^cPost Graduate Research Center in Organic Chemistry and Department of Chemistry
Hutatma Rajguru Mahavidyalaya, Rajgurunagar Pune 410505, Maharashtra, India

^dAnnasaheb Awate College Manchar, Pune 410503, Maharashtra, India

(Affiliated to Savitribai Phule Pune University, Pune)

*Corresponding author email: pramodskulkarni3@gmail.com

Mobile No. +919850658087

Abstract: The new organocatalyst amine-iodine-iodide complex was prepared and used as a catalyst for the synthesis of arylidene derivatives of pyrazole from ethyl acetoacetate, substituted aryl aldehyde and phenylhydrazine. The direct one-step multicomponent efficient synthesis was achieved with remarkable green advantages offered by this protocol such as short reaction time, the broad scope of a substrate, simple experimental procedure and moderate to a good yield of the desired product. The synthesized molecules were confirmed by spectroscopic analysis ¹H-NMR and ¹³C-NMR.

Keywords: DBU-iodine-iodide complex, Pyrazole, Condensation, Arylidene pyrazole, Multicomponent.

Introduction:

Pyrazole derivatives are very useful scaffolds of five-membered heterocyclic compounds, found in numerous natural and medicinal products.^{i,ii} They are a precursor for the synthesis of numerous valuable organic molecules, pharmaceutical compounds, biologically active molecules and agrochemicals.ⁱⁱⁱ The innumerable advantages of pyrazole in medicinal chemistry as they display a broad spectrum of biological activities such as anticancer,^{iv} antibacterial, antifungal,^v anti-inflammatory,^{vi} anti-viral,^{vii} antiplatelet,^{viii} anti-tubercular^{ix} and so on.^x Pyrazole are privileged five-membered heterocyclic compounds in human and veterinary medicine as well as a versatile building block in organic synthesis, therefore have attracted much attention of synthetic organic chemist.^{iv,xi}

The traditional protocol for the synthesis of 4-arylidene-3-methyl-1-phenyl-pyrazol-5(4H)-one derivative consists of two consecutive steps^{xii,xiv} viz, a) reaction between phenyl hydrazine and ethyl acetoacetate condensation followed by cyclisation produce 3-methyl-1-phenyl-5-pyrazolone, b) Knoevenagel condensation between 3-methyl-1-phenyl-5-

pyrazolone and aryl aldehyde. Most recently, only a few alternative reports indicate one step multicomponent reaction between phenyl hydrazine, ethyl acetoacetate and aryl aldehyde give corresponding arylidene pyrazole. Few multicomponent one-pot the synthesis of 4-arylidene-3-methyl-1-phenyl-pyrazol-5(4H)-one was reported earlier using silica-supported zinc chloride^{xv} and microwave.^{xvi}

The synthetic method survey of pyrazole, concludes that each synthetic method has certain merits and demerits. The demerit of a previous protocol is long reaction time, stringent reaction conditions, tedious steps (preparation of nano catalyst) and special conditions (grinding, high temperature, ultrasound, irradiation). Hence there is ample scope to develop a new efficient method for the synthesis of pyrazole. We have prepared a new organocatalyst amine-iodine-iodide complex, fortunately, it catalyses efficiently with process optimization protocol and synthesis of pyrazole. The present protocol offers an eco-friendly and sustainable approach with excellent substrate and functional group compatibility viz, use of organocatalyst, operationally simple, mild condition, inexpensive catalyst, low cost, simple and quick isolation of the product. To the best of my knowledge, no report is available on amine-iodine-iodide complex as a catalyst for the synthesis of pyrazole. The predicted protocol was one pot, one-step, multicomponent reaction for arylidene pyrazole synthesis. Iodine catalysis known for more than a hundred years has potent advantages over transition metal base catalysts but molecular iodine has a drawback such as sublimation and moisture sensitivity.^{xvii} To overcome this drawback, convert molecular iodine to amine-iodine-iodide complexes.^{xviii} These complexes were shown potent catalysts for the synthesis of arylidene pyrazole.

Experimental Section:

Melting points were determined in open capillary tubes and are uncorrected. All chemicals and solvents were used laboratory grade. The purity and progress of reactions were monitored on TLC. Products were purified by re-crystallization process. NMR data of as-synthesized compounds were recorded on Bruker 500 MHz instrument for their structural identification.

Synthesis of Pyrazolone derivatives using DBUH-I₃ Catalyst.

The Phenyl hydrazine (1mmol), ethyl acetoacetate(1mmol), aryl aldehyde (1 mmol) and 10 mL ethanol were taken in 25 mL single neck round bottom flask equipped with a condenser. Then, 15 mol % DBUH-I₃ catalyst was added to the reaction mixture. The reaction mass was refluxed for 30 min. The progress and completion of the reaction was confirmed by TLC. After completion of the reaction, solvent was evaporated to get the crude product. The reaction mixture was quenched with an excess 20% sodium thiosulfate solution and extracted with ethyl acetate. The organic layer dried over sodium sulphate and evaporated to obtain a crude solid. The crude solid product was purified by recrystallisation to get a pure product and report the yield. The pure products were characterized by ¹H-NMR, ¹³C-NMR and physical constant comparison with reported derivatives.

Result and Discussion:

We have prepared and confirmed the DBU-iodine-iodide complex by the reported procedure, with minor modifications replacing potassium iodide with ammonium iodide^{xviii-xix}. This iodine bearing complex is a good alternative for molecular iodine as they overcome sublimation and moisture sensitivity problem^{xix}. We have prepared the above complex by dissolving iodine in ammonium iodide aqueous solution and then adding this solution dropwise to the aqueous DBU solution, complex gets precipitated. The amine-iodine-iodide complex has quaternary nitrogen, molecular iodine and iodide ions important constituent responsible for catalytic activity and iodination.

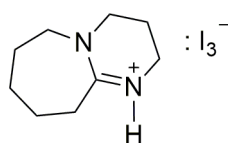
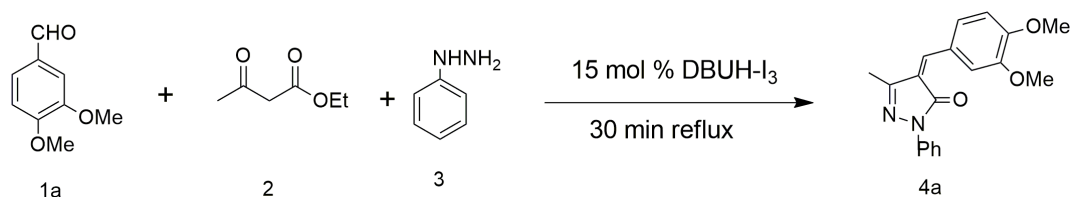


Figure 1 Structure of DBUH + I₃ Complex

The DBUH + I₃ complexes were screened for synthesis of 3-methyl-4-(3,4-dimethoxyaryl)methylene-pyrazole-5-(4*H*)-one in various solvents. The synthesis of pyrazole was achieved by one pot multi-step process, first Knoevenagel condensation of aryl aldehyde with ethyl acetoacetate led to the formation of α, β unsaturated carbonyl compound formation followed by the addition of phenyl hydrazine and cyclisation. All the above processes are efficiently catalysed by DBUH-I₃ complexes with the green chemistry principle.

Firstly, the solvent effect was studied in a multicomponent reaction of 3,4-dimethoxy benzaldehyde, phenyl hydrazine and ethyl acetoacetate as selected as a model reaction to optimize the reaction condition (**Scheme 1**). The screening result of different solvents in DBUH-I₃ complex catalyst indicates ethanol solvent was found better for the synthesis of pyrazole (**Table 1**). We have optimized the process at various temperature and amount of catalyst. In general, polar solvents are better for the synthesis of pyrazole.

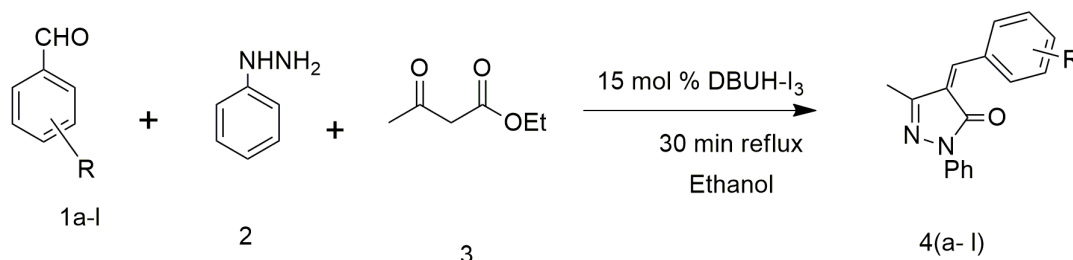


Scheme 1 : Screening of solvent for DBUH-I₃ catalyzed synthesis of 3-methyl-4-(3,4-dimethoxyaryl)methylene-pyrazole-5-(4*H*)-one

Table 1 : Screening of solvent for DBUH-I₃ catalyzed synthesis of 3-methyl-4-(3,4-dimethoxyaryl)methylene-pyrazole-5-(4*H*)-one^a

Sr. No.	Name of solvent	% Yield ^b
1	Ethanol	86
2	DMF	84
3	DMSO	81
4	Acetonitrile	61
5	Acetic Acid	51
6	Toluene	63
7	CHCl ₃	54
8	Dioxane	45

^aReaction Condition: 3,4-dimethoxy benzaldehyde (1 mmol), Ethyl acetoacetate (1 mmol), Phenyl hydrazine (1 mmol), Catalyst (15 mol %), ethanol (10 mL) Reflux 30 min. ^b isolated yield after purification.

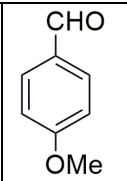
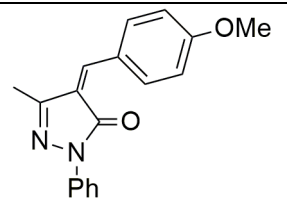
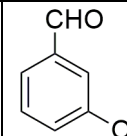
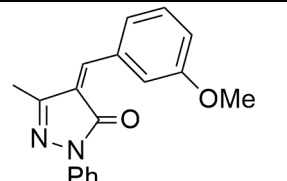
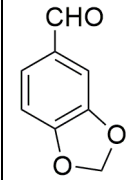
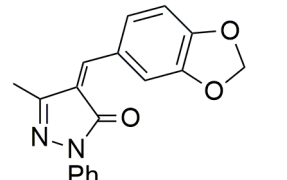
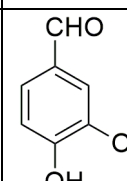
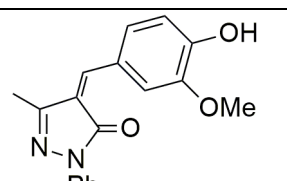
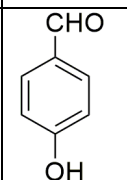
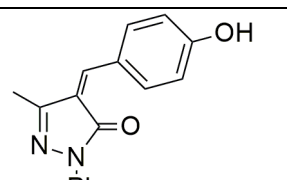
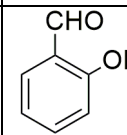
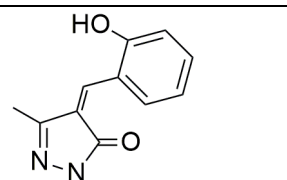
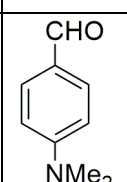
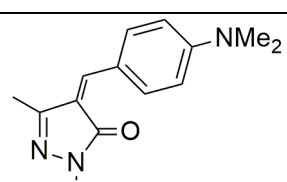


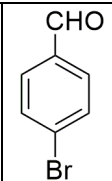
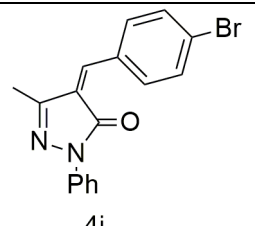
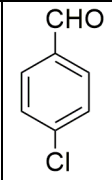
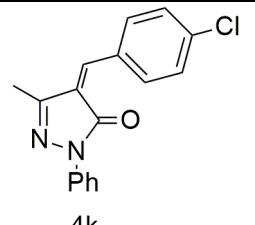
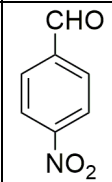
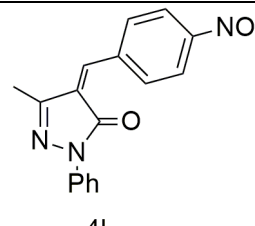
Scheme 2 : Synthesis of substituted arylidene pyrazole

In this work, DBUH-I₃ complex is explored as a catalyst for a three-component reaction to achieve the synthesis of 3-methyl-4-(aryl substituted) methylene-pyrazole-5-(4*H*)-one derivatives (**4a-l**) (**Scheme 2**). The multicomponent reaction of ethyl acetoacetate, phenyl hydrazine and substituted aryl aldehyde catalysed efficient synthesis of pyrazole. The aryl aldehyde bearing electron donating groups such as methoxy and amino more efficiently catalysed by DBUH-I₃ lead to the formation of product (**4a**, **4c**, **4e**, **4f**, **4g**, **4i**) and aryl aldehyde bearing electron withdrawing group such as 3-methoxy and the nitro group also formed the product comparatively in lower yield form (**4d** & **4l**). The halogen group bearing aryl aldehyde gets converted to pyrazole with moderate yield (**4j**, **4k**) and ortho-substituted aryl aldehyde gave comparatively poor yield (**4h**). The substituted electron rich aryl aldehyde gives high yield than electron deficient aryl aldehyde. The product was purified by recrystallisation in ethanol and the yield reported. The product formation was confirmed by ¹HNMR, methyl signal (~2.25 δ) olefinic hydrogen singlet in aromatic region and corresponding ¹³CNMR signal. The yield was reported after purification and physical constant compared with reported derivatives. The proposed multicomponent reaction catalysed by DBUH-I₃ for the synthesis of arylidene pyrazole was efficiently applicable to electron rich aryl aldehyde (**Table 2**).

Table 2 : Synthesis of 4-arylidene-3-methyl-1-phenyl-pyrazol-5(4*H*)-one^a

Entry	Arylaldehyde	Product (4)	% Yield ^b	Observed M. P.	Reported M. P.
1		<p style="text-align: center;">4a</p>	86	156-158°C	---
2		<p style="text-align: center;">4b</p>	81	197-199°C	195-197°C ^{XX}

3	 <p>CHO OMe</p>	 <p>4c</p>	85	105-107°C	100-106°C ^{xiv}
4	 <p>CHO OMe</p>	 <p>4d</p>	75	228-230°C	227-228°C ^{xx}
5	 <p>CHO</p>	 <p>4e</p>	88	158-160°C	---
6	 <p>CHO OMe OH</p>	 <p>4f</p>	78	165-167°C	160-164°C ^{xiv}
7	 <p>CHO OH</p>	 <p>4g</p>	71	238-240°C	208-212°C ^{xiv}
8	 <p>CHO OH</p>	 <p>4h</p>	65	170-172°C	173-175°C ^{xx}
9	 <p>CHO NMe₂</p>	 <p>4i</p>	82	200-202°C	204-205°C ^{xx}

10		 4j	73	119-121°C	117-120°C ^{xxvi}
11		 4k	71	198-200°C	201-203°C ^{xx}
12		 4l	62	195-197°C	192-195°C ^{xx}

^a Reaction Condition: Arylaldehyde (1 mmol), Ethyl acetoacetate (1m mol), Phenyl hydrazine (1 mmol), Catalyst (15 mol %), ethanol (10 mL) reflux 30 min.

^b Isolated yield after purification by recrystallisation in ethanol.

Conclusion: We have developed an efficient homogeneous catalysis system for the synthesis of arylidene pyrazole. The proposed protocol offers several advantages over traditional methods.

Acknowledgment: The authors are grateful to the Savitribai Phule Pune University Pune for spectral analysis.

References:

- i Brogden R. N. Pyrazolone derivatives, *Drugs*, 1986, **32**, 60-70
- ii John M. F., Joseph C., Joseph B., Robert K. M., Joseph H. L., Pancras C. W. Preparation of 1-(4-methoxyphenyl)-1H-pyrazolo[4,3-d]pyrimidin-7(6H)-ones as potent, selective and bioavailable inhibitors of coagulation factor Xa, *Bioorg. Med. Chem. Lett.*, 2006, **16**, 3755.
- iii Mohd J. N., Ozair A., Farah N., Md. Jahangir A., and Perwaiz A. Current status of pyrazole and its biological activities, *J Pharm Bioallied Sci.* 2016, **8** (1), 2–17.
- iv Salehl N. M., El-Gazzar M. G., Aly H. M. Novel Anticancer Fused Pyrazole Derivatives as EGFR and VEGFR-2 Dual TK Inhibitors Othman *Frontiers in Chemistry*, 2020, **7**, article 917. <https://doi.org/10.3389/fchem.2019.00917>
- v Seham Y and Hassan Synthesis antibacterial and antifungal activity of some new pyrazoline and pyrazole derivatives, *Molecule*, 2013, **18**, 2683-2711.
- vi Karabasanagouda T., Adhikari A. V. and Girisha M. Synthesis of some new pyrazolines and isoxazoles carrying 4-methylthiophenyl moiety as potent analgesics and anti-inflammatory agents, *Indian Journal Chem.*, 2009, **48B**, 430-437.
- vii Osama I. El-Sabbagh, Mohamed M. Baraka, Samy M. Ibrahim, Christophe

- Pannecouque, Graciela Andrei, Robert Snoeck, Jan Balzarini, Adel A. Rashad, Synthesis and antiviral activity of new pyrazole and thiazole derivatives, *European Journal of Medicinal Chemistry*, 2009, **44**, 3746–3753.
- viii Serkan L., Burcu Ç., Murat Ç., Yesim O., Idil Y., Huseyin U., Erden B., Pyrazole derivatives as inhibitors of arachidonic acid-induced platelet aggregation, *European Journal of Medicinal Chemistry* 2013, **64**, 42-53.
- ix Zhi X., Chuan G., Qing-cheng R., Xu-Feng S., Lian-shun F., Zao-sheng Lv. Recent Advances of Pyrazole-containing Derivatives as Anti-tubercular Agents *Eur. Journal of Med. Chem.* 2017, **139**, 429-440.
- x Khalid K., Smaail R., Youssef R., Jamal T., Yahia N. M., Faiz A. Al-aizari and M'hammed, Synthesis and Pharmacological Activities of Pyrazole Derivatives: A Review *Molecules*, 2018, **23**, 134. <https://doi.org/10.3390/molecules23010134>
- xi Giomi D., Cardero F. M. and Machetti, F. *Comprehensive Heterocyclic Chemistry*, III, 2008, **4**, 365-485. ISBN: 9780080449913
- xii Mohamed, Spectral, thermal, antimicrobial studies for silver(I) complexes of pyrazolone derivatives, *BMC Chemistry*, 2020, **14**, 69. <https://doi.org/10.1186/s13065-020-00723-0>
- xiii Ramajayam R., Tan K., Liu H. Liang P. Synthesis and evaluation of pyrazolone compounds as SARS-coronavirus 3C-like protease inhibitors *Bioorg. Med. Chem.* 2010, **18**, 7849–7854.
- xiv Verma R., Chawla P. and Saraf S. K. Synthesis, characterization and evaluation of some 1,3,4-tri substituted-5- pyrazolone derivatives as dual anti-inflammatory and antimicrobial agents *Pelagia Research Library Der Pharmacia Sinica*, 2012, **3**, 5, 546-555.
- xv Neelima G, Lakshmi K. and Maheswaramma Sessa, Development of novel pyrazolones by using SiO₂/ZnCl₂ – green approach *J. Chemical Sciences* 2019, **131**, 105.
- xvi Ruoqun Ma, Jin Z., Jie L., Lili C., Xu S., Hualiang J. and Jian L. Microwave-Assisted One-Pot Synthesis of Pyrazolone Derivatives under Solvent-Free Conditions *Molecules* 2010, **15**, 3593-3601 <https://doi.org/10.3390/molecules15053593>
- xvii Koenig J. Jonas, Breugst M., Halogen bonding in solution, Wiley online book, ISBN: 9783527825738, 2021, **Chapt. 7**. <https://doi.org/10.1002/9783527825738.ch7>
- xviii Frota L. C. R. M. da, Canavez R. C. P., Gomes S. L. da S., Costa P. R. R., Silva A. J. M. da, Iodination of Phenols in Water using Easy to Handle Amine-Iodine Complexes *J. Braz. Chem.* 2009, **20** (10), 1916-1920.
- xix Rafat M. S., Didamony H. Al., El-Nour K. M. A., El-Zayat L., Synthesis and spectroscopic characterization on the tri-iodide charge transfer complex resulted from the interaction between morpholine as donor and iodine σ -acceptor *J. Saudi Chem. Soc.*, 2010, **14**, 323–330.
- xx Shaglof A., Elzlatene H. and Mohamad F. Ali synthesis and evaluation of biological activity of pyrazolone compounds *J. Pharm. Appl. Chem.* 2021, **7**, 1, 9-23

Received on August 23, 2022.



Synthesis of Benzimidazole and Benzothiazole Derivatives using Reusable Waste Stem of *Trigonella Foenum-graecum* Assisted Zinc Sulphide Nanoparticles: A Green and Efficient Solid Acid Catalyst

Arun K. Valvi^a, Hemangi J. Gavit^a, Shubhada S. Nayak^b, Vitthal S. Shivankar^c, Gurumeet C. Wadhawa^{b,*}

^a Annasaheb Awate Arts, Commerce and Hutatma Babu Genu Science College, Manchar, Pune, Maharashtra, India

^b Rayat Shikshan Sanstha's Karmaveer Bhaurao Patil College, Vashi, Navi Mumbai, India

^c Rayat Shikshan Sanstha's Chhatrapati Shivaji College, Satara, Maharashtra, India

ARTICLE INFO

Article history:

Available online 21 October 2022

Keywords:

Benzimidazole
Benzothiazole
Condensation reaction
Nanoparticles
Plant extract

ABSTRACT

In this study, the simple and rapid methods for the preparation of benzimidazole and benzothiazole by the condensation of *o*-phenylenediamine with the aromatic aldehyde in presence of the zinc sulphide nanoparticles derived from the waste stem of the *Trigonella foenum-graecum*. The catalyst was prepared by using the waste stem of the *Trigonella foenum-graecum*. Most of the reaction carried under the mild condition with very high excellent yield. The method is used for the aromatic, unsaturated and heteroaromatic aldehyde. The main advantage of this method is that it takes very short reaction time, solvent free reaction condition, reusable catalyst, milder reaction, easy workup and waste stem of the plant was used. © 2022 Elsevier Ltd. All rights reserved.

Selection and peer-review under responsibility of the scientific committee of the Integrative Nanotechnology Perspective for Multidisciplinary Applications - 2022. All rights reserved.

1. Introduction

Naturally occurring nucleotides, i.e., adenine base of the DNA, as well as a component of vitamin B12 have extensively been used in drug synthesis and medicinal chemistry containing the benzimidazole or 1H-1,3-benzothiazole-based heterocyclic compounds (shown in fig.) [1–6]. Due to the presence of aromatic ring and nitrogen present in the ring of Benzimidazoles, it can show the large number of the biological activity such as antiviral activities [7–8], anticancer [9–11], antidiabetics [12,13], level modulators [14], antimicrobial [15–17], anti-inflammatory [18–20], and antioxidant [21].

There are various methods for the synthesis of benzimidazole derivatives. The most common traditional methods are coupling of the nitriles, amides, esters, chlorides, carboxylic acids with the *o*-phenylenediamine [22–23]. There are several methods in which thermal, microwave or the sonication method was used, most of time the benzimidazoles synthesized using the condensation of orthophenyl diamine with 2-nitroamines [24], aldehydes [25], car-

boxylic acids [26], carbonitriles, [27], arylamino oximes [28], cyclization of *o*-bromoaryl derivatives [29] and orthoesters [30].

The second route involves condensation reactions between *o*-phenylenediamine and aldehyde or alcohols via a dehydrogenated coupling, followed by oxidative cyclode hydrogenation [24,25], but in many of these methods, a stoichiometric number of oxidizing agents is a prerequisite [26–29].

Other important method which involves the direct regioselective C-2 arylation of imidazole with aryl halides using Pd(II)/Cu(I) catalytic amount at the high temperature, or pressure with low yield. There are several green catalyst like the inorganic salts zeolites [31–33], micelles [34], heterogeneous ionic liquid gel [35], metal oxides [36–40] *p*-toluenesulfonic acid/graphite and *N,N*-dimethyl aniline/graphite [41], benzimidazoles using various catalysts such as rose bengal [42], NH₄Cl [43] ytterbium perfluorooctane sulfonates (Yb(OPf)₃) [44] and base or metal catalysts [45] produces benzimidazoles. Generally, the condensation of *o*-phenylenediamines with aldehydes in the presence of acid [20], the dehydration of *N*-acylated, *o*-phenylenediamines using acetic acid [46], *p*-TSA [47] or amberlyst-15 Other methods include condensation of *o*-phenylenediamines with carboxylic acids, nitriles and *ortho*-esters under dehydrating conditions [48].

* Corresponding author.

E-mail addresses: arunvalvi99@gmail.com (A.K. Valvi), wadhava.gurumeet@gmail.com (G.C. Wadhawa).

Benzothiazole derivatives are known for different biological properties, including antitubercular, antimalarial, anticonvulsant, antihelmintic, analgesic, antidiabetic, antimicrobial, antibacterial, antifungal, herbicidal, antiproliferative and anti-inflammatory activities [49–52]. These compounds have shown antitumor activity against a range of human breast, ovarian, and colon cancers [53,54]. They are also useful for the *in-vivo* diagnosis of Alzheimer's disease [55,56].

Conventionally, 2-substituted benzothiazoles are synthesized by condensation of 2-aminothiophenol with aldehyde derivatives in different conditions. Various catalysts such as ZnO-beta zeolite [56], solid silica supported ferric chloride ($\text{SiO}_2\text{-FeCl}_3$) [57], glucose oxidase (GOX)/chloroperoxidase (CPO) [58], perchloric acid-doped polyaniline ($\text{HClO}_4/\text{PANI}$) [59], $\text{Sc}(\text{OTf})_3$ [60], YCl_3 and mixed metal oxide nano crystals of $\text{Al}_2\text{O}_3\text{-Fe}_2\text{O}_3$, $\text{Al}_2\text{O}_3\text{-V}_2\text{O}_5$ and $\text{Al}_2\text{O}_3\text{-CuO}$ were used in the synthesis of benzothiazoles. However, there is still room for improvement in the present methods to overcome the limitations and disadvantages of using organic solvents, long reaction times, lower yields and tedious work-up procedures. In this paper, we have reported the development of an environmental friendly protocol for the synthesis of 1,3-benzothiazole derivatives.

Nowadays, ZnS is an important member of this family as it has been extensively investigated [26]. ZnS nanoparticles have attracted a tremendous amount of attention because of their remarkable properties such as low cost, easy synthesis, high stability, small size etc [27]. Because of the importance of benzimidazoles and the catalytic ability of ZnS nanoparticles in the organic reactions, we wish to report a facile and efficient method for the synthesis of benzimidazole derivatives in the presence of catalytic amounts of ZnS nanoparticles in ethanol as solvent at 70°C.

2. Experimental

Chemicals are used of the S.D.Fine chemicals and Loba Chemicals products were characterized by their physical constant via the comparison with the authentic samples. Samples are purified by using column chromatography and progress of the reaction was monitored by using thin layer chromatography. Thin layer chromatography was performed using the aluminium plates with silica coating.

2.1. Synthesis of ZnS nanoparticles

ZnS nanoparticles were prepared by chemical method [5]. The reactants used for synthesis of ZnS nanoparticles were sodium sulphide ($\text{Na}_2\text{S}\cdot 7\text{H}_2\text{O}$) and Zinc sulphate ($\text{ZnSO}_4\cdot 5\text{H}_2\text{O}$). Using stoichiometric ratio in grams, 1 M solution of each reactant was prepared in distilled water. Freshly prepared aqueous solutions of these chemicals were used for the synthesis of nanoparticles at room temperature. The ZnS nanoparticles were prepared in the following sequence: First the extract prepared from waste stem of the *Trigonella foenum-graecum* (0.25 g) was added to the Zinc sulphate solution. The solution containing sodium sulphide was then added drop wise in solution of zinc sulphate and extract under continuous stirring until the white precipitates were formed. Stirring was done for 20 min to complete the reaction.

These precipitates were washed several times with distilled water to remove the impurities of sodium. After washing, the precipitates were centrifuged and dried at 100°C for 24 h. After drying, nanoparticles were grinded to achieve fine powder for characterization.

2.2. General procedure for the synthesis of benzimidazole derivatives

o-phenylenediamine (1 mmol) was added to a mixture of plant assisted nanoparticles (30 mg) and aldehyde (1 mmol) and the

resulting mixture was sonication on the probe sonicate. After completion of the reaction, as monitored by TLC (EtOAc: hexane 5:5), ethyl acetate (20 mL) was added and the catalyst was separated by filtration. The solvent was then removed under reduced pressure and the resulting solid product was recrystallized from ethanol, producing the pure product in good to high yields.

2.3. General procedure for the synthesis of benzothiazole derivatives

o-phenylenediamine (1 mmol) was added to a mixture of Plant assisted nanoparticles (30 mg) and aldehyde (1 mmol) and the resulting mixture was sonication on the probe sonicate. After completion of the reaction, as monitored by TLC (EtOAc: hexane 8:2), ethyl acetate (20 mL) was added and the catalyst was separated by filtration. The solvent was then removed under reduced pressure and the resulting solid product was recrystallized from ethanol, producing the pure product in good to high yields.

2.4. UV-visible spectrum for ZnS nanoparticles

The UV-Visible spectrum of the prepared ZnS nanoparticles is shown in the Fig. 1. It shows a strong absorption peak around 265–270 nm which is large blue shifted from the bulk absorption. From the absorption peak the optical energy band gap of ZnS nanostructure has been calculated using the formula, $E_{gn} = h\nu_{gn} = hc/\lambda_{gn}$ where h is plank's constant and E_g is energy band gap of the semiconducting nanoparticles in the optical spectra.

2.5. XRD study

X-ray diffraction patterns of the synthesized ZnS colloidal powders have been depicted in Fig. 2. The XRD traces shows that the prepared zinc sulphate is crystalline having zinc blende type structure. The cubic zinc blende structure was confirmed from the agreement of 2θ values with standard data. Fig. 2, showed three diffraction peaks at 2θ values of 28.96, 48 and 56.52. The peaks were identified to originate from (111), (220) and (311) planes of the cubic zinc-blende phase of ZnS, respectively.

The particle size calculated using Debye Scherer formula was 2.8 nm. The Debye Scherer formula is $D = 0.9 \lambda / (\beta \cos \theta)$ (2) where D is the mean grain size, λ is the X-ray wavelength, θ is the diffraction angle and β is full width at half maximum.

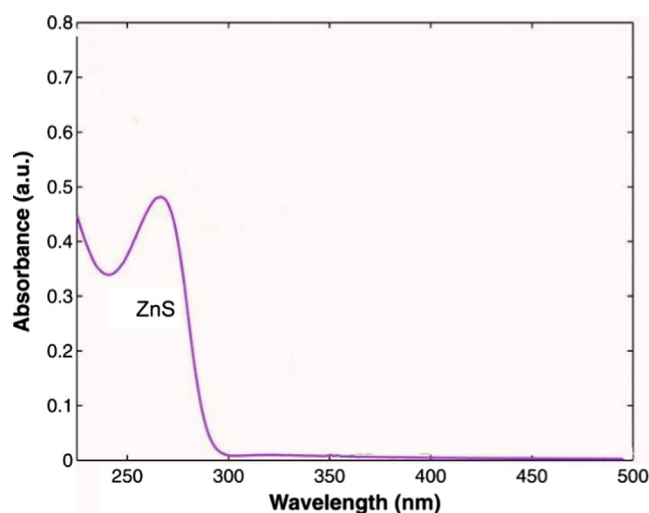


Fig. 1. UV spectrum of prepared ZnS nanoparticles.

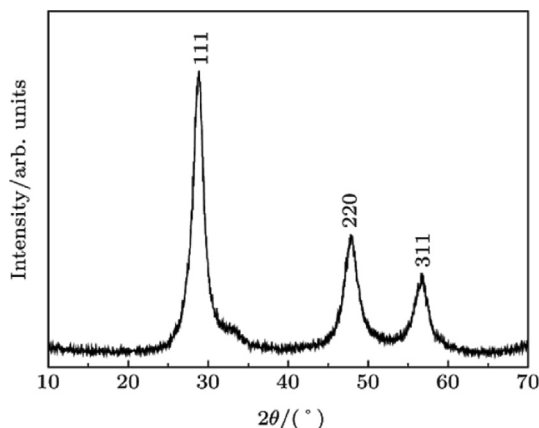


Fig. 2. X-ray diffraction patterns of the synthesized ZnS colloidal powders.

2.6. FTIR

The FTIR spectrum of ZnS nanoparticles at room temperature is shown in Fig. 3. This spectrum shows the IR absorption due to the various vibration modes. The characteristic major peaks of ZnS can be observed at about 1060, 1236, 1404, 788, 592, which are in good agreement with the reported results. The observed peaks at 1538 cm^{-1} – 1659 cm^{-1} are assigned to the C=O stretching modes, and also the broad absorption peaks in a range of 3434 cm^{-1} – 3965 cm^{-1} correspond to O–H stretching modes arising from the absorption of water on the surface of nanoparticles via –COOH group.

2.7. SEM

The SEM microstructural analysis shows that the synthesized ZnS contains mainly the grains of ZnS particles (crystallite) with regular shape (Fig. 4). One can see that nearly spherical nanoparticles have an almost homogenous size distribution with a mean size of 80–90 nm. In the absence of EDTA, a bulk ZnS sample is formed (not shown here). In the synthesis process, the usage of EDTA causes the stabilization of the small particles and the inhibition of this agglomeration. Due to the existence of –COOH group in EDTA molecules which absorbed on the particle surface, EDTA-

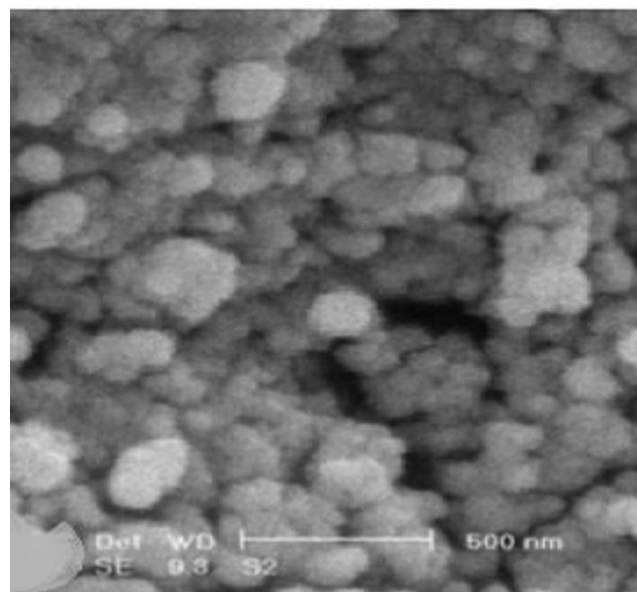


Fig. 4. The SEM image of ZnS nanoparticles.

capped ZnS sample is formed. The maximum particle size does not exceed 70 nm.

In order to establish the better catalytic activity of nano-ZnS, the reaction in the presence of other catalysts in ethanol at 70°C was investigated. The results showed that the nano-ZnS, as compared to other catalysts, gave the better yield of the desired product.

To determine the optimum quantity of nano-ZnS, the reaction of benzaldehyde and *o*-phenylenediamine was carried out in ethanol at 70°C using different quantities of nano-ZnS. The results showed that 0.03 g for benzimidazole and for benzothiazole 0.09 of the catalyst gave the excellent yield of the product. (See Tables 1–6).

3. Results and discussion

On the basis of the research information obtained on the applicability of plant assisted nanoparticles in the promotion of different types of organic reactions, we expected that this reagent

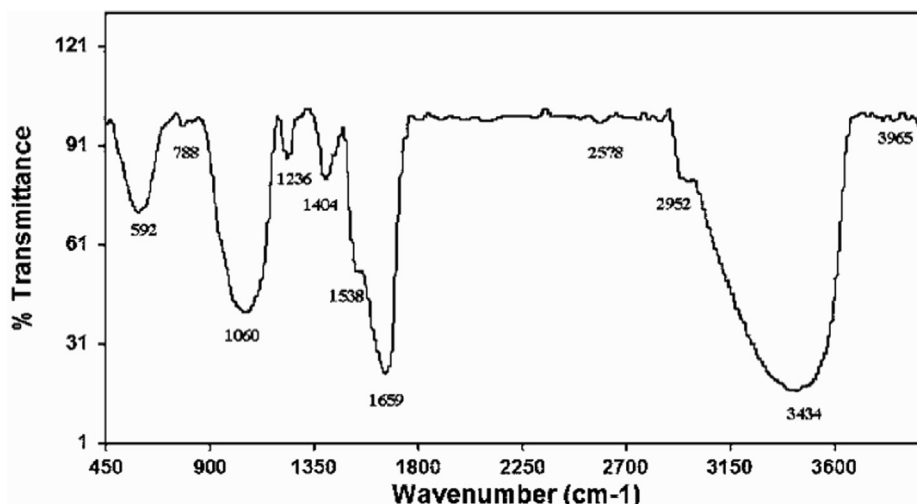


Fig. 3. The FTIR spectrum of ZnS nanoparticles.

Table 1
Evaluation of the activity of different catalysts for the synthesis of 2-phenyl-1H-benzimidazole.

Entry	Catalyst	Time (min)	Yield (%) (Benzimidazole)	Yield (%) (Benzothiazole)
1	–	60	25	35
2	Zinc Oxide	60	70	45
3	Alum	60	65	67
4	Hydrochloric Acid	60	65	55
5	Para-toluene Sulphonic Acid	60	67	54
6	NH ₄ Cl	60	87	86
7	Nano ZnS	60	97	96

Table 2
Optimization amount of nano-ZnS for the synthesis of 2-phenyl-1H-benzimidazole.

Entry	Catalyst (g)	Time (min)	Yield (%) (Benzimidazole)	Yield (%) (Benzothiazole)
1	–	60	40	43
2	0.01	60	56	67
3	0.03	60	98	56
4	0.09	60	78	97
5	0.20	60	67	78

Table 3
Optimization of the reaction temperature in the synthesis of 2-phenyl-1H-benzimidazole using nano-ZnS.

Entry	Temperature (°C)	Time (min)	Yield (%) (Benzimidazole)	Yield (%) (Benzothiazole)
1	70	60	97	95
2	60	60	70	80
3	40	60	78	70
4	25	60	67	45

Table 4
Reaction between *o*-phenylenediamine and different aldehydes catalyzed by nano-ZnS (0.03 g) in EtOH at 70 °C.

Entry	Ar	Time (min)	Yield (%) (Benzimidazole)	Yield (%) (Benzothiazole)
1	2-NO ₂ C ₆ H ₄	60	95	92
2	3-NO ₂ C ₆ H ₄	60	95	94
3	4-NO ₂ C ₆ H ₄	60	96	91
4	4-NHCH ₃ C ₆ H ₄	60	91	89
5	2-OH-3CH ₃ OC ₆ H ₄	60	85	81
6	4-ClC ₆ H ₄	60	87	86
7	4-OHC ₆ H ₄	60	98	95
8	3,4(CH ₃ O) ₂ C ₆ H ₃	60	89	92

Table 5
Catalyst Reusable for Benzimidazole.

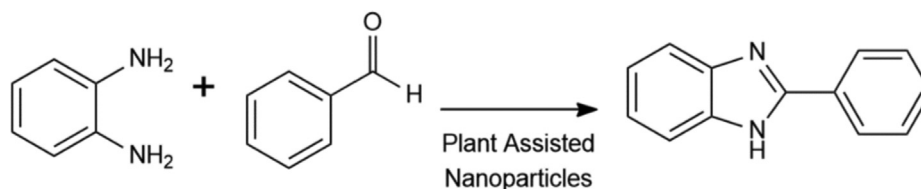
Entry	Catalyst (g)	Time (min)	Catalyst Cycle	Yield (%) (Benzimidazole)
1	0.03	60	1	96
2	0.03	60	2	82
3	0.03	60	3	78
4	0.03	60	4	56
5	0.03	60	5	40

Table 6
Catalyst Reusable Benzothiazole.

Entry	Catalyst (g)	Time (min)	Catalyst Cycle	Yield (%) (Benzothiazole)
1	0.03	60	1	94
2	0.03	60	2	78
3	0.03	60	3	67
4	0.03	60	4	56
5	0.03	60	5	45

could also be efficiently used in promoting the synthesis of benzimidazole and benzothiazole; these compounds function as acidic catalysts and speed up the reaction. Initially, optimize reaction conditions were studied by investigating the effect of various reac-

tant molar ratios and solvents. and also, solvent-free conditions, on the reaction of substituted benzaldehyde (10 mmol) and *o*-phenylenediamine (10 mmol) in terms of time and the product yield. The obtained results showed that the reaction using 30 mg



Scheme 1. Organic transformation using plant assisted nanoparticles.

of the catalyst at room temperature under a solvent-free condition in sonication produced the highest yield during a very short time.

Any further increase of the temperature or the catalyst amount did not improve the reaction time and yield. After optimizing the reaction conditions and in order to show the general applicability of this method, the preparation of benzimidazoles derivatives with a variety of simple, readily available substrates under the optimal conditions was investigated. Several aldehydes having electron donating and electron withdrawing groups underwent the conversion to form a series of aryl benzimidazoles in good to excellent yields. As can be seen, o-phenylenediamines with electron-withdrawing groups gave the desired products in higher yields within longer times in excellent yields.

After the successful synthesis of benzimidazoles, the preparation of benzothiazole derivatives, as the other useful heterocyclic compounds, in the presence of plant assisted nanoparticles, was nominated for further study.

Our investigations clarified that by using this method, the best results can be obtained when the reaction proceeded using lower amounts of the catalyst (90 mg) under solvent-free conditions at ambient temperatures. It is important to note that this reaction was not completed in different types of solvents even after a long time under reflux conditions. The selected conditions are shown in Scheme 1. To assess the efficiency of plant assisted nanoparticles in the preparation of benzothiazole derivatives, various aromatic aldehydes were subjected to the optimal conditions. It was observed that under the selected conditions, all the substrates containing electron-withdrawing groups, as well as electron-donating groups, were easily reacted in short reaction times with good to excellent isolated yields.

To check the reusability of the catalyst, the reaction of o-phenylenediamine with benzaldehyde or aromatic aldehyde under the optimized reaction condition was studied again. When the reaction was completed, ethyl acetate was added and the catalyst was separated by filtration. The recovered catalyst was washed with dichloromethane, dried and reused for the same reaction. The recovered catalyst was reused five times with a slight decrease in reusability in comparison to fresh catalyst. In order to show the efficiency of the present method, our result obtained from the reaction between o-phenylenediamine and benzaldehyde in the presence of plant assisted nanoparticles was compared with some of the other results reported in the literature for the same reaction. This method avoids the disadvantages of other procedures such as long reaction times, excess reagents and organic solvents.

4. Conclusion

We have used plant assisted nanoparticles as a highly catalyst for the simple and efficient synthesis of benzimidazole and benzothiazole and their derivatives. The procedure has several advantages, such as ease of preparation and handling of the catalyst, being a simple experimental procedure, having high reaction rates, producing excellent yields and the use of inexpensive and reusable catalyst. Furthermore, this process avoids problems associated with the use of organic solvents and liquid acids, which makes it

a useful and attractive strategy in view of these economic and environmental advantages.

Data availability

Data will be made available on request.

Declaration of Competing Interest

The authors declare that they have no known competing financial interests or personal relationships that could have appeared to influence the work reported in this paper.

Acknowledgments

We are thankful to Rayat Shikshan Sanstha, Satara for providing research facilities.

References

- [1] M. Boiani, M. Gonzalez, Imidazole and benzimidazole derivatives as chemotherapeutic agents, *Mini-Rev. Med. Chem.* 5 (2005) 409–424.
- [2] B. Narasimhan, D. Sharma, P. Kumar, Benzimidazole: A medicinally important heterocyclic moiety, *Med. Chem. Res.* 21 (2012) 269–283.
- [3] Y. Bansal, O. Silakari, The therapeutic journey of benzimidazoles: a review, *Bioorg. Med. Chem.* 20 (2012) 6208–6236.
- [4] K. Shah, S. Chhabra, S.K. Shrivastava, P. Mishra, Benzimidazole: a promising pharmacophore, *Med. Chem. Res.* 22 (2013) 5077–5104.
- [5] G. Yadav, S. Ganguly, Structure activity relationship (SAR) study of benzimidazole scaffold for different biological activities: a mini-review, *Eur. J. Med. Chem.* 97 (2015) 419–443.
- [6] M. Gaba, C. Mohan, Development of drugs based on imidazole and benzimidazole bioactive heterocycles: recent advances and future directions, *Med. Chem. Res.* 25 (2016) 173–210.
- [7] Starcevic, K.; Kralj, M.; Ester, K.; Sabol, I.; Grce, M.; Pavelić, K.; Karminski-Zamola, G. Synthesis, antiviral and antitumor activity of 2-substituted-5-amidino-benzimidazoles. *Bioorg. Med. Chem.* **2007**, 15, 4419–4426.
- [8] A. Gellis, H. Kovacic, N. Boufatah, P. Vanelle, Synthesis and cytotoxicity evaluation of some benzimidazole-4,7-diones as bioreductive anticancer agents, *Eur. J. Med. Chem.* 43 (2008) 1858–1864.
- [9] Purushottamachar, P.; Ramalingam, S.; Njar, V.C. Development of benzimidazole compounds for cancer therapy. In *Chemistry and Applications of Benzimidazole and Its Derivatives*; Marinescu, M., Ed.; IntechOpen: Rijeka, Croatia, 2019; ISBN 978-1-78984-552-5.
- [10] Hranjec, M.; Starcević, K.; Pavelić, S.K.; Lucin, P.; Pavelić, K.; Karminski Zamola, G. Synthesis, spectroscopic characterization and antiproliferative evaluation in vitro of novel Schi_ bases related to benzimidazoles. *Eur. J. Med. Chem.* **2011**, 46, 2274–2279.
- [11] N. Shrivastava, M.J. Naim, M.J. Alam, F. Nawaz, S. Ahmed, O. Alam, Benzimidazole sca_old as anticancer agent: Synthetic approaches and structure-activity relationship: Benzimidazole Sca_old as Anticancer Agent, *Arch. Pharm. Chem. Life Sci.* 350 (2017) e201700040.
- [12] R.V. Shingalapur, K.M. Hosamani, R.S. Keri, M.H. Hugar, Derivatives of benzimidazole pharmacophore: synthesis, anticonvulsant, antidiabetic and DNA cleavage studies, *Eur. J. Med. Chem.* 45 (2010) 1753–1759.
- [13] M. Ishikawa, K. Nonoshita, Y. Ogino, Y. Nagae, D. Tsukahara, H. Hosaka, H. Maruki, S. Ohyama, R. Yoshimoto, K. Sasaki, et al., Discovery of novel 2-(pyridine-2-yl)-1H-benzimidazole derivatives as potent glucokinase activators, *Bioorg. Med. Chem. Lett.* 19 (2009) 4450–4454.
- [14] D.A. Powell, Y. Ramtohol, M.-E. Lebrun, R. Oballa, S. Bhat, J.-P. Falgueyret, S. Guiral, Z. Huang, K. Skorey, P. Tawa, et al., 2-Aryl benzimidazoles: Human SCD1-specific stearyl coenzyme-A desaturase inhibitors, *Bioorg. Med. Chem. Lett.* 20 (2010) 6366–6369.
- [15] Kazimierzczuk, Z.; Upcroft, J.A.; Upcroft, P.; Górska, A.; Starósciak, B.; Laudy, A. Synthesis, antiprotozoal and antibacterial activity of nitro- and halogeno-substituted benzimidazole derivatives. *Acta Biochim. Pol.* **2002**, 49, 185–195.

- [16] K.F. Ansari, C. Lal, Synthesis and evaluation of some new benzimidazole derivatives as potential antimicrobial agents, *Eur. J. Med. Chem.* 44 (2009) 2294–2299.
- [17] K.F. Ansari, C. Lal, Synthesis, physicochemical properties and antimicrobial activity of some new benzimidazole derivatives, *Eur. J. Med. Chem.* 44 (2009) 4028–4033.
- [18] L.K. Labanauskas, A.B. Brukštus, P.G. Gaidelis, V.A. Buchinskaitė, Ė.B. Udrenaitė, V.K. Daukšas, Synthesis and antiinflammatory activity of some new 1-acyl derivatives of 2-methylthio-5,6-diethoxybenzimidazole, *Pharm. Chem. J.* 34 (2000) 353–355.
- [19] G. Tsukamoto, K. Yoshino, T. Kohno, H. Ohtaka, H. Kagaya, K. Ito, 2-Substituted azole derivatives. 1. synthesis and antiinflammatory activity of some 2-(substituted-pyridinyl)benzimidazoles, *J. Med. Chem.* 23 (1980) 734–738.
- [20] K. Ito, H. Kagaya, T. Fukuda, K. Yoshino, T. Nose, Pharmacological studies of a new non-steroidal antiinflammatory drug: 2-(5-ethylpyridin-2-yl)benzimidazole (KB-1043), *Arzneimittelforschung* 32 (1982) 49–55.
- [21] B. Can-Eke, M. Orhan Puskullu, E. Buyukbingol, M. Iscan, A study on the antioxidant capacities of some benzimidazoles in rat tissues, *Chem. Biol. Interact.* 113 (1998) 65–77.
- [22] J.B. Wright, The chemistry of the benzimidazoles, *Chem. Rev.* 48 (1951) 397–541.
- [23] P.N. Preston, Synthesis, reactions, and spectroscopic properties of benzimidazoles, *Chem. Rev.* 74 (1974) 279–314.
- [24] S.I. Alaqeel, Synthetic approaches to benzimidazoles from o-phenylenediamine: a literature review, *J. Saudi Chem. Soc.* 21 (2017) 229–237.
- [25] E.J. Hanan, B.K. Chan, A.A. Estrada, D.G. Shore, J.P. Lyssikatos, *Synlett* 18 (2010) 2759.
- [26] D. Yang, D. Fokas, J. Li, L. Yu, C.M. Baldino, *Synthesis* 1 (2005) 47.
- [27] W. Cui, R.B. Kargbo, Z. Sajjadi-Hashemi, F. Ahmed, J.F. Gauuan, *Synlett* 23 (2012) 247.
- [28] J. Sluiter, J. Christoffers, *Synlett* 1 (2009) 63.
- [29] B.C. Wray, J.P. Stambuli, *Org. Lett.* 12 (2010) 4576.
- [30] P. Saha, T. Ramana, N. Purkait, M.A. Ali, R. Paul, T. Punniyamurthy, *J. Org. Chem.* 74 (2009) 8719.
- [31] A. Hegedüs, Z. Hell, A. Potor, Zeolite-catalyzed environmentally friendly synthesis of benzimidazole derivatives, *Synth. Commun.* 36 (2006) 3625–3630.
- [32] A. Mobinikhaledi, N. Forughifar, M. Zendehtdel, M. Jabbarpour, Conversion of aldehydes to benzimidazoles using NaY zeolite, *Synth. React. Inorg. Met. Org. Nano-Met. Chem.* 38 (2008) 390–393.
- [33] A. Mobinikhaledi, M. Zendehtdel, F. Goudarzi, G.R. Bardajee, Nano-Ni(II)/Y Zeolite catalyzed synthesis of 2-aryl- and 2-alkyl benzimidazoles under solvent-free conditions, *Synth. React. Inorg. Met. Org. Nano-Met. Chem.* 46 (2016) 1526–1531.
- [34] K. Bahrami, M.M. Khodaei, A. Nejati, Synthesis of 1,2-disubstituted benzimidazoles, 2-substituted benzimidazoles and 2-substituted benzothiazoles in SDS micelles, *Green Chem.* 12 (2010) 1237–1241.
- [35] a) T.T. Nguyen, X.-T.-T. Nguyen, T.-L.-H. Nguyen, P.H. Tran, Synthesis of benzoxazoles, benzimidazoles, and benzothiazoles using a Brønsted acidic ionic liquid gel as an efficient heterogeneous catalyst under solvent-free condition, *ACS Omega* 4 (2019) 368–373; b) M. Adharvana Chari, D. Shobha, T. Sasaki, Room temperature synthesis of benzimidazole derivatives using reusable cobalt hydroxide (II) and cobalt oxide (II) as efficient solid catalysts, *Tetrahedron Lett.* 52 (2011) 5575–5580.
- [36] B. Das, B.S. Kanth, K.R. Reddy, A.S. Kumar, Sulfonic acid functionalized silica as an efficient heterogeneous recyclable catalyst for one-pot synthesis of 2-substituted benzimidazoles, *J. Heterocycl. Chem.* 45 (2008) 1499–1502.
- [37] K. Bahrami, M. Bakhtiarian, Mesoporous titania-alumina mixed oxide: A heterogeneous nanocatalyst for the synthesis of 2-substituted benzimidazoles, benzothiazoles and benzoxazoles, *ChemistrySelect* 3 (2018) 10875–10880.
- [38] B. Chen, C. Zhang, L. Niu, X. Shi, H. Zhang, X. Lan, G. Bai, Biomass-derived N-doped carbon materials with silica-supported ultrasmall ZnO nanoparticles: robust catalysts for the Green synthesis of benzimidazoles, *Chem. Eur. J.* 24 (2018) 3481–3487.
- [39] P. Bandyopadhyay, M. Sathe, S. Ponmariappan, A. Sharma, P. Sharma, A.K. Srivastava, M.P. Kaushik, Exploration of in vitro time point quantitative evaluation of newly synthesized benzimidazole and benzothiazole derivatives as potential antibacterial agents, *Bioorg. Med. Chem. Lett.* 21 (2011) 7306–7309.
- [40] R. Fazaeli, H. Aliyan, A Heterogeneous catalyst for efficient and green synthesis of 2-arylbenzothiazoles and 2-arylbenzimidazoles, *Appl. Catal. A Gen.* 353 (2009) 74–79 [CrossRef].
- [41] K. Jeshma, B. Nagaraju, A. Kamal, K.S. Ajay, *ACS Comb. Sci.* 18 (2016) 644.
- [42] H. Sharghi, O. Asemani, S.M.H. Tabaei, *Chem. Susc.* 45 (2008) 1293.
- [43] D. Kathirvelan, P. Yuvaraj, K. Babu, A.S. Nagarajan, B.S.R. Reddy, *J. Indian. Chem. B* 52 (2013) 1152.
- [44] M.S. Kedar, N.S. Dighe, S.H.R. Pattan, D.S. Musmade, T. Dipak, M. Bhosale, G.V. M. Der, *Pharma Chem.* 2 (2010) 249.
- [45] a) H. Baars, A. Beyer, S.V. Kohlhepp, C. Bolm, *Org. Lett.* 16 (2014) 536; b) J. Sluiter, J. Christoffers, *Synlett* (2009) 63; c) P. Saha, T. Ramana, N. Purkait, M.A. Ali, R. Paul, T. Punniyamurthy, *J. Org. Chem.* 74 (2009) 8719.
- [46] a) Zhang Z.H., Yin L., Wang Y.M. *Catal. Commun.*, 2007, 8:1126; b) Kommi D.N., Kumar D., Bansal R., Chebolu R., Chakraborti A.K. *Green Chem.*, 2012, 14:3329; c) Bressi J.C., Jong R.D., Wu Y., Jennings A.J., Brown J.W., Connell O.S., Tari L.W., Skene R.J., Vu P., Naver M., Cao X., Gangloff A.R. *Bioorg. Med. Chem. Lett.*, 2010, 20:3138.
- [47] a) D. Mahesh, P. Sadhu, T. Punniyamurthy, *J. Org. Chem.* 80 (2015) 1644; b) A.J. Blacker, M.M. Farah, M.I. Hall, S.P. Marsden, O. Saidi, J.M.J. Williams, *Org. Lett.* 11 (2009) 2039.
- [48] a) Dudd L.M., Venardou E., Garcia-Verdugo E., Licence P., Blake A.J., Wilson C., Poliakov M. *Green Chem.*, 2003, 5:187; b) Rambabu D., Murthi P.R.K., Dulla B., Rao B.M.V., Pal M. *Synth. Commun.*, 43:3083.
- [49] Z. Wang, X.H. Shi, J. Wang, T. Zhou, Y.Z. Xu, T.T. Huang, Y.F. Li, Y.L. Zhao, L. Yang, S.Y. Yang, L.T. Yu, Y.Q. Wei, *Bioorg. Med. Chem. Lett.* 21 (2011) 1097.
- [50] M. D. Altıntop, Z. A. Kaplancıklı, G. I. T. Zitouni, A. O. zdemir, F. Demirci, G. k. Is, can, G. Revial, *Synth. Commun.*, 41, 2234 (2011).
- [51] P. Datta, D. Sardar, A.P. Mukhopadhyay, E.L. Torres, C.J. Pastor, C. Sinha, *J. Organomet. Chem.* 696 (2011) 488.
- [52] Y. Q. Yuan, S. R. Guo, *Synth. Commun.*, 41, 2169 (2011).
- [53] a) T. H. Al-Tel, R. A. Al-Qawasmeh, R. Zaarour, *Eur. J. Med. Chem.*, 46, 1874 (2011), b) B. H. Yousefi, A. Manook, A. Drzezga, B. V. Reutern, M. Schwaiger, H. J. Wester, G. Henriksen, *J. Med. Chem.*, 54, 949 (2011).
- [54] T.I.A. Gerber, K.C. Potgieter, P. Mayer, *Inorg. Chem. Commun.* 14 (2011) 1115.
- [55] S.S. Katkar, P.H. Mohite, L.S. Gadekar, K.N. Vidhate, M.K. Lande, *Chin. Chem. Lett.* 21 (2010) 421.
- [56] M.H. Mosslemin, A. Fazlinia, Phosphorus, Sulfur Silicon Relat. Elem. 185 (2010) 2165.
- [57] A. Kumar, S. Sharma, R.A. Maurya, *Tetrahedron Lett.* 51 (2010) 6224.
- [58] M. Abdollahi-Alibeik, S. Poorirani, Phosphorus, Sulfur Silicon Relat. Elem. 184 (2009) 3182.
- [59] T. Itoh, K. Nagata, H. Ishikawa, A. Ohsawa, *Heterocycles* 62 (2004) 197.
- [60] L.-J. Zhang, J. Xia, Y.-Q. Zhou, H. Wang, S.-W. Wang, *Synth. Commun.* 42 (2012) 328.



Development of value-added cookies supplemented with giloy and tulsi powder

Disha Sunil Gawade, Karuna Wasudeo Patil, Gavit Hemangi Jayram *

Rayat Shikshan Sansths's Annsaheb Awate College Manchar, Pune 410503, India

ARTICLE INFO

Article history:
Available online 26 December 2022

Keywords:
Giloy Powder
Tulsi powder
Wheat Flour
Cookies
Phytochemical

ABSTRACT

Medical plants are widely used in various industries like agriculture, cosmetics, pharmaceuticals, and food. In some pandemic situations, every-one focused on developing immunity. The best way to increase the nutritional value of a person's daily diet is through a variety of ayurvedic practices. In this research conducted, herbal biscuits were developed. Cookies are eaten worldwide so it is the largest confectionary product and it is suitable for all age groups. In the present work, cookies are especially replaced with jaggery, wheat flour, and milk. Giloy stem powder was optimized by replacing whole wheat flour 100gm with (0.5gm, 1gm, 1.5gm, 2gm, 2.5gm, 3gm, 3.5gm, 4gm) and Tulsi leaves powder ((0.5gm, 1gm, 1.5gm, 2gm, 2.5gm, 3gm, 3.5gm, 4gm). Then final 1.5gm of giloy stem powder and 3gm of tulsi leaves powder were finalized based on sensory score. Both herbal powders which is an effective anti-aging herb. It also nourishes the skin. It is an anti-bacterial, antiviral and anti-fungal property that protects from a variety of infections. The use of this herbal powder focuses on developing organic products for human consumption and medicament.

© 2022 Elsevier Ltd. All rights reserved.

Selection and peer-review under responsibility of the scientific committee of the Integrative Nanotechnology Perspective for Multidisciplinary Applications - 2022. All rights reserved.

1. Introduction

Cookies are a popular form of bakery snack consumed all over the world for taste as well as nutrition. With long shelf life they also have high sugar and fat content thereby providing healthy nutrients. [1]. Due to fat rich content, they are highly susceptible to rancidity or oxidation. Hence, the quality of food deteriorates leading to unpleasant flavor, negative impact on health, and economic devaluation [2].

Creating novel meals by incorporating functional ingredients into a carrier food, like cookies, gives food producers better marketing prospects [3]. The majority of these investigations concentrate on organic substances having a range of physiological functions. It is intriguing to employ these herbs as food supplements due to their rising consumption. These herbs can provide a potent biochemicals including antioxidants, antimutagens, anticarcinogens and so on. [4,5].

Tinospora cordifolia Miers (Wild.) belonging to family Menispermaceae, is called by various local names in India such as giloy,

guduchi, or amrita. Ayurveda and conventional medicine highly regard this species for its wonderful therapeutic efficacy. [6]. India is home to this big deciduous climbing shrub whose extract is used as a treatment for a variety of illnesses, such as diabetes and hepatitis. This ancient herb giloy is rich in various phytochemicals such as ascorbic acid, lycopene alkaloids, terpenoids, lignans, carotene, etc. [7].

According to reports, giloy have phytochemicals having potent cytotoxic and immune-modulating properties. They work by stimulating immune cells exhibiting i-tumor effects. They increase the phagocytic activity of macrophages and boosts the generation of nitric oxide. According to Ayurveda, eating giloy with jaggery is more effective and cures the majority of ailments thereby lengthening a person's life. [8].

Additionally, the stem of giloy is used to treat a number of viral disorders as well as fever, jaundice, emaciation, skin conditions, diabetes, and anaemia. The proximate analyses of stem of giloy are carried out using standard methods, while mineral elements were analyzed using Atomic Absorption Spectrophotometer, equipped with air acetylene flame [9]. Numerous fascinating results have been published following thorough phytochemical,

* Corresponding author.

E-mail addresses: dishagawade2010@gmail.com (D.S. Gawade), gavit.hemangi@gmail.com (G. Hemangi Jayram).

pharmacological, and clinical examinations into the substance [10].

The scented perennial plant *Ocimum sanctum* L. also known as tulsi, belongs to the Lamiaceae family. The medicinal relevance of these plants is due to their bioactive phytochemical components, which have specific physiological effects on the human body [11]. *Ocimum sanctum* has been used and is known as the “Queen of Herbs” since the beginning of Bangladesh’s ancient civilization. It has been employed in ayurvedic and traditional medicine since ancient times. Tulsi is grown for its aromatic leaves. Due to its numerous therapeutic characteristics, it has also significantly influenced contemporary study. The plant’s various parts have been proven to have antibacterial, anti-inflammatory, analgesic, antipyretic, antiulcer, antidiabetic, and anticancer properties. [12]. When coupled with vitamin C, tulsi has helpful antiviral and antibacterial properties. Tulsi leaves and jaggery are a great combo for treating viral infections of the digestive system as well as the common cold and flu. It is known to improve cardiovascular health, promote immunity, and speed up the healing process after infections [13].

Apart from many significant components present in plants, dietary fiber cannot be digested by human digestive enzymes present in the small intestine [14]. It is mostly a complex carbohydrate, is a crucial component of a balanced diet because it aids in the effective passage of food and waste through the digestive system. These are of two types, viz., soluble and insoluble dietary fibre. [15]. If the soluble dietary fibre is present in food, it dissolves in water and makes the passage of food slowly. It also aids in maintaining a healthy cholesterol level, normalizes blood sugar levels in diabetics, and may help reduce blood pressure. Gums and Pectins are examples of soluble fibers, and they are also found in herbs like Tulsi. [16].

Jaggery is frequently used in Indian families and boosts immunity. Minerals like zinc and selenium, which are known to have antioxidant properties, are found in jaggery [17].

Children in rural areas of developing countries like India are especially at risk since the food that is easily accessible to them does not support their ability to develop physically or to resist disease. According to research conducted by the Nutrition Monitoring Bureau and The National Institute of Nutrition in 12 Indian states, the rural population’s diets are inadequate and low in the majority of nutrients, including calories, vitamins, and other nutrients, particularly protein. [18].

2. Materials and methods

2.1. Materials

Refined wheat flour, jaggery, fat, baking powder, baking soda, and milk, were obtained from the local market of Manchar. Flavor powder was obtained from naturally giloy stem powder and tulsi leaves powder to prepared at the college level by using the tray dryer method. All chemicals and reagents used were of analytical grade.

2.2. Preparation of giloy stems powder

Giloy stems creeping over neem were collected and washed thoroughly. After the stem were washed under running water, disinfected for the rinsed. Giloy stem covering were removed manually or by using stainless steel knives and weighed to determine the yield. Material preparation and physico-chemical properties analyses were performed at the laboratory. After the weighed the giloy stem, was cut into small slices and then dried in a tray dryer

at 40 °C – 60 °C for 8 h and ground. The crushed material was sieved through a 50 mesh to obtain a powder. The giloy stem powder was again weighed to calculate the yield, then giloy stem powder was vacuum packed and stored at 4 °C for future analysis.

2.3. Preparation of tulsi leaves powder

Tulsi was collected near the farm of Manchar. It was washed under the running tap water and disinfected. Tulsi was weighed to determine the yield. Material preparation and Physico-chemical properties analyses were performed at the laboratory. After tulsi leaves were removed manually and then dried in a tray dryer at 40 °C – 65 °C for 24 h and grind. The crushed material was sieved through a 50 mesh to obtain a powder. The tulsi leaves powder was again weighed to calculate the yield, then tulsi leaves powder was vacuum packed and stored at 4 °C for future analysis.

2.4. Development of herbal cookies by supplementing giloy stem powder and tulsi leaves powder.

Herbal cookies were formulated using giloy stem powder and tulsi leaves powder. Giloy stem and tulsi leaves were collected from the college campus. They were further processed and used as ingredients for development of herbal cookies. Giloy stem powder, tulsi leaves powder, wheat flour, milk, baking soda, baking powder and salt was used as raw material for development of herbal cookies. See Fig. 1

3. Result and discussion

3.1. Optimization and development of herbal cookies

In the case of final cookies wheat flour, fat, baking powder, baking soda, salt, and milk, were kept constant while giloy stem powder was optimized by replacing whole wheat flour 100gm with (0.5gm, 1gm, 1.5gm, 2gm, 2.5gm, 3gm, 3.5gm, 4gm) Then final 1.5gm of giloy stem powder (trial 3) was finalized based on the sensory score. (Table 1).

Tulsi leaves powder was optimized by replacing whole wheat flour 100gm with ((0.5gm, 1gm, 1.5gm, 2gm, 2.5gm, 3gm, 3.5gm, and 4gm). The final 3 gm of tulsi stem powder (trial 6) was finalized based on the sensory score (Table 2). So sensory evaluation was done with the 1.5 % incorporation of giloy stem powder or 3 % of tulsi leaves. The powder was used development of herbal cookies. The prepared cookies were baked at 160 °C at the top and 150 °C at the bottom for 25 min in the baking oven. The baked cookies are cooled at room temperature and packed in LDPE and HDPE pouches for another analysis. Cookies were prepared with whole wheat flour to serve as a control.

3.2. Quality characteristics of cookies:

3.2.1. Physical analysis of cookies

The physical properties of Before and After cookies were analyzed for their weight using a balance (ELB3000, Shimadzu, Japan), and the Thickness(T) of the cookies (distance between top to the bottom surface of cookies) and Width(W) (distance across the cookies) were determined using Vernier caliper.

Giloy stem powder and tulsi leave powder in the herbal cookies were analyzed for weight, Diameter, thickness, and spread ratio, by following the respective procedures (AACC, 2000). [19].

Spread ratio – The spread ratio of baked cookies was determined by the ratio of width and ratio of thickness.

$$SF = W/T$$

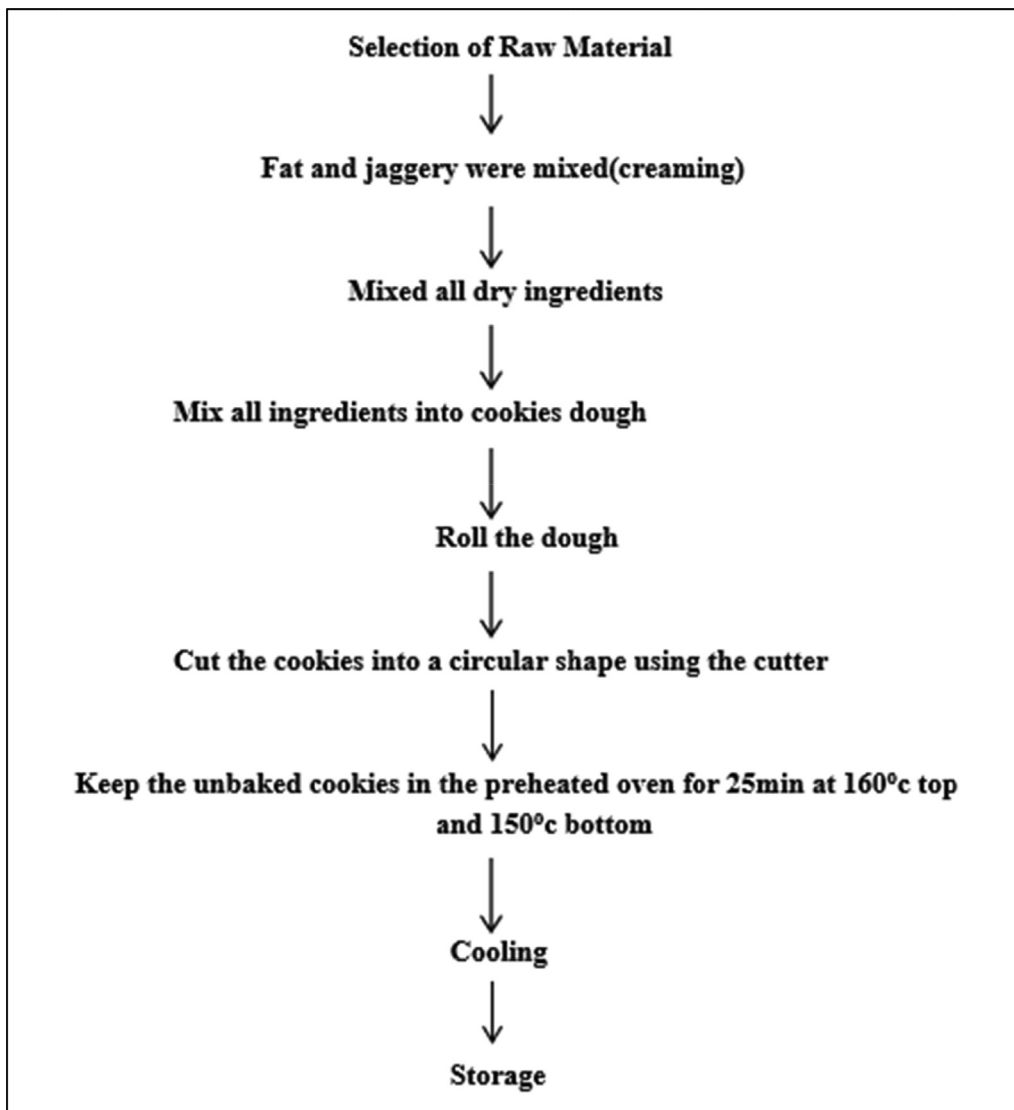


Fig. 1. Flowchart of preparation of cookies.

Table 1
Optimization of cookies based on Giloy stem powder.

Materials	T1	T2	T3	T4	T5	T6	T7	T8
Wheat flour	100	100	100	100	100	100	100	100
Fat	70	70	70	70	70	70	70	70
Baking soda	2	2	2	2	2	2	2	2
Baking powder	2	2	2	2	2	2	2	2
Milk	43	43	43	43	43	43	43	43
Salt	0.5	0.5	0.5	0.5	0.5	0.5	0.5	0.5
Giloy powder	0.5	1	1.5	2	2.5	3	3.5	4
Tulsi powder	3	3	3	3	3	3	3	3

Table 2
Optimization of cookies based on tulsi leaves powder.

Materials	T1	T2	T3	T4	T5	T6	T7	T8
Wheat flour	100	100	100	100	100	100	100	100
Fat	70	70	70	70	70	70	70	70
Baking soda	2	2	2	2	2	2	2	2
Baking powder	2	2	2	2	2	2	2	2
Milk	43	43	43	43	43	43	43	43
Salt	0.5	0.5	0.5	0.5	0.5	0.5	0.5	0.5
Giloy powder	1.5	1.5	1.5	1.5	1.5	1.5	1.5	1.5
Tulsi powder	0.5	1	1.5	2	2.5	3	3.5	4

Results of the physical analysis of before and after cookies are shown in (Table 3) (Figs. 2,3). The product parameters like weight, thickness, width, spread ratio, and spread factor in the case of cookies have a direct relation to product uniformity, quality, and consumer acceptance [20]. The quality of cookies is widely determined by the spread factor. As shown in (Table 3). The highest spread ratio before cookies is (5.2) and the lowest spread ratio after cookies is (4.3).

3.3. Sensory evaluation of cookies:

Sensory evaluation of cookies added with giloy stem powder was done and the results were noted. (Table 4). The sample prepared by using 100 g whole wheat flour, 45 ml milk, 0.5 g salt, 2 g baking powder, 2 g baking soda, 50 g jaggery, and 70 g fat was used control sample. Baking this formulation at 160°C top and 150°C bottom for 25 min was used as a control procedure. The whole wheat flour was replaced with giloy stem powder at a level (0.5gm, 1gm, 1.5gm, 2gm, 2.5gm, 3gm, 3.5gm, and 4gm) of from the results of a sensory analysis it was observed that flavor, color, and the taste was affected significantly by addition 1.5gm of giloy stem powder selected.

Sensory evaluation of cookies added with tulsi powder was done and the results were noted. (Table 5). The sample prepared by using 100 g whole wheat flour, 45 ml milk, 0.5 g salt, 2 g baking powder, 2 g baking soda, 50 g jaggery, and 70 g fat was used control sample. Baking this formulation at 160°C top and 150°C bottom for 25 min was used as a control procedure. The whole wheat flour was replaced with tulsi stem powder at a level (0.5gm, 1gm, 1.5gm, 2gm, 2.5gm, 3gm, 3.5gm, and 4gm) of from the results of a sensory analysis it was observed that flavor, color, and taste were affected significantly by the addition of 3gm of Tulsi leaves powder selected.

3.4. Proximate composition of herbal Cookies:-

The proximate composition of refined wheat flour, giloy stem powder, and tulsi leaves powder was estimated using standard AACC methods [21]. Moisture: Estimation of moisture content is determined by using the hot air oven method at 105°C for 4 hrs. (AOAC, 1995). [21].

Ash: By using the muffle furnace method up to constant weight. Ignite in a muffle furnace at 550+/- 250c for 4 hrs. [22].

Fat: Extracting the sample in a Soxhlet apparatus for 6-8h using petroleum ether. The solvent is evaporated and the residue is weighed [22].

3.5. Shelf life study of prepared cookies:

The prepared cookies were packed in PP and LDPE bags at room temperature for the shelf life study (Fig. 4). The moisture content of cookies was analyzed at a regular interval of 15 days along with sensory analysis. Results summarized in the Sensory evaluation showed that prepared cookies were of good quality throughout the storage period. The sensory quality mainly in terms of taste

Table 3 Physical analysis of before and after cookies.

Parameter	Before cookies	After cookies
Weight	14.80	15.82
Thickness	5.2	6.1
Width	1.0	1.4
Spread ratio	5.2	4.3



Fig. 2. Cookies before baking.



Fig. 3. Cookies after baking.

Table 4 Sensory evaluation of giloy stem powder.

Attribute	Sensory Score								
	GP 0	GP 1	GP 2	GP 3	GP 4	GP 5	GP 6	GP 7	GP 8
Color	7	7	7.5	8.5	8	7.5	7	7.2	6.5
Texture	7.5	7.5	8	8	8	8	8	8	8
Taste	8	7.5	7.7	8.3	7.5	7	7.2	6.5	6
Flavor	7.5	7.5	8	8.5	8	7.5	7	6.5	6
Overall	7.5	7.3	7.8	8.3	7.8	7.5	7.3	7	6.6
Acceptability									

Table 5 Sensory evaluation of Tulsi leaves powder.

Attribute	Sensory Score								
	TL 0	TL 1	TL 2	TL 3	TL 4	TL 5	TL 6	TL 7	TL 8
Color	7	7	7.5	8	8	7.5	8.5	7.2	6.5
Texture	7.5	7.5	8	8	8	8	8	8	8
Taste	8	7.5	7.7	7.6	7.5	7	8.7	6.5	6
Flavor	7.5	7.5	8	7	8	7.5	8.5	6.5	6
Overall	7.5	7.3	7.8	8.2	7.8	7.5	8.5	7	6.6
Acceptability									

was decreased to some extent but the product was acceptable. There was a gradual increase in the moisture content during the storage period.



Fig. 4. Value added cookies supplemented with giloy powder and tulsi powder.

4. Conclusion

The use of giloy stem powder and tulsi leaves powder is partially replaced by whole wheat flour in the preparation of herbal cookies. They are supplemented with nutritional properties such as anti-cancer, anti-inflammatory, antioxidant, and anti-microbial properties and the richness of dietary fibers.

The found sensory evaluation, textural and color properties that the overall acceptability of 1.5 % giloy stem powder and 3 % of tulsi leaves powder based on herbal cookies. The herbal cookies are suitable for the best nutritional value as well as sensory score.

Ayurveda has several advantages in India. It helps the body digest food more easily while also preventing some illnesses and infections. In a pandemic emergency, every-one concentrates on building their body's energy and immune system in order to make herbal cookies that are both good for testing and beneficial to our health. Every generation consumes cookies on a daily basis, which is a terrific way for some medicinal components to originate from our bodies or our food.

Although the sensory evaluation of the prepared value-added cookies supplemented with giloy and tulsi powder have good acceptability rate, it is also important to analyze the composition of final product.

CRedit authorship contribution statement

Gawade Disha Sunil: Data curation, Investigation. **Patil Karuna Wasudeo:** Conceptualization, Methodology, Supervision. **Gavit Hemangi Jayram:** Visualization, Investigation.

Data availability

Data will be made available on request.

Declaration of Competing Interest

The authors declare that they have no known competing financial interests or personal relationships that could have appeared to influence the work reported in this paper.

References

- [1] L.C. Okpala, E.C. Okoli, Development of cookies made with cocoyam, fermented sorghum, and germinated pigeon pea flour blends using response surface methodology, *J. Food Sci. Technol.* 51 (10) (2012) 2671–3267.
- [2] J. Ullah, M. Humayun, T. Ahmad, M. Ayub, M. Zarafullah, Effect of light, natural and synthetic antioxidants on stability of edible oil and fats, *Asian Journal Plant Science.* 2 (17–24) (2003) 1192–1194.
- [3] R. Krutulyte, K.G. Grunert, J. Scolderer, L. Lähteenmääki, K.S. Hagemann, P. Elgaard, B. Neilsen, J.P. Graverholt, Perceived Fit of Different Combinations of Carriers and Functional Ingredients and Its Effect on Purchase Intention, *Food Qual. Prefer.* 22 (2011) 11–16.
- [4] C.J. Dillard, J.B. German, *Phytochemicals: Nutraceuticals and Human Health*, *J. Sci. Food Agric.* 80 (2000) 1744–1756.
- [5] V.J. Sharma, P.M. Patel, Evaluation of Antibacterial Activity of Methanolic Extract of Plant *Rivea Ornata*, *International Research Journal of Pharmacy* 4 (2013) 233–234.
- [6] L.N. Sankhala, R.K. Saini, B.S. Saini, A review on chemical and biological properties of *Tinospora Cordifolia*, *Int J Med AromatPlants* 2 (2012) 340–344.
- [7] P. Srivastava, Study of medicinal properties of herb *Tinospora cordifolia* (Giloy) in preventing various diseases/abnormalities by increasing immunity naturally in human bodies, *Int. J. Eng. Res. and Gen. Sci.* 8 (4) (2020) 10–14.
- [8] S. Saha, S. Ghosh, *Tinospora Cordifolia: One plant, many roles*, *Anc. Sci. Life* 31 (4) (2012) 151–159, <https://doi.org/10.4103/0257-7941.107344>.
- [9] A.K. Sharma, M. Tafazul, Y. Badkhane, D.K. Raghuvanshi, A review on *Adhatodavasica* Nees- An important and high demanded medicinal plant, *Indo American Journal of Pharmaceutical Research* 2 (2014) 2231–6876.
- [10] A.K. Nadkarni, *Indian Materia Medica*, 3 edn., M/s Popular Prakashan Pvt Ltd, Bombay, 2005, p. 1(II).
- [11] C.A. Akinmoladun, E.O. Ibukun, E.M. Obuotor, E.O. Farombi, Phytochemical constituent and antioxidant activity of extract from leaves *Ocimum gratissimum*, *Science Research Essay* 2 (2007) 163–166.
- [12] R. Maheshwari, B. Rani, R.K. Yadav, M. Prasad, "Usage of Holy Basil for Various Aspects" (2012). *Bull. Env. Phar. and Life Sci.* 1: 63 – 65.
- [13] R.K. Upadhyay, *Tulsi: A holy plant with high medicinal and therapeutic value*, *Int. J. Green Pharma.* 11 (1) (2017) S1–S12.
- [14] *Dietary Fiber*. The University of California, Berkeley Bancroft Way Berkeley, CA 9472.
- [15] D.J.A. Jenkins, T.M.S. Wolever, A.R. Leeds, et al., *Dietary fiber, Fiber Analogues, and Glucose Tolerance: Importance of Viscosity*. 1 (1978) 1392–1394p.
- [16] S. Holt, R.C. Heading, D.C. Carter, et al., Effect of gel fiber on gastric emptying and absorption of glucose and paracetamol, *Lancet* 1 (1979) 636–639p.
- [17] A.K. Shrivastava, P. Singh, *Jaggery (Gur): The Ancient Indian Open-pan Non-centrifugal Sugar*. In: Mohan N, Singh P (eds) *Sugar and Sugar Derivatives: Changing Consumer Preferences*. Springer, Singapore, 2020, pp 283–307 https://doi.org/10.1007/978-981-15-6663-9_19.
- [18] K. Vijayaraghavan, H.D. Rao, *Diet and nutrition situations in rural India*, *IndJMed Res* 108 (1998) 243–253.
- [19] AACC, *Approved Methods of the American Association of Cereal Chemists*, America Association of Cereal Chemists. Inc., St. Paul, Minnesota, 2000.
- [20] A. Chauhan, D. Saxena, S. Singh, Total dietary fiber and antioxidant activity of gluten-free cookies made from raw and germinated amaranth (*Amaranthus spp.*) flour, *LWT Food Sci. Technol* 63 (2) (2015) 939–945.
- [21] AOAC, *Official methods of analysis*, 16th ed., Association of Official Analytical Chemists, Washington, DC, 1995, pp. 27–29.
- [22] S. Rangana, *Hand Book of Analysis and Quality Control for the Fruit and Vegetable Products*, Tata McGraw Hills Limited New Delhi, 1986.



Formulation of healthy cookies incorporated with orange peel powder and *Moringa oleifera* leaf powder

Nikita Vilas Teke, Karuna Wasudeo Patil, Hemangi Jayram Gavit*

Rayat Shikshan Sanstha's Annasaheb Awate College, Manchar, Pune 410503, India

ARTICLE INFO

Article history:

Available online 9 December 2022

Keywords:

Moringa leaf powder
Orange peel powder
Wheat flour
Cookies
Waste utilization
Phytochemicals

ABSTRACT

Studies were conducted for the incorporation of OPP (Orange peel powder) and MLP (Moringa leaves powder) in cookies. The OPP and MLP were analyzed and used in whole WF 100gm (0.5 gm, 1 gm, 1.5 gm, 2 gm, 2.5 gm, 3 gm, 3.5 gm, 4 gm) and MLP (0.5 gm, 1 gm, 1.5 gm 2 gm, 2.5 gm, 3 gm, 3.5 gm, 4 gm) proportion respectively. Based on sensory evaluation, 3% of OPP and 1% of MLP were selected for the preparation of healthy cookies. In the present work, OPP and MLP were prepared by using the tray dryer method. Jaggery and whole wheat flour were used instead of sugar and maida. The final formulation of the cookie mixture containing wheat flour (WF), OPP, and MLP was in the 96:3:1 ratio and resulted in the highest sensory score. The cookies were analyzed for various nutrients and phytochemical compounds. The utilization of waste orange peel and Moringa leaves was the most significant aspect of this study.

Copyright © 2022. Elsevier Ltd. All rights reserved.

Selection and peer-review under responsibility of the scientific committee of the Integrative Nanotechnology Perspective for Multidisciplinary Applications - 2022.

1. Introduction

Health-promoting foods including cookies have recently been in focus and of great interest to consumers, dieticians, experts, and producers. Cookies were classified as one of the most highly distributed bakery products in the market worldwide, because it is ready to eat, cheap, nutritionally rich, available in different tastes and have a longer shelf life [1].

The nutritional composition of Moringa of the South African ecotype has also been reported that including the profiling of chemical composition, fatty acids, amino acids, and vitamins. Amino acids, fatty acids, minerals, and vitamins are essential in animal feed. These nutrients are used for osmotic adjustment; activate enzymes, hormones, and other organic molecules that enhance growth, function and maintenance of life process [2].

Studies have also revealed that the leaves have immense nutritional value to combat malnutrition, especially among infants and nursing mothers. In addition, nutrition plays a crucial role in both humans and livestock as short-term alternative to chemoprophylaxis. In animals, nutrition plays a major role in animal's ability to overcome the detrimental effects of parasitism and diseases [3].

It is important to emphasize that orange peel, a byproduct of citrus manufacturing that is typically discarded, is actually valued as a functional food. Citrus peels may therefore boost health in addition to the usual nutrients they contain and help ward off disorders linked to food, such as osteoporosis, metabolic syndrome, type II diabetes, coronary heart disease, obesity, and hypertension [4].

The nutritional benefits of Moringa vary widely and are influenced by things like genetic makeup, environmental conditions, and production practices [5]. As a potential inhibitor of some microorganisms, such as bacteria (*Escherichia coli*, *Staphylococcus aureus*, *Vibrio parahaemolyticus*, *Enterococcus faecalis*, *Pseudomonas aeruginosa*, *Salmonella enteritidis*, and *Aeromonas caviae*) and fungi (*Trichophyton rubrum*, *Trichophyton mentagrophytes*, *Epidermophyton floccosum* and *Microsporium canis*), moringa leaf extracts were also able to act as a biocidal agent [6].

In addition to energy, proteins, minerals (zinc, copper, and iron), and vitamins (A and E) are all necessary for an animal to develop immunity (for the production of antibodies and cells) [7]. These nutrients also help organs and tissues communicate with one another to fight infections. Due to its several uses, moringa oleifera is regarded as a plant of versatility. Its leaves are an excellent source of calcium, iron, and vitamins A, B, and C [8].

* Corresponding author.

E-mail address: nikitateke03@gmail.com (N.V. Teke).

The majority of the world's population enjoys eating baked items made only with wheat flour. In nations like Nigeria, these goods have continually been consumed [9]. A well-fed animal is more resistant to disease than one that is already weak from starvation, even when exposed to infection. An animal's immune system responds to pathogen exposure by mounting an attack to ward off infection. This includes raising antibodies to fight the infection, as well as using white blood cells to attack pathogens [10]. In Africa, nursing mothers have been shown to produce much more milk when they add Moringa leaves to their diet. Severely malnourished children were reported to have made significant weight gains when caregivers add the leaves to their diet to increase their nutritional content [11].

Citrus by-products, if utilized fully, could be major sources of phenolic compounds. The peels, in particular, are an abundant source of natural flavonoids and contain a higher amount of phenolics compared to the edible portions [12].

The healing of abdominal tumors, hysteria, scurvy, paralytic attacks, helminthic bladder, prostate issues, ulcers, skin infections, inflammation, cardiovascular, and liver illnesses are just a few of the health issues and diseases that moringa is helpful for. Moringa, also protects body from arsenic-induced oxidative stress and in the depletion of arsenic concentration. Moringa is considered as a hypocholesterolemic agent, regulation of thyroid hormone status, anti-diabetic agent, antipyretic, antiepileptic gastric ulcers, antitumor agent, and hypotensive agent [13–15]. It is considered as one of the World's most useful trees, as almost every part of the Moringa tree can be used for food, medication and industrial purposes [16].

The wastes of fruits and vegetables are inexpensive, abundantly available, and are a good source of dietary fiber [17]. The orange peel is thought to contain some essential nutrients and has certain qualities that help the gastrointestinal tract operate properly. It is also great for diabetics and heart patients. Besides the nutritional aspect, it is having an affordable aspect as well. A segment membrane of citrus fruits appears to be able to prevent prostate and other cancers by acting as a mediator in cell communication, a factor known to reduce the likelihood of abnormal cell growth. Sour fruits such as lemon appear to have the greatest effect [18]. Moringa leaves are more potent in nutritional value. Its vitamin C content is seven times more than that of oranges, it has thirteen times more vitamin than spinach, and is on a lead on its own when it comes to the amino acid, 2,000 times more than green tea and 242 times more than apples. The leaves are sources of sulfur-containing amino acid such as methionine and cystine which are often in short supply in most legumes [19].

Bakery products have become more popular in India since earlier times. Among the different bakery products cookies constitutes the most popular group. Cookies were created fairly early. Because of their extremely low moisture content, they can be preserved for a long period. Cookies are chemically leavened bakery items with a high fat and sugar content [20].

Wheat as a major source of raw material for the production of these baked products such as cookies also lacks some nutrients. *Moringa oleifera* is an important food commodity that has had enormous attention as the 'natural nutrition of the tropics. The leaves, seeds, and flowers of *Moringa oleifera* all have great nutritional and therapeutic value [21].

The seeds are eaten like peas or roasted like nuts when still green; the dry seeds are apparently not used for human consumption, perhaps because the bitter coating becomes hardened while the flowers are eaten when cooked and taste like mushrooms [22]. The leaves are outstanding as a source of vitamins A, B group and (C when raw) and are among the best sources of minerals. They are also excellent sources of protein, but poor sources of car-

bohydrate and fat. Moringa leaves are one of the best plant foods available in nature.

The leaves of Moringa was considered as a very nutritional material as it contains vitamin A, vitamin C, iron, calcium and potassium in concentrations as much as in carrot, orange, spinach and banana. It is also a good protein source based on a comparison between its amino acid profiles and FAO/WHO/UNO reference protein for children. Its content of protein are more than that found in egg and soybean and contains a wide range of amino acids including zeatin, glutamic, arginine, and aspartic acid. Also, it contains carotenoid pigments, flavonoids, minerals, sterols and some phenolic compounds. Moringa leaves was proved to possess a high antioxidant activity values which played a potential rule in cancer chemoprevention, protein oxidation reduction and lipid peroxidation inhibition [23].

Since ancient times, 70 percent of the total production of oranges is used for the manufacture of derivative products, but 30 percent of processed fruits are converted into citrus peels waste, so these wastes contain many nutrients. Fruit peels serve as a barrier, shielding the edible components of the fruit from external elements as well as microorganisms and enzymes. They may or may not be considered fruits depending on their thickness and flavor. People frequently discard the peels of fruits after eating them, although the peels contain many of the fruit's nutritional benefits. They help protect our bodies from many diseases and increase disease resistance. Apart from this, various types of dishes, cosmetics, and medicines are also prepared by using these nutritious peels properly [24].

According to the World Health Organization (2003) report, "Dietary nutrition and prevention of chronic disease", it prevents heart disease due to folate present in citrus fruits, which is essential to lower levels of the heart. Potassium helps lower blood pressure, prevents stroke and kidney disease, and vitamins, carotenoids, and flavonoids are found in citrus fruits, all of them as protective cardiovascular effects.

2. Methodology

Refined wheat flour, jaggery, hydrogenated vegetable oil, baking powder, baking soda, salt, and milk were obtained from the local market of Manchar. Essence was obtained from the natural orange peel powder, moringa leaves powder to prepare at a college level by using the tray dryer method. All chemicals and reagents used were of analytical grade.

2.1. Preparation of orange peel powder

First, The orange fruits were washed under running water, disinfected and rinsed. The orange peels were manually removed using stainless steel knives and weighed to determine the yield. Material preparation and physicochemical analyses were performed at the laboratory. After the peels were weighed, they were cut into small pieces then dried in a tray dryer at 40 °C for 24 h and ground, then sieved through a 50 mesh sieve to obtain a powder. The peel powder was again weighed to calculate the yield, then orange peel powder was vacuum packed and stored at room temp for future analysis.

2.2. Preparation of Moringa leaves powder

First, the fresh moringa leaves were separated from the stalks of the ties, it was then removed from the leaf petal by hand. The leaves were placed on a tray dryer 45 °C for 24 h. After drying, dried moringa leaves were ground in the grinder to reduce the particle size. The ground material is then allowed to pass through a sieve

size 50 mesh, the larger particle on the sieve was again taken for grinding and passed through the sieve to obtain a fine powder. The moringa leaves powder was vacuum-packed and stored at room temperature for future analysis.

2.3. Preparation of cookies

Cookies were prepared by using the standardized recipe and method given by (Table 1):

According to the recipe, blends were made by combining milk, wheat flour, moringa leaf powder, and orange peel powder in various dry-weight ratios. These mixtures were standardized to produce products with acceptable physical characteristics and greater nutritional value. The dry ingredients i.e. wheat flour, MLP(moringa leaves powder), OOP(orange peel powder), baking powder, baking soda, salt, and flavour (cardamom and nutmeg powder) were mixed. A homogenous paste of fat and jaggery was prepared by hand to obtain a uniformly mixed dough. The prepared dough was rolled in a uniform shape and cut into round shape cookies with the help of a cutter. These cookies were baked at 160 °C top and 150 °C bottom for 25 min. Preparation of cookies was carried out using wheat flour samples replaced separately with (0.5, 1, 1.5, 2, 2.5, 3, 3.5, 4) OOP and MLP (0.5, 1, 1.5, 2, 2.5, 3, 3.5, 4) The method of cookies is a flow sheet in Fig. 1.

2.3.1. Optimization of Moringa powder in final cookies

Moringa powder optimization in the final cookies is shown in Table 2. Wheat flour, fat, baking powder, baking soda, salt, milk, and jaggery were all used in constant amount as mentioned in the Table 2. While the amount of Moringa leaf powder was changed in respective sample, to achieve an acceptable level of quality for optimization. The range of the MLP was 0.5gm to 4.0gm. Further, the sensory assessment of the product was carried out using 9 point Hedonic scale depending on which the suitable sample was selected. Sample T2 was chosen based on the sensory assessment.

2.3.2. Optimization of orange peel powder in final cookies

Orange peel powder optimization in the finished cookies is shown in Table 3. Wheat flour, fat, baking powder, baking soda, salt, milk, jaggery, and moringa powder were all kept constant in the final cookies while orange peel powder was changed to achieve an acceptable level of quality. The range of the OPP was 0.5gm to 4.0gm. Further, the sensory assessment of the product was carried out using 9 point Hedonic scale depending on which the suitable sample was selected. Sample T6 was chosen based on the sensory assessment.

Table 1
Ingredients used for preparation of cookies.

Sr. no	Ingredient Quantity
1	Wheat flour
2	Jaggery
3	Fat
4	Salt
5	Baking powder
6	Baking soda
7	Milk

2.4. Analysis of orange peel powder and Moringa leaves powder cookies

2.4.1. Physical analysis

Orange peel powder and moringa leaves powder cookies were analyzed for weight, Diameter, thickness, spread ratio, by following the respective procedures (AACC, 2000) [25].

Diameter (D): Six cookies were placed horizontally (edge to edge) and rotated at 90°angle for reading. Measured by vernier caliper.

Thickness (T): biscuits thickness was measured with a vernier caliper in triplicate. Means were recorded. Six cookies were measured one-by-one.

Spread ratio (SF): It was calculated according to the following equation.

$$SF = D/T$$

2.4.2. Chemical analysis

Moisture: Estimation of moisture content by hot air oven method at 105 °C for 4 hrs (AOAC, 1995) [26].

Ash: By using muffle furnace method up to constant weigh. Ignite in a muffle furnace at 550+/- 250c for 4 hrs. [27].

Fat: Extracting the sample in a Soxhlet apparatus for 6-8h using petroleum ether. The solvent is evaporated and the residue is weighed [27].

2.4.3. Sensory analysis

Sensory evaluation: Evaluate the products for acceptability based on its flavour, texture, appearance, amount of bitterness and overall acceptability using nine-point hedonic scale.

(1 = dislike extremely to 9 = like extremely; Meilgaard et al., 1999).

Shelf life analysis: The Orange peel powder and moringa leaves powder cookies samples were packed in LDPE packaging material under ambient temperature for 45 days has evaluated.

3. Result and discussion

3.1. Optimization

The optimization of control cookies was carried out by varying proportion of different components such as flour, jaggery, salt, milk and fat. In the 1st trial Wheat flour content was varied to get an acceptable quality of cookies. The preparation of control cookies the amount of wheat flour was varied as 90 %, 95 % and 100 %. sample 100 % was finalized due to its good characteristics (Fig. 2).

In 2nd trial the control cookies were prepared by using wheat flour, jaggery, baking powder, baking soda milk. In this case of fat were optimized i.e. 50, 70, and 90 gm respectively. Depending upon sensory evaluation cookies having good taste, texture and overall acceptability 70 gm were finalized.

In 3rd trial the control cookies were prepared by using wheat flour, fat, baking powder, baking soda milk. In this case of jaggery were optimized i.e. 25, 50, 75 gm respectively. Depending upon sensory evaluation cookies having good taste, texture and overall acceptability 50 gm were finalized.

In 4th trial, the control cookies were prepared by using wheat flour, fat, baking powder, baking soda, and jaggery. In this case of milk was optimized. i.e. 30, 45, 60 ml respectively. Depending upon sensory evaluation cookies having good taste, texture, and overall acceptability 45 ml were finalized.

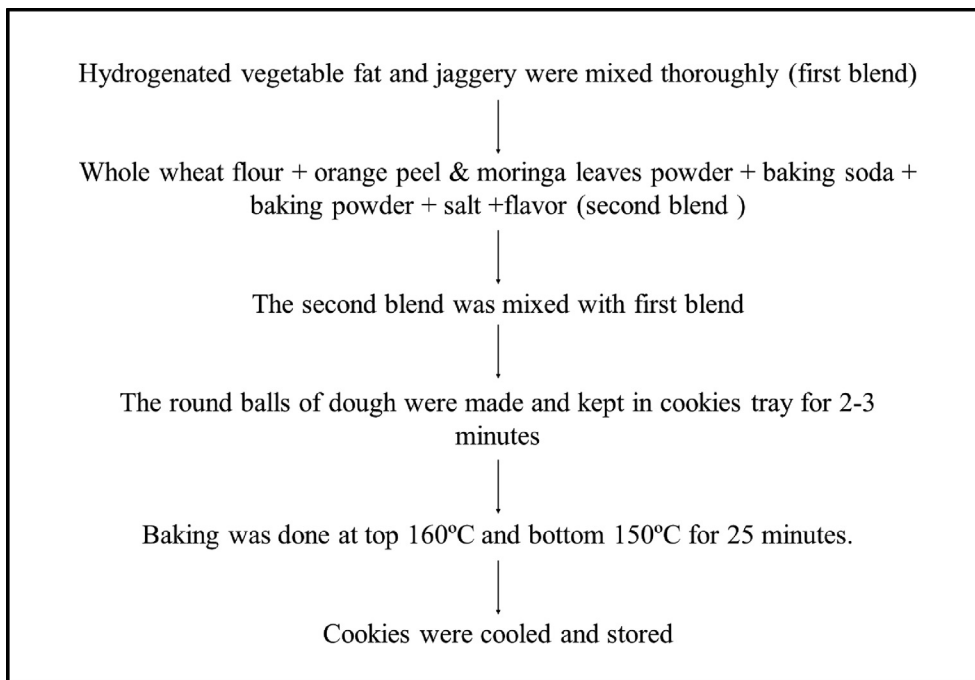


Fig. 1. Flow sheet for preparation of cookies.

Table 2
Optimization process of Moringa powder.

Sample code	Wheat flour (gm)	Fat (gm)	Baking powder (gm)	Baking soda (gm)	Salt (gm)	Milk (ml)	Jaggery (gm)	Moringa powder (gm)
T1	100	70	2	2	0.5	45	50	0.5
T2	100	70	2	2	0.5	45	50	1
T3	100	70	2	2	0.5	45	50	1.5
T4	100	70	2	2	0.5	45	50	2
T5	100	70	2	2	0.5	45	50	2.5
T6	100	70	2	2	0.5	45	50	3
T7	100	70	2	2	0.5	45	50	3.5
T8	100	70	2	2	0.5	45	50	4

Table 3
Optimization of orange peel powder.

Sample code	Wheat flour (gm)	Fat (gm)	Baking powder (gm)	Baking soda (gm)	Salt (gm)	Milk (ml)	Jaggery (gm)	Moringa powder (gm)	Orange peel powder (gm)
T1	100	70	2	2	0.5	45	50	1	0.5
T2	100	70	2	2	0.5	45	50	1	1
T3	100	70	2	2	0.5	45	50	1	1.5
T4	100	70	2	2	0.5	45	50	1	2
T5	100	70	2	2	0.5	45	50	1	2.5
T6	100	70	2	2	0.5	45	50	1	3
T7	100	70	2	2	0.5	45	50	1	3.5
T8	100	70	2	2	0.5	45	50	1	4

In 5th trial, all ingredients were kept constant only varied salt content based on taste parameters i.e. 0.3, 0.5, 0.7gm respectively. Depending upon sensory evaluation cookies having good taste, texture, and overall acceptability of 0.5 gm were finalized.

In the 6th trial, whole wheat flour 100gm with *Moringa oleifera* leaves powder 0.5gm, 1gm, 1.5gm, 2gm, 2.5gm, 3gm, 3.5 gm, 4gm based on taste parameters. Depending upon sensory evaluation cookies having good taste, texture, and overall acceptability of 1 gm were finalized.

In 7th trial whole wheat flour 100gm with orange peel powder 0.5gm, 1gm, 1.5gm, 2gm, 2.5gm, 3gm, 3.5 gm, 4gm based on taste

parameter. Depending upon sensory evaluation cookies having good taste, texture, and overall acceptability 3 gm were finalized.

In 8th trial, all ingredients were kept constant only varied time and temperature. i.e. top and bottom temp (180–160 for 15 min, 160–160 for 18 min, 160–150 °C for 25 min).

After the trails, the final cookies were prepared using ingredients as per mentioned in Table 4. These cookies were used for sensory evaluation.

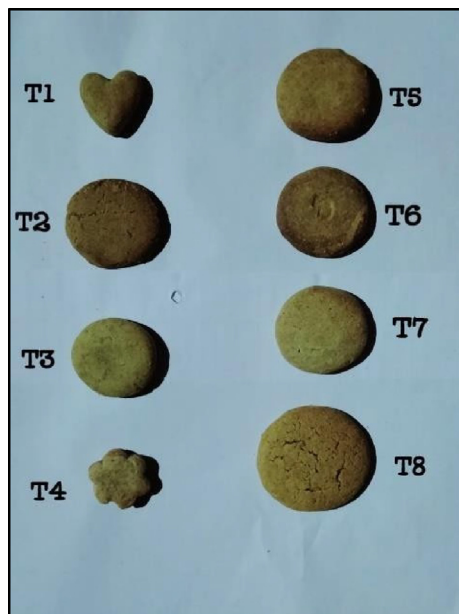


Fig. 2. Image of cookies trial (trial 1 to 8).

Table 4 Standardized recipe for cookies.

Sr. no	Ingredient	Quantity
1	Wheat flour	100 gm
2	Jaggery	50 gm
3	Fat	70 gm
4	Salt	0.5 gm
5	Baking powder	2.0 gm
6	Baking soda	2.0 gm
7	Milk	45 ml

3.2. Sensory evaluation of cookies

The effect of MLP fortification on sensory characteristics (color, taste, flavour, texture and overall acceptability) of wheat flour cookies is shown in Table 5 and Table 6. The color, taste, flavour and texture of control sample and cookies fortified with 1 % MLP and 3 % OPP extract were significantly superior to MLP and OPP cookies. Cookies fortified with 1 % MLP and 3 % OPP extract had the highest scores of flavour, texture and overall acceptability being (8.5, 8.3, 8.4) and (8.3, 8.5, 8.5) respectively. Cookies fortified with above 1 % MLP and 3 % were not acceptable. The results of

Table 5 Sensory evaluation of moringa leaves powder in cookies.

Sample Ccode	Sensory attributes				
	Color and appearance	Texture	Flavour	Taste	Overall acceptability
Control	8.5	8.5	8.5	8.5	8.5
MLP (0.5)	8.0	8.0	8.5	8.0	8.0
MLP (1.0)	8.5	8.3	8.3	8.4	8.3
MLP (1.5)	8.0	8.5	8.0	8.3	8.3
MLP (2.0)	8.0	8.5	8.5	7.0	7.0
MLP (2.5)	7.5	8.5	7.5	7.5	7.5
MLP (3.0)	7.5	8.5	6.0	6.5	6.5
MLP (3.5)	6.5	8.5	5.5	6.0	6.0
MLP (4.0)	6.5	8.5	5.0	5.5	5.5
Mean	7.66	8.42	7.31	7.3	7.28

MLP =Moringa leaves powder.

sensory evaluation indicated that 1 % MLP and 3 % OPP extract can be successfully used in wheat flour cookies.

3.3. Physical parameters of cookies

Various physical parameters such as thickness, diameter, weight and spread ratio were studied before and after baking and are shown in Table 7. The cookies observed are shown in Fig. 3 and Fig. 4.

3.4. Shelf life of orange peel powder and moringa leaves powder cookies

Shelf life of orange peel powder and moringa leaves powder cookies was carried out from 0 days to 45 days packed in LDPE pouches at ambient temperature (Fig. 5).

4. Conclusion

The present investigation focused on utilization of orange peel powder and moringa leaves powder for formulation of healthy cookies. The development and consumption of such products can also aid in improving the nutritional status of developing children. Orange peel powder and moringa leave powder are waste products derived from orange and moringa oleifera and possess good nutritional value, functional properties, dietary fiber, antioxidant, and antimicrobial properties. The MLP and OPP were optimized and the best sample was selected on the basis of sensory evaluation using nine-point Hedonic scale. Different optimization techniques were tested, and among those formulations, the product made with moringa powder was chosen for a 1 % sample based on sensory analysis, and the product made with orange peel powder for a 3 % sample.

Seven trials were conducted to formulate the ingredients in final cookies which included wheat flour, fat, jaggery, milk, salt, MLP and OPP. In the last eight trial, time and temperature were optimized. The final cookies were prepared according to the optimized ingredients and parameters. Further, the final product was subjected to the sensory evaluation. The cookies were evaluated depending on the color, texture and taste.

The results of Moringa’s nutrient characterization provide strong evidence that the plant’s leaves are nutrient-rich. Orange peel is thought to include several essential nutrients and possesses particular qualities that help the gastrointestinal tract work properly and is great for diabetics and heart patients. This study suggest that the moringa leaves and orange peels can be incorporated in the diet through the bakery products and be used as a nutritional supplement. The products can further be analyzed for its nutritional components.

Table 6
Sensory evaluation of orange peel powder in cookies.

Sample code	Sensory attributes				
	Color & appearance	Texture	Flavour	Taste	Overall acceptability
Control	8.5	8.5	8.5	8.5	8.5
OPP (0.5)	8.0	8.5	8.0	8.3	8.3
OPP (1.0)	8.5	8.5	8.4	8.3	8.0
OPP (1.5)	8.0	8.5	8.0	8.3	8.3
OPP (2)	8.3	8.5	8.0	8.0	8.0
OPP(2.5)	8.0	8.5	8.3	8.3	8.3
OPP(3)	8.3	8.5	8.4	8.5	8.5
OPP (3.5)	8.0	8.5	7.5	7.5	7.5
OPP (4)	8.0	8.5	7.0	7.0	7.0
Mean	8.17	8.5	8.01	8.07	8.04

OPP = Orange peel powder.

Table 7
Testing of physical parameters.

Sr.No	Timing	Thickness(T)	Diameter(D)	Weight (mg)	Spread ratio
1	Before baking	1.0	4.9	20.34	4.9
2	After baking	1.4	6.5	20.34	4.5



Fig. 3. Prepared cookies before baking.



Fig. 4. Prepared cookies after baking.



Fig. 5. Packaging of cookies.

CRedit authorship contribution statement

Teke Nikita Vilas: Data curation, Investigation. **Patil Karuna Wasudeo:** Data curation, Investigation. **Gavit Hemangi Jayram:** Visualization, Investigation.

Data availability

Data will be made available on request.

Declaration of Competing Interest

The authors declare that they have no known competing financial interests or personal relationships that could have appeared to influence the work reported in this paper.

References

- [1] C.M. Ajila, K. Leelavathi, U.J.S. Prasada Rao, Improvement of dietary fiber content and antioxidant properties in soft dough biscuits with the incorporation of mango peel powder, *J. Cereal Sci.* 48 (2) (2008) 319–326.
- [2] T.S. Anjorin, P. Ikokoh, S. Okolo, Mineral composition of *Moringa oleifera* leaves, pods and seeds from two regions in Abuja, Nigeria. *Int. J. Agric Biol.* 12 (2010) 431–434.
- [3] F. Anwar, S. Latif, M. Ashraf, A.H. Gilani, *Moringa oleifera*: a food plant with multiple medicinal uses, *Phytotherapy Res.* 21 (1) (2007) 17–25.
- [4] G. Block, B. Patterson, A. Subar, Fruit, vegetables and cancer prevention: A review of the epidemiological evidence, *Nutri. Cancer* 18 (1992) 1–29.
- [5] E.A. Brisibe, U.E. Umoren, F. Brisibe, P.M. Magalhaes, J.F.S. Ferreira, D. Luthria, X. Wu, R.L. Prior, Nutritional characterization and antioxidant capacity of different tissues of *Artemisia annua* L, *Food Chem.* 115 (2009) 1240–1246.
- [6] P.H. Chuang, C.W. Lee, J.Y. Chou, M. Murugan, B.J. Shieh, H.M. Chen, Anti fungal activity of crude extracts and essential oil of *Moringa oleifera* Lam, *Bioresource Techno.* 98 (1) (2007) 232–236.
- [7] R.L. Coop, P.H. Holmes, Nutrition and Parasite Interaction, *Int. J. Parasitol.* 26 (8-9) (1996) 951–962.
- [8] M.U. Dahot, Vitamin Contents of the Flowers and Seeds of *Moringa oleifera*, *Pakistan J. Biochem.* 21 (1988) 21–24.
- [9] M.O. Edema, L.O. Sanni, A.L. Sanni, Evaluation of maize –soybean flour blends for soy-maize bread production in Nigeria, *Afr. J. Biotechnol.* 4 (2005) 911–918.
- [10] FAO, Improved animal health for poverty reduction and sustainable livelihoods, *FAO Animal Prod. Health Papers.* 153 (2002).
- [11] L.J. Fuglie, *The Miracle Tree: the multiple attributes of Moringa.* Church world service, west African regional office, Dakar, Senegal, 2001, pp 103–36.
- [12] S.O. Gorinstein, Y.S. Martín-Belloso Park, Trakhtenberg, Comparision of some biochemical characteristics of different citrus fruits, *Food Chem* 74 (2001) 309–315.
- [13] A.P. Guevara, C. Vargas, H. Sakurai, Y. Fujiwara, K. Hashimoto, T. Maoka, M. Kozuka, Y. Ito, H. Tokuda, H. Nishino, An antitumor promoter from *Moringa*

- oleifera* Lam, Mutation Res./Genetic Toxicol. Environ. Mutagenesis 440 (2) (1999) 181–188.
- [14] R. Gupta, G.M. Kannan, M. Sharma, S. Flora, Therapeutic effects of *Moringa oleifera* Lam. on arsenic-induced toxicity in rats, Environ. Toxicol. Pharmacol. 20 (3) (2005) 456–464.
- [15] A.A. Hamza, A meliorative effects of *Moringa oleifera* Lam. seed extract, Food Chem. Toxicol. 48 (1) (2010) 345–355.
- [16] M.M. Khalafalla, E. Abdellatef, H.M. Dafalla, A.A. Nassrallah, K.M. Aboul-Enein, D.A. Lightfoot, F.E. El-Deeb, H.A. El-Shemy, Active principle from *Moringa oleifera* Lam Leaves effective against two leukemias and a hepatocarcinoma, Afr. J. Biotechnol. 9 (49) (2010) 8467–8471.
- [17] B. Knudsen, A. Serena, Chemical and physicochemical characterization of co-products from vegetable food and agro industries, Anim. Feed Sci. Technol 139 (2007) 109–124.
- [18] Y. Liu, H. Ahmad, Y. Luo, D.T. Gardina, R.S. Guasekera, W.L. Mc Keehan, B.S. Patil, Citrus pectin: Characterization and inhibitory effect on fibroblast growth factor-receptor interaction, J. Agric. Food Chem. 49 (6) (2001) 3051–3057.
- [19] F.W. Martin, R.M. Ruberte, L.S. Meitzner, Edible leaves of the tropics. 3rd ed. Educational concerns for hunger organization, Inc., N.ft. Meyers, Fl. 1998, 194pp.
- [20] N. Navy, Bakery products in the middle east especially in the Arab countries obtained in Egypt, J. Food Sci. Technol 22 (8) (1980) 342–347.
- [21] A.T.E. Olushola, The Miracle tree", *Moringa oleifera* (Drumstick), in : Achieve Vibrant Health with Nature, Keep Hope Alive Series 1, Unijos Consultancy Limited press, Jos, Nigeria, 2006, pp. 120–136.
- [22] L.L. Price, The *Moringa* tree. www.echonet.org. Accessed on 14/11/2010. Samphal metz; 2000, (1998) hand book of bakery and confectionary.
- [23] S. Sreelatha, A. Jeyachitra, P.R. Padma, Antiproliferation and induction of apoptosis by *Moringa oleifera* Lam. leaf extract on human cancer cells, Food Chem. Toxicol. 49 (6) (2011) 1270–1275.
- [24] M.K.E. Youssef, Foods that fight cancer, in: Proceedings of the sixth Conference of Woman and Scientific Research & Development in Upper Egypt. 17–19 April 2007, Assiut University, 2007, pp. 213–228.
- [25] American Association of Cereal Chemists AACC, Approved methods of The AACC. 10th Ed. The Association: St. Paul, MN, 2000.
- [26] AOAC, Official methods of analysis, 16th ed., Association of Official Analytical Chemists, Washington, DC, 1995, pp. 27–29.
- [27] S. Rangana, Hand Book of Analysis and Quality Control for the Fruit and Vegetable Products, Tata McGraw Hills Limited, New Delhi, 1986.



Effect of Divalent / Trivalent Doping on Structural, Electrical and Magnetic Properties of Spinel Ferrite Nanoparticles

Mahesh B. Khanvilkar,^{1,2,*} Arvind K. Nikumbh,¹ Ramdas A. Pawar,¹ Neeta J. Karale,¹ Pratik A. Nagwade,¹ Deepak V. Nighot,¹ Gulab S. Gugale,¹ Mohan D. Sangale,¹ Sham B. Misal¹ and Sharad P. Panchgalle²

Abstract

Five nanosized divalent/trivalent doped spinel ferrites (a) Cu-Zn co-doped nickel ferrite ($\text{Ni}_{0.6}\text{Cu}_{0.2}\text{Zn}_{0.2}\text{Fe}_2\text{O}_4$), (b) Cd-doped cobalt ferrite ($\text{Co}_{0.9}\text{Cd}_{0.1}\text{Fe}_2\text{O}_4$), (c) Al-doped cobalt ferrite ($\text{CoAl}_{0.3}\text{Fe}_{1.7}\text{O}_4$), (d) Ru-doped cobalt ferrite ($\text{CoRu}_{0.04}\text{Fe}_{1.96}\text{O}_4$), and (e) Ni-doped gamma ferric oxide ($\text{Fe}_{2.55}\text{Ni}_{0.12}\square_{0.33}\text{O}_4$; where \square , is Fe vacancy) are synthesized by coprecipitation method. Energy dispersive X-ray (EDS) and ICPE analysis confirm the stoichiometry of the elemental composition of the synthesized materials. The X-ray diffraction pattern (XRD) confirmed the cubic structure with enlarged lattice parameters as compared to undoped compounds. The size and crystalline structure are confirmed by scanning electron micrographs (SEM), transmission electron microscopy (TEM), and Histogram found approx. 18-52nm. Selected area electron diffraction (SAED) pattern exhibited the lattice planes which indicates the particle is crystalline in nature. Electrical conductivity, Seebeck voltage and Hall effect measurements for these samples showed n-type semiconductors. All samples show typical hysteresis behavior with a decrease in saturation magnetization, and an increase in coercivity as compared to respective undoped ferrites. The remanence ratio was found in the range of 0.11 to 0.47 indicating multi-domain structure for all samples except $\text{Fe}_{2.55}\text{Ni}_{0.12}\square_{0.33}\text{O}_4$, which have single domain structure ($M_R/M_S=0.58$). The observed irreversibility of zero-field cooled (ZFC)-field cooled (FC) curve for $\text{Fe}_{2.55}\text{Ni}_{0.12}\square_{0.33}\text{O}_4$, is indicative of ferromagnetism.

Keywords: Nanosized doped spinel ferrites; Ferromagnetism; Electrical conductivity; Magnetization; Exchange interaction.

Received: 19 October 2022; Revised: 16 March 2023; Accepted: 19 March 2023.

Article type: Research article.

1. Introduction

In recent decades, the preparation and characterization of nanoparticles and nano-structured materials of various chemical compositions, structures, and morphologies have become a topic area in inorganic materials research. These issues have emerged in the development of nanotechnologies for manufacturing nanopowders for structural and functional applications. Magnetic nanoparticles, especially nanocrystalline spinel ferrites have across-the broad applications in medicine, photocatalysis, microwave devices, transformers, electric generators, storage instrumentations, multilayer chip inductors, ferrofluids, rod antenna, ferrite cores, humidity sensors, magnetic recorders, *etc.*^[1-3] The spinel

ferrite has the general formula (A)[B₂]O₄ that can be portrayed as a cubic closed pack of oxygen ions. The round brackets (A) represent tetrahedral interstitial sites and square brackets [B] corresponds to larger octahedral sites. Both of these sites are occupied by cations, with divalent ions occupying tetrahedral and trivalent ions occupying octahedral sites. The magnetic moments of the cations occupying octahedral lattice sites are oriented in the same direction, whereas the magnetic moments of the cations at tetrahedral sites are oriented antiparallel to that of the cations at octahedral sites. The resultant of these two magnetic moments gives rise to the net magnetization in spinel ferrite.

The unit cell of the spinel structure is obtained by doubling approximately face-centered cubic oxygen sublattices along each of the three directions. Of the resulting 64 tetrahedral (A) sites and 32 octahedral [B] sites, only 8 and 16 are occupied, respectively, by cations in stoichiometric spinel. Most spinel compounds belong to the space group Fd3m.^[4]

¹ Department of Chemistry, Savitribai Phule Pune University (Formerly University of Pune), Ganeshkhind, Pune 411 007, India.

² K. M. C. College, Khopoli, Tal-Khalapur, Dist. Raigad – 410203, India.

*Email: mb.khanvilkar@gmail.com (M. B. Khanvilkar)

Occupation of the tetrahedral sites entirely with a divalent metal ion produces a normal spinel structure, while the occupation of the octahedral site with the divalent metal ion yields an inverse spinel structure. If divalent metal ions are present on both (A) and [B] sublattices, the structure is of mixed or disordered spinel.^[5] Information on cation distribution and spin alignment is essential to understand the magnetic properties of spinel ferrites. The interesting physical and chemical properties of ferros spinels arise from their ability to distribute the cations among the available tetrahedral (A) and octahedral [B] sites. The determination of cation distribution at the tetrahedral (A) and octahedral [B] sites have been the subject of many studies. X-ray diffraction, Mossbauer spectroscopy, Magnetization measurement, electron spin resonance (ESR), Neutron diffraction, Thermoelectric, and Nuclear magnetic resonance (NMR), Quantum mechanical method, and Rietveld refinement have been employed to determine the cation distribution in spinels.^[5,6]

In recent decades, the doped metal ions can substitute either (A) site or [B] site or both depending upon its valency and site type, which in turn affects the structural, electrical, and magnetic properties of the spinel ferrites.^[7] One of the difficulties regarding the crystal chemistry of spinel ferrites is determining the metal oxidation states and cation distribution among the tetrahedral (A) and octahedral [B] sites of the spinel structure. This determination becomes more complex when two or more metallic cations with relatively similar oxidation states share the lattice sites and which has been determined by X-ray photoelectron spectroscopy (XPS). Thermodynamic considerations have shown that trivalent or tetravalent cations are usually positioned on octahedral sites, while divalent have no preference.^[8] The dependency of any particular doped composition adopting the normal, inverse, or mixed spinel structure lies in lattice energy, crystal field stabilization, and covalency effects. Similarly, the site preference for any particular dopant will arise from the balance of energy considerations. The ferrimagnetic properties of cobalt ferrite (CoFe_2O_4) or nickel ferrite (NiFe_2O_4) are closely related to the cation arrangements and oxidation states in the two crystallographic sites (*i.e.*, A and B sites) and are inverse spinel structures.^[9] The antiferromagnetic properties of Zinc ferrite (ZnFe_2O_4) or Cadmium ferrite (CdFe_2O_4) are closely related to the cation arrangements and oxidation states in the same crystallographic site (*i.e.*, B-site), which are antiparallel and normal spinel.^[10] The ferrimagnetic properties of gamma- Fe_2O_3 (maghemite) are believed to be close to that of Fe_3O_4 (magnetite) and are inverse spinel structures, of which one-third of Fe^{3+} at the B-site is vacant. It is frequently written as $(\text{Fe}^{3+})_A[\text{Fe}^{3+}_{5/3}\square_{1/3}]_B\text{O}_4^{2-}$, where \square it stands for Fe vacancy.^[11]

Most of the research is emphasized the modification of magnetic properties for a substitution or doped of Fe^{3+} ions for cobalt ferrites with transition metal ions (Mn, Cr, Cd, Ni, Zn, Ru, *etc.*) and rare-earth ions (Gd, Pr, Nd, Sm, *etc.*).^[12-14] The electrical and magnetic properties of nonmagnetic Al^{3+} doped cobalt ferrites are also reported by various groups.^[15] The effect of rare-earth ion doped on magnetization and initial permeability of Mn-Zn, Cu-Zn, Ni-Zn, Mg-Zn, and Ni-Cd ferrite systems have also been extensively studied.^[16,17] The nano Cobalt ferrite (CoFe_2O_4) particles are worthy contenders in the medical field for isolation and purification of genomic (DNA) and the separation of polymerase chain reaction (PCR) ready DNA and especially in hyperthermia treatment.^[18] Mn-doped Co-Zn ferrites ($\text{Co}_{0.6}\text{Zn}_{0.4}\text{Mn}_x\text{Fe}_{2-x}\text{O}_4$) and Cd-doped Co-Zn ferrites ($\text{Co}_{0.5}\text{Zn}_{0.5}\text{Cd}_{1.5x}\text{Fe}_{2-x}\text{O}_4$) were synthesized by standard solid-state reaction method and electrical, magnetic, mechanical properties and photocatalytic degradation activities reported.^[19] While nanosized doped-gamma ferric oxide has increased the coercivity and saturation magnetization to a large extent for its use in high-density recording disks or high-speed digital tape.^[20] Structural and dielectric studies of Zn, Gd, and Ga doped NiFe_2O_4 are synthesized by two different routes as solid-state reaction and citrate method.^[21] The samples synthesized using solid-state reaction showed magnetic order, whereas the samples prepared through the citrate method exhibited super magnetic nature. From this literature, it is learned that the physical and chemical properties of spinel ferrites are strongly affected by synthesis conditions and methods as these influence the chemical composition, stoichiometry, point defect concentration (*i.e.*, dopants), and used in energy technology.^[21]

With this view in mind, the doped spinel ferrites have attracted much interest due to their novel magnetic and electrical properties and are still the subject of much research aimed at a better understanding of the magnetic interaction between A site and B site. These properties are associated with the distribution and occupancy of cations in the spinel crystal structure. The aim for both divalent and/or trivalent dopants is with ionic radii comparable to that of Fe^{3+} . Hence they would be expected at different crystallographic sites (A or B sites) of spinel ferrites. Also, different substituting cations have their own preferential sites when doping in the spinel ferrites. When doping in the spinel ferrite phase by partial reduction of Fe^{3+} to Fe^{2+} took place, but overall charge neutralization, oxygen vacancies are created at the octahedral site, thus decreasing the electrical and magnetic parameters.

In general, the synthesis technique of spinel ferrite plays a vital role in determining the structural, electrical, and magnetic properties. The main novel synthesis methods of

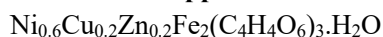
nanosized spinel ferrites are sol-gel, co-precipitation, oxidation, micro-emulsion, hydrothermal, spray pyrolysis, reverse micelles, and ultrasound-assisted synthesis.^[3] In the present study, five nano-sized divalent and /or trivalent doped inverse spinel ferrites such as (a) Cu-Zn codoped nickel ferrite ($\text{Ni}_{0.6}\text{Cu}_{0.2}\text{Zn}_{0.2}\text{Fe}_2\text{O}_4$), (b) Cd-doped cobalt ferrite ($\text{Co}_{0.9}\text{Cd}_{0.1}\text{Fe}_2\text{O}_4$), (c) Al-doped cobalt ferrite ($\text{CoAl}_{0.3}\text{Fe}_{1.7}\text{O}_4$), (d) Ru-doped cobalt ferrite ($\text{CoRu}_{0.04}\text{Fe}_{1.96}\text{O}_4$), and (e) Ni-doped gamma ferric oxide ($\text{Fe}_{2.55}\text{Ni}_{0.12}\square_{0.33}\text{O}_4$; where \square is a vacancy, it stands for Fe vacancy) were synthesized using tartrate / Succinate or hydroxide coprecipitation method (soft chemical route). This method is simple, low cost, exhibits high purity, and ability to produce a fine and homogeneous nano particle powder with any risk of contamination in shorted duration than other methods. This work aims to explain the effect of dopants on the structural, and electrical properties of the as-synthesized doped samples. The magnetic measurements are also undertaken to gain information about the cation distribution, and possible canted spin structures at both A and B sites in these doped inverse spinel ferrites.

2. Experimental

Nanoparticles of undoped and doped ferrites were synthesized by the coprecipitation method. All the reagents in this study were supplied by Sigma-Aldrich and were used without further purification.

2.1 Synthesis of tartrate/succinate and hydroxide precursors

2.1.1 Nickel-copper-zinc-iron tartrate mono hydrate,



The tartrate precursor was prepared using stoichiometric amounts of $\text{NiSO}_4 \cdot 6\text{H}_2\text{O}$ (1.9593 g), $\text{CuSO}_4 \cdot 5\text{H}_2\text{O}$ (0.7110 g) $\text{ZnSO}_4 \cdot 7\text{H}_2\text{O}$ (1.1154 g), and $\text{FeSO}_4 \cdot 7\text{H}_2\text{O}$ (8.1267 g) dissolved in 100 mL double distilled de-ionized water. The solution was placed in a three-necked round bottom flask under a stream of dry nitrogen atmosphere and the solution was stirred on amagnetic stirrer with a hot plate. Then, the pH was adjusted to about 5.90 with dilute H_2SO_4 . To this diammonium tartrate solution (8.7468 g dissolved in 40 mL double distilled water) was added drop by drop with stirring till a permanent precipitate occurred. Then acetone was added in equal amounts to get a more homogeneous, stoichiometric, fine-grained precursor powdered, and the resulting solution was digested at 50 °C for 30 minutes. The obtained precipitate was filtered and washed with double-distilled deionized water. The as-synthesized precipitate was air-dried at room temperature. The flow sheet diagram for Nickel-copper-zinc-iron tartrate monohydrate and subsequent conversion to

nanosized doped inverse spinel ferrites is depicted in Fig. S1 of the supplementary information file.

A similar procedure was used for the synthesis of (a) undoped nickel-iron and cobalt-iron tartrate, (b) Cadmium-cobalt-iron tartrate one and half hydrate ($\text{Cd}_{0.1}\text{Co}_{0.9}\text{Fe}_2(\text{C}_4\text{H}_4\text{O}_6)_3 \cdot 1.5\text{H}_2\text{O}$), (c) Aluminium-cobalt-iron succinate seven hydrate ($\text{Al}_{0.3}\text{CoFe}_{1.7}(\text{C}_4\text{H}_4\text{O}_4)_3 \cdot 7\text{H}_2\text{O}$), (d) Cobalt-ruthenium-iron tartrate mono hydrate ($\text{CoRu}_{0.04}\text{Fe}_{1.96}(\text{C}_4\text{H}_4\text{O}_6)_3 \cdot \text{H}_2\text{O}$) by taking the stoichiometric amount of respective salts.

2.1.2 γ -Ferric-nickel oxy-hydroxide, ($\gamma\text{-Fe}_{0.96}\text{Ni}_{0.04}\text{O}(\text{OH})$)

The preparation of gamma-Ferric-Nickel oxy-hydroxide in a definite morphology is achieved by gas-liquid-solid phase reaction involving the oxidation of precipitated ferrous-nickel hydroxide by air.^[22]

0.347g of iron metal powder was dissolved in 3mL of concentrated hydrochloric acid in a three-neck flask under the nitrogen atmosphere and evaporated slowly to obtain a green ferrous chloride. It was then dissolved in distilled water to make the volume 250 mL giving a 0.025M FeCl_2 solution. From this, take 150 mL FeCl_2 solution was mixed with 0.0446 g $\text{NiCl}_2 \cdot 6\text{H}_2\text{O}$ and 100mL ammonium chloride solution (0.1M) and was introduced into a 500 mL three-neck flask. The solution was maintained at 50 °C. Air was introduced into the mixture at a rate of 500 mL min^{-1} . The hydrogen ion concentration of the solution was maintained at pH 6.00 by adding aqueous ammonia (0.1 M) drop wise from a separatory funnel. An addition of about 130 mL of aqueous ammonia (0.1M) during 2 h was required for the completion of the reaction. The yellowish-brown precipitate of γ -ferric oxy-hydroxide containing nickel was filtered through Whatman filter paper No.42 and washed thoroughly with distilled water till free from chloride. It was air-dried at the ambient temperature.

The same procedure was used for the synthesis of undoped gamma ferric oxide by taking 150 mL FeCl_2 (0.025M) and 100 mL ammonium chloride (0.1M). Then add drop by drop 130 mL NH_4OH (0.1 M) over two h.

2.2 Synthesis of nanosized doped spinel ferrites

The above undoped and doped precursors except gamma ferric oxi hydroxide were calcined slowly at 700 °C for two hours in a platinum crucible under a normal air atmosphere. This sample was then reground and recalcined at the same temperature for another 2h. The obtainable doped spinel ferrites such as $\text{Ni}_{0.6}\text{Cu}_{0.2}\text{Zn}_{0.2}\text{Fe}_2\text{O}_4$, $\text{Cd}_{0.1}\text{Co}_{0.9}\text{Fe}_2\text{O}_4$, $\text{Al}_{0.3}\text{CoFe}_{1.7}\text{O}_4$, $\text{CoRu}_{0.04}\text{Fe}_{1.96}\text{O}_4$ and undoped samples such as NiFe_2O_4 and CoFe_2O_4 were restored in a desiccator.

The nickel-containing gamma ferric oxy-hydroxide and undoped gamma ferric oxy-hydroxide (γ FeOOH) was placed in a platinum boat and kept in a tubular furnace. The sample was heated at a constant temperature of 250 °C in the air. After one hour, the sample was reground and reheated at the same temperature yielding reddish-brown nickel doped and undoped gamma ferric oxide.

2.3 Characterization Technique

Precursors were characterized at the first stage of carbon and hydrogen by the microanalytical technique. The composition of metals in the precursors and doped spinel ferrites was carried out by inductively coupled plasma spectrometer (ICPES) (ICP-AES instrument ARCOS from M/S. Spectro Germany) and Energy dispersive X-ray analysis (EDS) on PHILIPS XL 30 CP instrument. The infrared spectra of compounds were carried out with Perkin-Elmer 1600 series FTIR spectrophotometer on KBR pellets. The thermal behavior (TGA and DTA) of the precursors was conducted on Mettler Toledo 850 instrument. The crystal structure was characterized by X-ray diffraction (XRD) carried out using a Siemens D 500 diffractometer with $\text{CuK}\alpha$ radiation ($\lambda = 1.5418 \text{ \AA}$ and $\theta = 20 - 80^\circ$) at room temperature. Philips 30 XL FEG scanning electron microscope (SEM) was used to examine the surface morphology and particle size distribution of prepared doped spinel ferrites. The morphology and the size of resultant powders were obtained by Transmission electron microscopy (TEM) and corresponding selected area electron diffraction (SAED) pattern on a JEOL-2010 transmission electron microscope, operating at an accelerating voltage of 208 kV. (The TEM specimen of doped spinel ferrites was prepared from the dispersed by dispersing in 2-propanol and ultrasonicated. Then, one or two drops of the mixed solution were cast on an amorphous carbon film-coated copper TEM grid). The electrical conductivity, Seebeck voltage (*i.e.* thermoelectric voltage), and Hall effect measurements were performed similarly to describe in the literature.^[12,23] For Seebeck voltage measurements, the sample in the form of a pellet of 10 mm thickness was pressed between two platinum discs fixed at the ends of two ceramic blocks. One of these blocks was spring-loaded two obtained good pressure contact. This sample holder along with the sample was placed in a constant temperature zone of a furnace, whose temperature was held to within $\pm 1^\circ\text{C}$. The temperature of the ends of the sample was measured with chrome-alumini thermocouples, placed in such a way as to touch the sample ends. These junctions were as to touch the sample ends. These junctions were insulated from platinum disks and ceramic blocks by means of thin mica sheets. During the measurements, the

sample was equilibrated at each temperature for about 10 mins. Temperature differences of 2 to 20°C were used along the sample. The thermoelectric voltage (or Seebeck voltage) developed across the sample and the temperature of the sample ends were read on a Philips PP 9004 micro voltmeter. A set of the values of thermoelectric voltage at various temperatures thus obtained ($\mu\text{V K}^{-1}$) was plotted against the respective absolute temperatures, T (K). The predominant charge carriers in a temperature gradient diffuse towards the cold end of the sample. The sign of the probe at the lower temperature is the sign of the Seebeck voltage or thermoelectric voltage. The dielectric measurement was carried out at room temperature using HIOKI model 3532-50 LCR Hi Tester (frequency range from 100 Hz to 5 MHz).

The magnetic behavior of the samples was investigated using a SQUID magnetometer (Quantum Design MPMS-55). The sample magnetization was carried out in a field of 100 Oe on warming through the temperature range $5 < T \text{ (K)} < 325$ after cooling the sample both in the measuring field (field cooling-FC) and in the absence of an applied field (zero-field cooling - ZFC). The magnetic hysteresis measurement was also studied at room temperature by using a vibrating sample magnetometer (PAREG and G model no.4508) with an applied field up to 20 k Oe. The saturation magnetization (M_s) and coercivity were determined from the hysteresis loop.

3. Results and discussion

3.1 Characterization of precursors

Mixed metal tartrate/succinate and hydroxide precursors were obtained by the reaction of stoichiometric respective metal salt in an aqueous solution with slow addition of 3% ammonium dicarboxylate or ammonium hydroxide. The optimum conditions such as the pH, solution temperature, precipitate age time, and stirring were chosen. Similarly, for stoichiometric precipitation of tartrate or succinate precursors along with an equal amount of distilled acetone, digested for half an hour to get the complete precipitation under controlled stirring. The composition of the dicarboxylate and hydroxide precursors such as C and H was carried out by a microanalytical technique, while metal analysis was carried out by the inductively coupled plasma spectrometer (ICPES). The observed compositions are summarized in Table T1 of the supplementary information file. They are found to be within $\pm 0.5\%$ of the calculated values. The results showed a close relationship with the nominal compositions of the precursors. The presence of water in the crystallization of these compounds was confirmed based on the thermal analysis curve. These results are also further supplemented by the infrared spectral data.

The infrared spectrums of these precursors (Figures are not shown) showed the band at 3443 cm^{-1} corresponds to the ν (O-H) vibration of water. The width of this band confirms the presence of intramolecular hydrogen bonds in these compounds.

The band at 1750 cm^{-1} in the infrared spectra of d-tartaric acid/succinic acid assigned to ν (C = O) is replaced in the tartrate/succinate complex (*i.e.*, precursor) spectra by the bands; ν_{asy} (OCO) at 1593 cm^{-1} and ν_{sy} (C = O) at $1415 - 1367\text{ cm}^{-1}$. The presence of these two bands in the infrared spectra for tartrate/succinate precursor suggests the coordination of both COO^- groups present in the tartaric acid/succinic acid molecule to the metallic ions. Infrared spectral analysis showed bidentate linkage to be more favorable for tartrate/succinate precursor due to the difference between the stretching vibration of antisymmetric and symmetric (C = O) groups. The infrared spectra in the range $1177 - 1001\text{ cm}^{-1}$ do not show any significant differences between tartaric acid / succinic acid and the mixed-metal complexes (*i.e.*, precursor). From these, it concludes that there is no bonding with the free C – OH group to the metal in a solid state.^[24] Other bands, which are all combination bands, may be assigned to the different normal modes of vibrations of the carboxylate group. The ν (M – O) vibrations have been identified for these precursors. Water molecules present in all precursors constitute only water of hydration and do not coordinate with the metal ions. These dicarboxylate/hydroxide precursors have a magnetic moment (by Faraday's Technique) in the range of 6.78 to 9.17 B.M. for all precursors (see Table T1 of supplementary information file). These magnetic moments (μ) at room temperature showed slightly less value than the theoretical ones in all compounds. These differences may be due to the antiferromagnetic interaction between the odd electrons of two or more paramagnetic metallic ions. All the precursors were isolated as a powder and not as a single crystal, meaning that no complete structural determination can be made. However, the infrared spectrum and magnetic susceptibility measurements suggested a chain-like polymeric octahedral structure of the precursors.^[25]

The TGA and DTA curve for tartrate/succinate and hydroxide precursors such as (a) $\text{Ni}_{0.6}\text{Cu}_{0.2}\text{Zn}_{0.2}\text{Fe}_2(\text{C}_4\text{H}_4\text{O}_6)_3 \cdot \text{H}_2\text{O}$, (b) $\text{Co}_{0.9}\text{Cd}_{0.1}\text{Fe}_2(\text{C}_4\text{H}_4\text{O}_6)_3 \cdot 1.5\text{H}_2\text{O}$, (c) $\text{Al}_{0.3}\text{CoFe}_{1.7}(\text{C}_4\text{H}_4\text{O}_4)_3 \cdot 7\text{H}_2\text{O}$, (d) $\text{CoRu}_{0.04}\text{Fe}_{1.96}(\text{C}_4\text{H}_4\text{O}_6)_3 \cdot \text{H}_2\text{O}$, (e) $\gamma\text{-Fe}_{0.96}\text{Ni}_{0.04}\text{O}(\text{OH})$ were recorded under normal air atmosphere and is shown in Fig. S2 of the supplementary information file. The representative of TGA and DTA curve for $\text{Ni}_{0.6}\text{Cu}_{0.2}\text{Zn}_{0.2}\text{Fe}_2(\text{C}_4\text{H}_4\text{O}_6)_3 \cdot \text{H}_2\text{O}$ is shown here in Fig. 1. The dehydration of this precursor can be detected on the DTA curve at $\sim 150^\circ\text{C}$.

The TGA curve shows weight loss for dehydration step up to 180°C corresponds to the loss of all water molecules (see eq. 1). The isothermal heating of the sample under normal air at 160°C , the infrared spectrum showed the absence of the –OH band and a considerable decrease in the intensity as compared to parent tartrate precursor. The observed mass loss and corresponding temperature ranges are shown in Table T2 of the supplementary information file. The oxidative decomposition of these precursors was indicated by the presence of strong and broad exothermic peaks on the DTA curve at around 250°C corresponds to the formation of the final oxide. The TGA curve showed one-step weight loss in the temperature range of $180 - 500^\circ\text{C}$, corresponding to the formation of Cu-Zn codoped nickel ferrite (see Table T2). In the isothermally heated sample at around 400°C , the infrared spectrum showed a band at 2365 cm^{-1} , indicating the presence of entrapped carbon dioxide, *i.e.*, adsorbed CO_2 is present in the final residue (see Eq. 2). The powdered XRD gave a slightly broad peak at a similar position of nickel ferrite. This entrapped CO_2 can be removed by heating the residue at 700°C for 2hr (see Eq. 3).

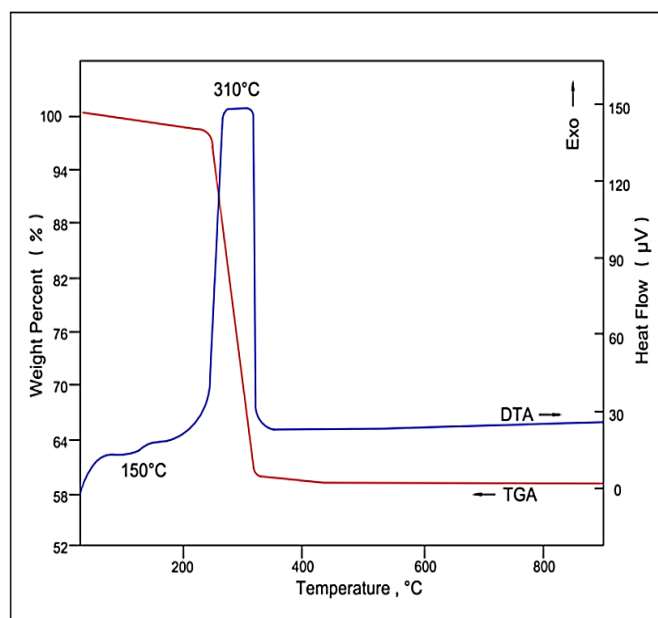
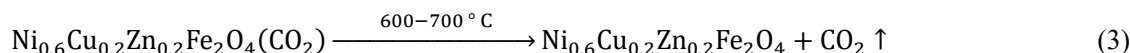
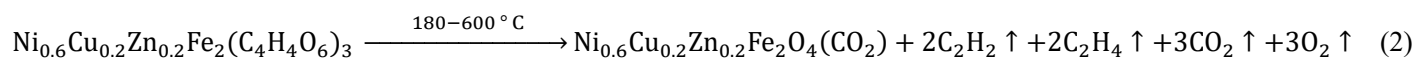
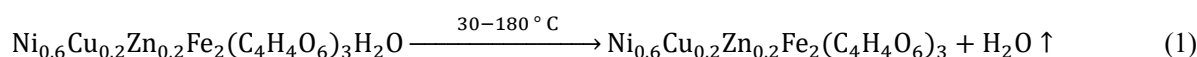


Fig. 1 TGA and DTA curves for nickel-copper-zinc-iron tartrate monohydrate, $\text{Ni}_{0.6}\text{Cu}_{0.2}\text{Zn}_{0.2}\text{Fe}_2(\text{C}_4\text{H}_4\text{O}_6)_3 \cdot \text{H}_2\text{O}$.

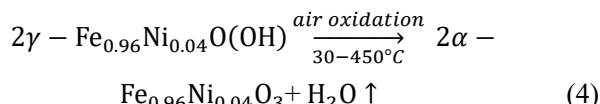
The gaseous product obtained by the thermal decomposition of this precursor was analyzed by qualitative gas detection method. The detailed detection procedure for CO , CO_2 , C_2H_4 , and C_2H_2 was reported elsewhere.^[26] On the basis of TGA/DTA and complimentary measurement (IR and XRD), the following thermal decomposition pathways of this studied compound may be assumed as follows:

(a) Nickel – copper – zinc – iron tartrate precursor.



A similar thermal decomposition reaction is observed for cobalt–cadmium–iron tartrate, aluminum–cobalt–iron succinate, and cobalt–ruthenium–iron tartrate in a normal air atmosphere.

(b) γ -Ferric–nickel oxyhydroxide



It should be noted here that the γ -phase is obtained at 250 °C and then it is converted to an α -phase above 450 °C.

3.2 Characterization of doped spinel ferrites

3.2.1 Compositional analysis

The composition of doped inverse spinel ferrites such as (a) $\text{Ni}_{0.6}\text{Cu}_{0.2}\text{Zn}_{0.2}\text{Fe}_2\text{O}_4$, (b) $\text{Co}_{0.9}\text{Cd}_{0.1}\text{Fe}_2\text{O}_4$, (c) $\text{Al}_{0.3}\text{CoFe}_{1.7}\text{O}_4$, (d) $\text{CoRu}_{0.04}\text{Fe}_{1.96}\text{O}_4$, and (e) $\text{Fe}_{2.55}\text{Ni}_{0.12}\square_{0.33}\text{O}_4$ was determined by ICPES and EDS analysis. The calculated and observed compositions of elements are summarized in Table 1. The proportion of ingredient elements showed that the weight proportions were correct in the final product.

To see the presence of any impurity element in the sample, we have performed an Energy dispersive X-ray (EDS)

spectroscopy measurement. The EDS studies excluded the presence of any impurity element in all samples. Energy dispersive X-ray analysis. (EDS) spectra (Fig. 2) in all doped ferrites confirmed the presence of the intended substituent’s (dopants) species within the lattice of each crystal examined, and the dopant peak heights relative to those parent elements varied in the correct sense according to the concentration of dopant expected by the nominal composition.

X-ray diffraction pattern (XRD) of all samples such as $\text{Ni}_{0.6}\text{Cu}_{0.2}\text{Zn}_{0.2}\text{Fe}_2\text{O}_4$, $\text{Co}_{0.9}\text{Cd}_{0.1}\text{Fe}_2\text{O}_4$, $\text{Al}_{0.3}\text{CoFe}_{1.7}\text{O}_4$, $\text{CoRu}_{0.04}\text{Fe}_{1.96}\text{O}_4$ and $\text{Fe}_{2.55}\text{Ni}_{0.12}\square_{0.33}\text{O}_4$ (*i.e.* nickel doped gamma ferric oxide) are presented in Fig. 3. There is an excellent agreement of observed XRD with the standard JCPDS (File No. 10-325, 21-045, 39-1346) pattern confirming the monophasic spinel structure of these doped ferrites.^[27-30] The X-ray diffraction peaks are found to be broad, and it is attributed to the nanosized of these spinels. The XRD peaks for these doped spinel ferrites appear approximately at the same position as the respective undoped spinel ferrites but with a slight difference in intensity. The hkl values assigned to the peaks in the XRD are shown in Fig. 3. The observed d-spacing values and relative intensities were compared with

Table 1. Observed ICPES and EDS analysis of nanosized doped spinel ferrites.

Compounds	Elemental analysis in wt % (± 0.5)							
	Req	Found	Req	Found	Req	Found	Req	Found
	Fe		Ni		Cu		Zn	
$\text{Ni}_{0.6}\text{Cu}_{0.2}\text{Zn}_{0.2}\text{Fe}_2\text{O}_4$	47.19	47.89 (47.81)*	14.88	15.05 (14.22)	5.37	4.93 (5.16)	5.53	5.85 (5.31)
NiFe_2O_4	47.65	47.80	25.04	24.91	--	--	--	--
	Fe		Co		Cd		--	--
$\text{Co}_{0.9}\text{Cd}_{0.1}\text{Fe}_2\text{O}_4$	46.54	46.72 (46.33)	22.10	21.91 (22.28)	4.68	4.34 (4.47)	--	--
CoFe_2O_4	47.60	47.51	25.11	25.01	--	--	--	--
	Fe		Al		Co		--	--
$\text{Al}_{0.3}\text{CoFe}_{1.7}\text{O}_4$	39.49	40.13 (39.37)	3.58	3.71 (3.31)	28.65	28.74 (29.15)	--	--
	Fe		Co		Ru		--	--
$\text{CoRu}_{0.04}\text{Fe}_{1.96}\text{O}_4$	46.29	45.74 (45.95)	24.93	25.04 (24.89)	1.71	1.52 (1.61)	--	--
	Fe		Ni		--	--	--	--
$\text{Fe}_{2.55}\text{Ni}_{0.12}\square_{0.33}\text{O}_4$	66.72	66.80 (66.59)	3.30	3.26 (3.33)	--	--	--	--
$\text{Fe}_{2.67}\square_{0.33}\text{O}_4$	69.97	69.71	--	--	--	--	--	--

* The figures in parenthesis indicate metal analysis obtained from the EDS method.

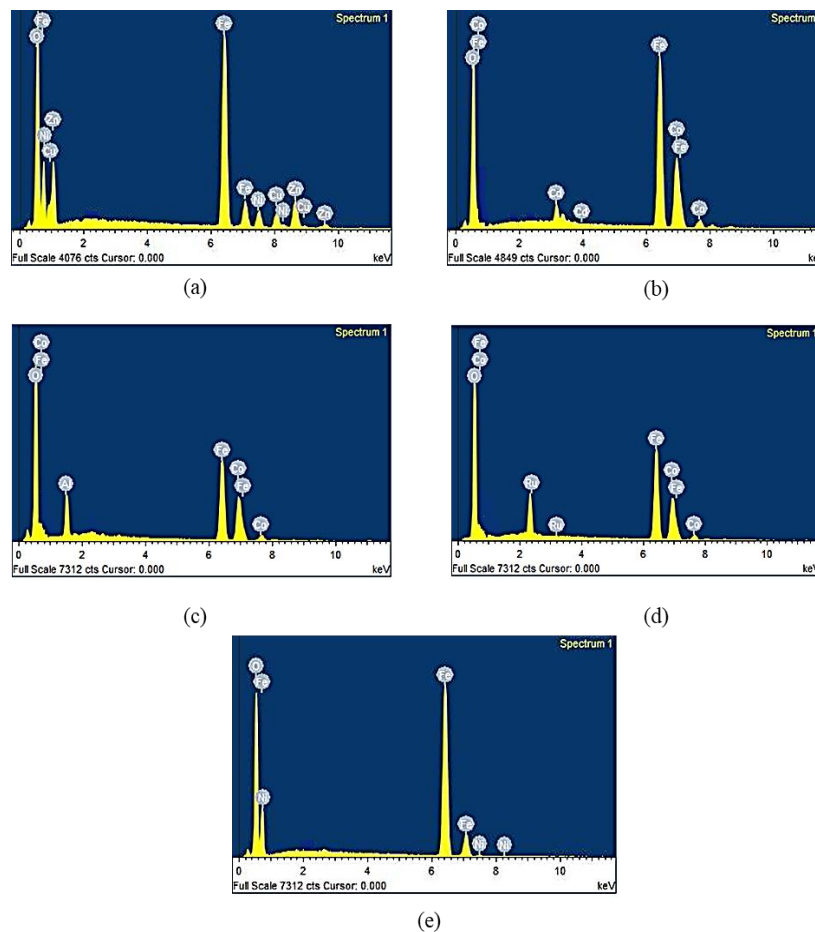


Fig. 2 Energy dispersive X-ray spectrum (EDS) of nanosized doped spinel ferrites.(a) $\text{Ni}_{0.6}\text{Cu}_{0.2}\text{Zn}_{0.2}\text{Fe}_2\text{O}_4$ (b) $\text{Cd}_{0.1}\text{Co}_{0.9}\text{Fe}_2\text{O}_4$ (c) $\text{Al}_{0.3}\text{CoFe}_{1.7}\text{O}_4$ (d) $\text{CoRu}_{0.04}\text{Fe}_{1.96}\text{O}_4$ (e) $\text{Fe}_{2.55}\text{Ni}_{0.12}\square_{0.33}\text{O}_4$.

those reported in the literature.^[27-30] The lattice parameters have been determined using the relation, $a = d\sqrt{h^2 + K^2 + l^2}$, where d is the inter planer spacing of the diffraction peak and hkl denotes the Miller indices of the corresponding peaks.

The lattice parameter is given in Table 2. The observed lattice constant of respective undoped spinel ferrites is comparable to the literature.^[11,12,17] It can also be seen from these tables, the lattice constant increases appreciably with the dopants as compared to respective undoped spinel ferrites (see Table 2). This can be explained based on the relative sizes of ionic radii of different substituent ions, which are relatively larger than that of Fe^{3+} ions. Replacement of slightly larger dopant cations for smaller Fe^{3+} cations in the prepared spinel ferrites causes an increase in lattice parameters. There is a correlation between the lattice parameter value and the $\text{M}-\text{O}$ distance for a particular site in the spinel structure which can directly be correlated to the fraction of every type of Co^{2+} , Fe^{3+} , and substitute cations among these sites.^[31]

The XRD line width and particle size are connected through the Scherrer equation.^[32] The crystallite size $\langle D \rangle_{\text{X-ray}} = 0.9\lambda / \beta \cdot \cos\theta$ with $\beta^2 = \beta_a^2 - \beta_b^2$, where $\langle D \rangle_{\text{X-ray}}$ is the

crystallite diameter, λ is the wavelength of the X-ray radiation, β is the measure of the broadening of diffraction peak due to size effect, β_a and β_b are the full-width at half-maximum of the XRD line of the sample and θ is the Bragg's angle. Using this relation, the observed mean values of the crystallite size $\langle D \rangle_{\text{X-ray}}$ are depicted in Table 2. As can be seen from Table 2, the mean crystallite size of substituted ferrites is in the range of 18.42 to 34.74 nm indicating the nanosized nature of the samples. The X-ray density of all compounds was determined using the formula $D_X = 8M / Na^3$, where 'M' is the molecular weight, 'N' is Avogadro's number, and 'a' is the lattice parameters. Also, the porosity of the samples was calculated using the relation $P = (1 - D / D_X)$, where D and D_X are the apparent density and X-ray density, respectively. The results of X-ray density (D_X), measured apparent density (D), and porosity (P) of doped ferrites are given in Table 2. It can be noticed that the X-ray density of each sample is higher than the corresponding apparent density of samples. This may be due to the existence of pores, which were formed and developed during sample preparation. Another reason for the presence of porosity may be the creation of more oxygen

Table 2. X-ray diffraction data, particulate properties, and infrared spectral data of nanosized doped spinel ferrites.

Compounds	Lattice constant 'a' nm	Unit cell volume (nm ³)	Mean crystallite size <D> _x -Ray nm ±10%	X-Ray density D _x (g.cm ⁻³)	Apparent density D (g.cm ⁻³)	Porosity P=1-D/D _x	Average particle size (from histogram) (nm)	Average particle size (from TEM) (nm)	Infrared spectral absorption band cm ⁻¹	
									v ₁	v ₂
Ni _{0.6} Cu _{0.2} Zn _{0.2} Fe ₂ O ₄	0.838	0.588	34.74	5.357	0.75	0.861	47	42	590	405
NiFe ₂ O ₄	0.832	--	--	--	--	--	--	--	600	410
Co _{0.9} Cd _{0.1} Fe ₂ O ₄	0.840	0.593	33.81	5.498	0.805	0.854	52	55	601	410
CoFe ₂ O ₄	0.835	--	--	--	--	--	--	--	606	417
Al _{0.3} CoFe _{1.7} O ₄	0.837	0.586	27.53	5.192	0.649	0.988	37	34	611	418
CoRu _{0.04} Fe _{1.96} O ₄	0.839	0.591	30.87	5.297	0.796	0.850	33	29	611	414
									435	
Fe _{2.55} Ni _{0.12} □ _{0.33} O ₄	0.837	0.586	18.42	4.874	0.926	0.810	18	20	543	(shoulder at 472)
Fe _{2.67} □ _{0.33} O ₄	0.834	--	--	--	--	--	--	--	550	443

vacancies (as required by the charge balance) in the doped samples as compared to undoped samples, and as a result, fewer cations are created in the system.^[33]

Microstructure plays an important role in obtaining the desired electric and magnetic particles of these materials for their microwave absorption applications. The microstructure and morphology of Ni_{0.6}Cu_{0.2}Zn_{0.2}Fe₂O₄, Co_{0.9}Cd_{0.1}Fe₂O₄, Al_{0.3}CoFe_{1.7}O₄, CoRu_{0.04}Fe_{1.96}O₄, and Fe_{2.55}Ni_{0.12}□_{0.33}O₄

samples were observed by scanning electron microscopy (SEM), as shown in Fig. 4. As it can be seen from the figure (a-d), the obtained nanoparticles get interlocked with each other to form a cluster. However, close observation shows the agglomerates of nearly spherical particles. The SEM image of the Fe_{2.55}Ni_{0.12}□_{0.33}O₄ sample indicates that the morphology is characterized by an acicular shape of particles and agglomerated due to the magnetic interaction (see Fig. 4 (e)).

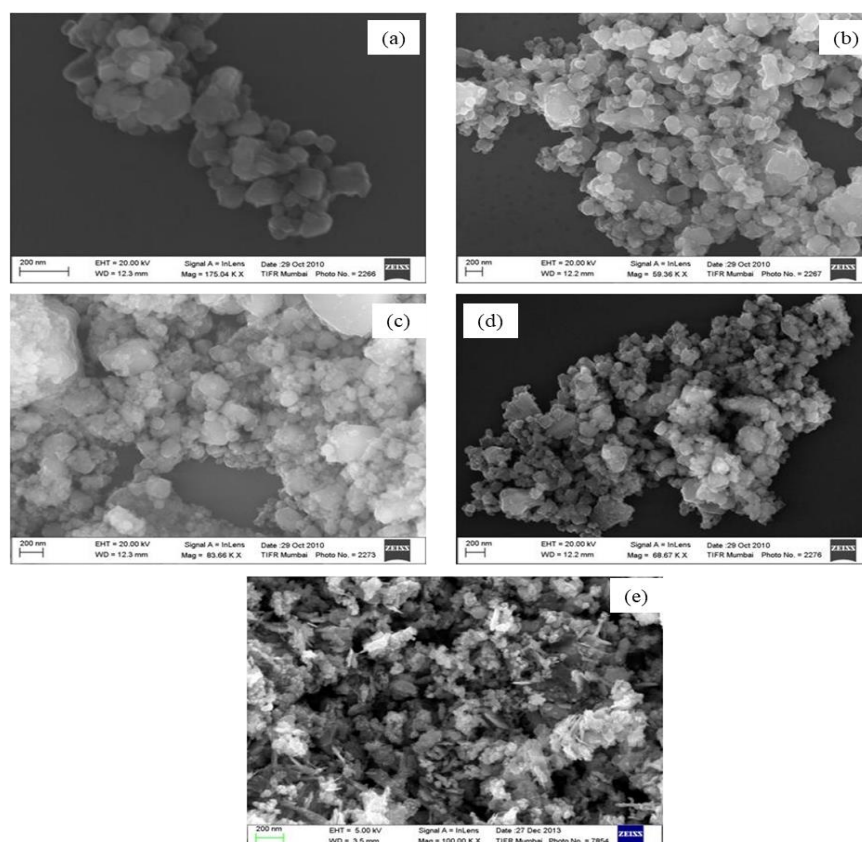


Fig. 4 Scanning electron micrographs (SEM) of nanosized doped spinel ferrites. (a) Ni_{0.6}Cu_{0.2}Zn_{0.2}Fe₂O₄, (b) Cd_{0.1}Co_{0.9}Fe₂O₄, (c) Al_{0.3}CoFe_{1.7}O₄, (d) CoRu_{0.04}Fe_{1.96}O₄, (e) Fe_{2.55}Ni_{0.12}□_{0.33}O₄.

Domain wall exists when grain size in the obtained spinel ferrites and grain size of these ferrites powder in the matrix become larger (*i.e.*, samples were coated by a gold thin film by using a sputtering technique, before observation in SEM) than critical grain size (D_c) is given by the following expression.^[34]

$$D_c = 18 \mu_0 \sigma_w / M_s^2 \quad (5)$$

where σ_w is the domain wall and M_s is the saturation magnetization of the sample. So, the magnetic loss (μ_0) due to displacement of the domain wall is added to magnetic losses.

The histogram of the particle size was drawn and has been shown in Fig. 5. The average size of all doped spinel ferrite ranges between 18nm and 52nm as per histogram obtained from SEM (see Table 2). The morphology of the particles formed was examined by transmission electron microscopy (TEM) for these doped spinel ferrites. The micrographs (TEM) and SAED patterns of all samples are given in Fig. 6. The variation of particle size is predominantly seen for these ferrites. TEM images of these doped spinel ferrites (Fig. 6(a)

(e)) show the grains to be in the nanometer size range, indicating the nanocrystalline nature of the compounds. The average grain sizes, measured by taking around 10 - 15 grains during the measurement stage, are found to be 20 to 55 nm range. The average particle sizes of these powders are given in Table 2. The grain shape of all samples is roughly spherical and not highly agglomerated (see Fig. 6(a)' to (e)'). The structural information from the selected area electron diffraction (SAED) pattern Fig. 6(a) - (e) shows the crystalline nature. It is apparent that all these lattice planes are clearly distinct in the SAED pattern (see Fig. 6(a)' to (e)'). The reflections correspond to (311), (511), and (440) lattice planes, which are also signatures of an FCC spinel phase. These values were indexed to the single-phase cubic structure of the doped inverse spinel ferrites. In addition, it may be noted that the High-Resolution Transmission Electron Microscopy (HRTEM) of semiconductor oxide reported in the literature^[35] could indicate the presence of lattice distinct fringes and confirming the nanocrystalline nature and good crystallinity.

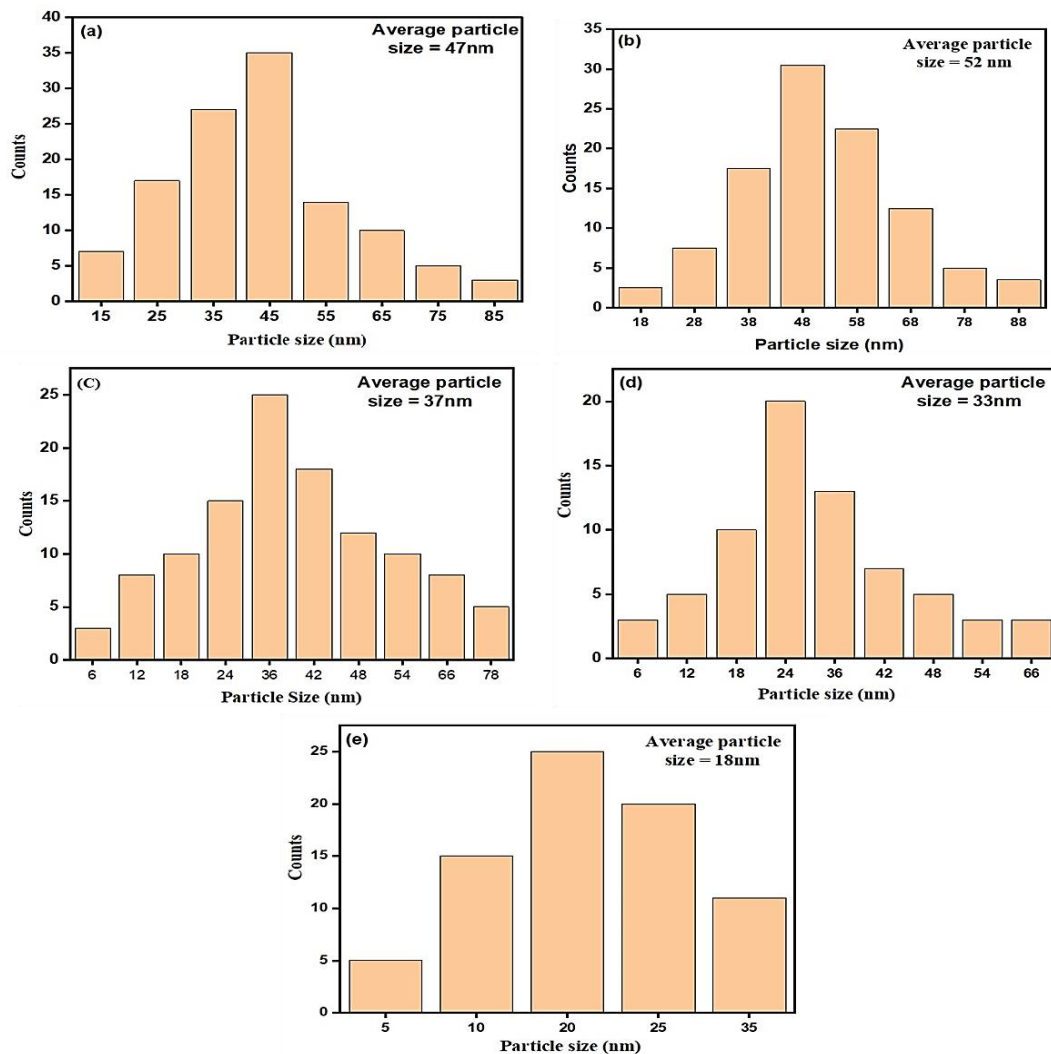


Fig. 5 Histogram of the particle size distribution for doped spinel ferrites. (a) Ni_{0.6}Cu_{0.2}Zn_{0.2}Fe₂O₄, (b) Co_{0.9}Cd_{0.1}Fe₂O₄, (c) Al_{0.3}CoFe_{1.7}O₄, (d) CoRu_{0.04}Fe_{1.96}O₄ (e) Fe_{2.55}Ni_{0.12}□_{0.33}O₄.

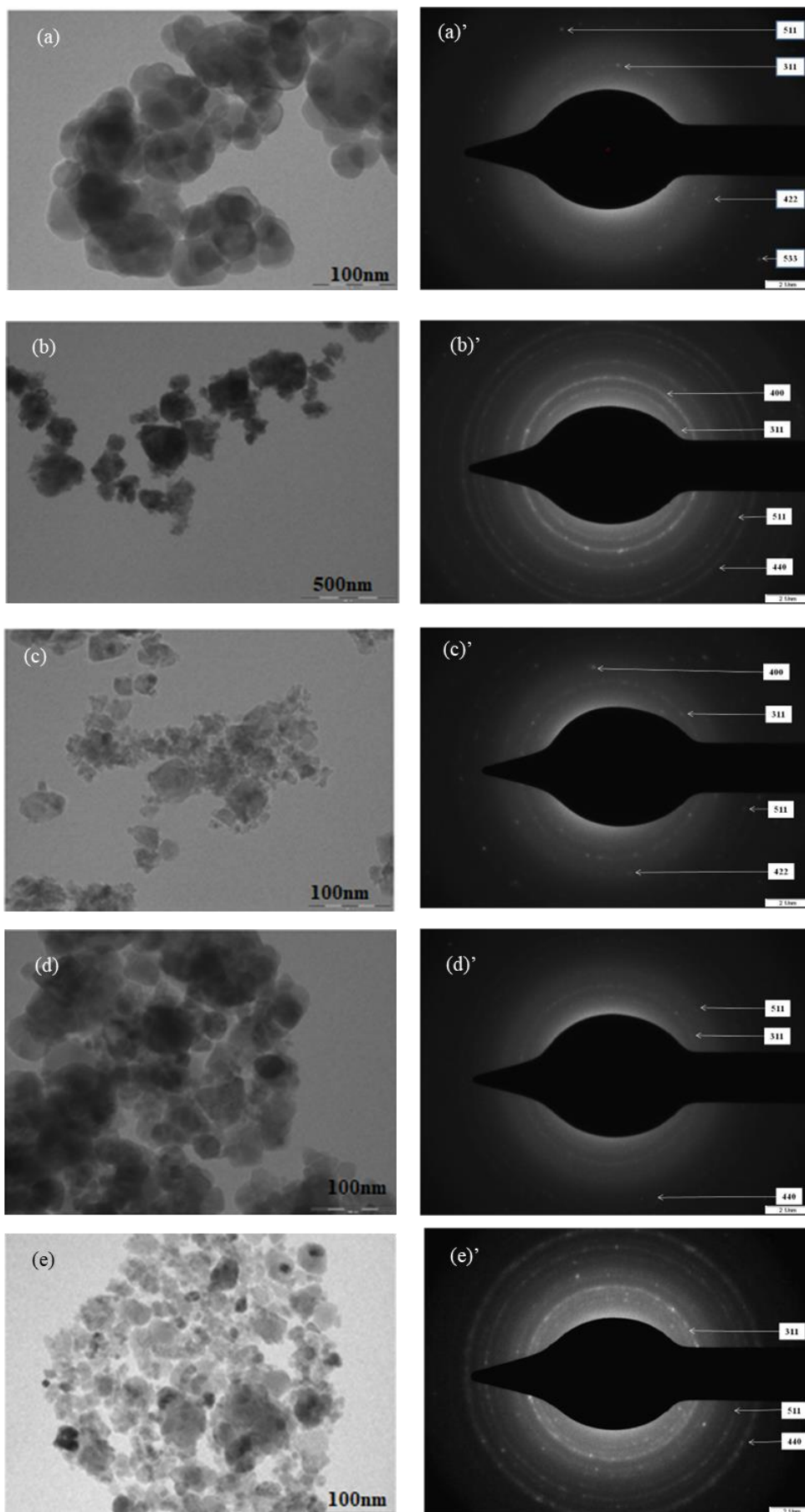


Fig. 6 Transmission electron micrographs (TEM) and Selected area electron diffraction (SAED) pattern of nanosized doped spinel ferrites. (a) $Ni_{0.6}Cu_{0.2}Zn_{0.2}Fe_2O_4$, (b) $Cd_{0.1}Co_{0.9}Fe_2O_4$, (c) $Al_{0.3}CoFe_{1.7}O_4$, (d) $CoRu_{0.04}Fe_{1.96}O_4$, (e) $Fe_{2.55}Ni_{0.12}\square_{0.33}O_4$.

The infrared spectra of investigated doped ferrites viz. $\text{Ni}_{0.6}\text{Cu}_{0.2}\text{Zn}_{0.2}\text{Fe}_2\text{O}_4$, $\text{Co}_{0.9}\text{Cd}_{0.1}\text{Fe}_2\text{O}_4$, $\text{Al}_{0.3}\text{CoFe}_{1.7}\text{O}_4$, $\text{CoRu}_{0.04}\text{Fe}_{1.96}\text{O}_4$ and $\gamma\text{-Fe}_{2.55}\text{Ni}_{0.12}\square_{0.33}\text{O}_4$ showed somewhat broad bands ν_1 at $\sim 590\text{ cm}^{-1}$ and ν_2 at 405 cm^{-1} (see Fig. 7). The ν_1 and ν_2 bands are assigned to intrinsic vibrations of tetrahedral and octahedral groups respectively.^[36] The infrared bands for all samples under investigation are given in Table 2. It can be seen that the frequencies ν_1 and ν_2 are shifted slightly to the lower frequency side on doping as compared to respective undoped spinel ferrite. A very small change is observed in the absorption band for doped samples, which may be due to the differences in the microstructures. The observed band position for all doped ferrites is at high-frequency band ν_1 ranging from 543 to 611 cm^{-1} , and the lower ν_2 band is in the range from 405 to 435 cm^{-1} . This difference is expected because of the difference in the $\text{Fe}^{3+} - \text{O}^{2-}$ distances for octahedral and tetrahedral complexes. The splitting in ν_2 is evidence of a contribution of Fe^{2+} on the octahedral sites, and the ferrite becomes normal ν_1 and ν_2 depending on the nature of the octahedral cations and less on the tetrahedral ions.

Thus, splitting of ν_1 and ν_2 into the shoulder has not been observed in the present doped compounds, except $\gamma\text{-Fe}_{2.55}\text{Ni}_{0.12}\square_{0.33}\text{O}_4$ compound, which also confirms the absence of excessive Fe^{2+} ions. While $\gamma\text{-Fe}_{2.55}\text{Ni}_{0.12}\square_{0.33}\text{O}_4$ (*i.e.*, nickel doped gamma ferric oxide) compound showed splitting of ν_2 into the shoulder (at 472 cm^{-1}), which shows the presence of Fe^{2+} ions at the octahedral site (see Fig. 7).

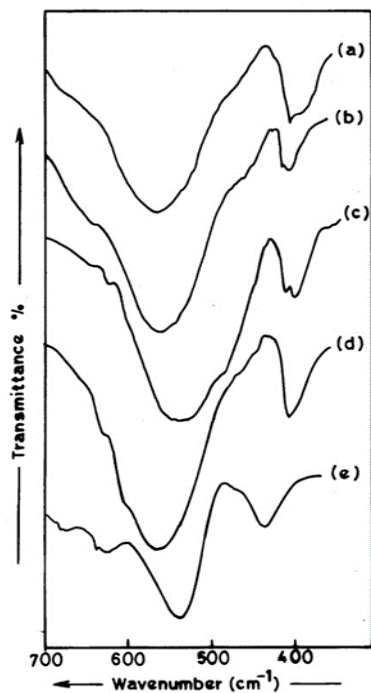


Fig. 7 Infrared spectra of nanosized doped spinel ferrites. (a) $\text{Ni}_{0.6}\text{Cu}_{0.2}\text{Zn}_{0.2}\text{Fe}_2\text{O}_4$, (b) $\text{Co}_{0.9}\text{Cd}_{0.1}\text{Fe}_2\text{O}_4$, (c) $\text{Al}_{0.3}\text{CoFe}_{1.7}\text{O}_4$, (d) $\text{CoRu}_{0.04}\text{Fe}_{1.96}\text{O}_4$ (e) $\text{Fe}_{2.55}\text{Ni}_{0.12}\square_{0.33}\text{O}_4$.

3.2.3 Electrical conductivity studies

The temperature dependence of electrical conductivity, σ , of $\text{Ni}_{0.6}\text{Cu}_{0.2}\text{Zn}_{0.2}\text{Fe}_2\text{O}_4$, $\text{Co}_{0.9}\text{Cd}_{0.1}\text{Fe}_2\text{O}_4$, $\text{Al}_{0.3}\text{CoFe}_{1.7}\text{O}_4$, $\text{CoRu}_{0.04}\text{Fe}_{1.96}\text{O}_4$, and $\text{Fe}_{2.55}\text{Ni}_{0.12}\square_{0.33}\text{O}_4$ compounds is presented in Fig. 8. The experiments are repeated three times, and the results are always found to be reproducible. The plot of $\log \sigma$ against T^{-1} obeys the Arrhenius relation $\sigma = \sigma_0 \exp(-E_a/KT)$, suggesting the semiconducting nature of all doped spinel ferrites, where E_a is the activation energy, σ_0 is temperature-independent constant, K is Boltzmann constant, and T is the absolute temperature. The electrical conductivity ($\log \sigma$) was plotted versus the reciprocal of absolute temperature (T^{-1}). The slope of these lines was considered to give the activation energy E_a for the semiconduction of these doped spinel ferrite compounds. The plot of $\log \sigma$ versus T^{-1} for these doped inverse spinel ferrites (Fig. 8) shows an initial decrease in electric conductivity in the temperature range of 35 to $130\text{ }^\circ\text{C}$. The σ values are then increased, showing two distinct slopes with a ‘break’. The initial decrease in conductivity in the temperature range 345 K to 400 K corresponds to the desorption of adsorbed water molecules, usually adsorbed water molecules behave as electron donors. These figures also show that there are two temperature regions with different activation energies. The temperature at which the break occurs was found to be about 525 K *i.e.*, transition temperature T_c (see Table 3). The break will be most marked for all compounds in which there is a strong exchange interaction between the outer and inner electrons. In addition, a different dopant can be affected by many factors like the nature of the dopant, the number of dopants incorporated, creating structural defects, and changing its microstructures. Therefore, we turn to the magnetic behavior of these compounds. The conductivity does not exhibit much variation with the temperature at region A due to the hopping of defect-related weakly bonded electrons are responsible for conduction, while conduction at high-temperature region B (above T_c) corresponds to the hopping of thermally activated charge carriers in these doped spinel ferrites.

The activation energies (E_a) are calculated for the two regions around breakpoints, firstly for ferrimagnetic (region A) and secondly for the paramagnetic region (region B) applying the above relates to the plot of $\log \sigma$ versus T^{-1} (Fig. 8), and the results are listed in Table 3. From this table, the values of activation energies (E_a) for doped ferrites are appreciably less than the respective undoped spinel ferrite. The activation energy (E_a) in the paramagnetic region is higher than that in the ferrimagnetic region. The observed E_a can be attributed to dopant ions in the present study such as Ni^{2+} , Cu^{2+} , Co^{2+} , Al^{3+} , Ru^{3+} , *etc.* ions that are known to have a strong preference for

Table 3. Electrical conductivity data and Hall effect of nanosized doped spinel ferrites.

Compounds	Temperature corresponding to desorption of adsorbed H ₂ O molecule T (K)	Conductivity measurements			Hall effect measurements					
		Region	Temp. range (K)	Activation energy Ea (ev)	Break temp. (transition temperature) T _c (K)	Current passed (nA)	Resistivity at room temp. Ohm cm	Types of charge carriers	Average Hall coefficient cm ³ /C	Mobility cm ² /Vs
Ni _{0.6} Cu _{0.2} Zn _{0.2} Fe ₂ O ₄	384	A	303-525	0.744	525	-	-	n-Type	-	-
		B	525-805	0.836						
NiFe ₂ O ₄	405	A	300-505	0.801	536	-	-	n-Type	-	-
		B	520-500	0.893						
Co _{0.9} Cd _{0.1} Fe ₂ O ₄	345	A	303-475	0.603	475	20	4.727 x 10 ⁷	n-Type	-1.290 x 10 ¹⁰	273.0
		B	475-825	0.912						
CoFe ₂ O ₄	340	A	305-481	0.713	500	-	-	n-Type	-	-
		B	450-830	0.978						
Al _{0.3} CoFe _{1.7} O ₄	400	A	303-558	0.694	558	20	2.085 x 10 ⁸	n-Type	-6.342x 10 ⁹	30.81
		B	558-750	0.970						
CoRu _{0.04} Fe _{1.96} O ₄	375	A	303-525	0.455	525	20	2.155 x 10 ⁷	n-Type	-9.571x 10 ⁹	444.1
		B	525-805	0.772						
Fe _{2.55} Ni _{0.12} □ _{0.33} O ₄	399	A	303-553	0.692	553	10	5.047 x 10 ⁷	n-Type	-3.399x 10 ⁹	67.35
		B	553-805	1.313						
Fe _{2.67} □ _{0.33} O ₄	380	A	300-545	0.850	--	--	--	n-Type	--	--
		B (α-phase)	550-800	1.350						

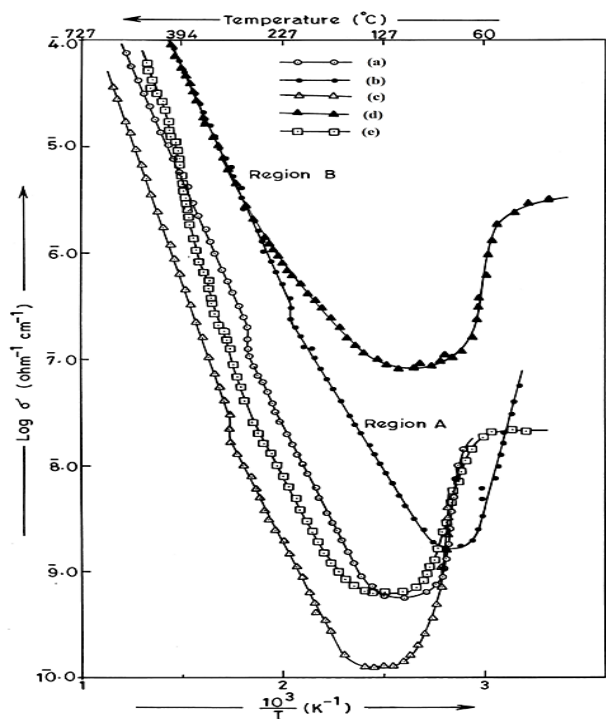


Fig. 8 Plot of log σ against T^{-1} of nanosized doped spinel ferrites. (a) Ni_{0.6}Cu_{0.2}Zn_{0.2}Fe₂O₄, (b) Co_{0.9}Cd_{0.1}Fe₂O₄, (c) Al_{0.3}CoFe_{1.7}O₄, (d) CoRu_{0.04}Fe_{1.96}O₄ (e) Fe_{2.55}Ni_{0.12}□_{0.33}O₄.

octahedral B-site, while Zn²⁺ and Cd²⁺ occupy at tetrahedral A-site. They are all depending on the crystal field stabilization energies of the metal ion.^[37] These dopants may be occupied at

interstitial or vacancy (i.e., point defect) of spinel lattices. Therefore, the conductivity of impurity (dopant) is a favour in the ferrimagnetic region, while the electron hopping in the sublattice between Fe²⁺ → Fe³⁺ ion results in increased activation energy (Ea) in the paramagnetic region. Magensen *et al.*^[38] as shown that dopants with lower valences may also lead to the introduction of vacancies, whereas dopants with higher valences may remove the oxygen vacancies. Apart from the charge state, these dopant ions do not participate in conduction processes but limit the degree of Fe²⁺ - Fe³⁺ condition, which is described by the Verway-deBoer mechanism.^[39] According to this phenomenon, the excess electrons on oxygen then bond with the neighboring Fe³⁺ ions in the spinel lattice due to electrostatic interaction giving rise to Fe²⁺ ions. The overall charge balance is restored by oxygen loss from the sample. The formation of Fe²⁺ ion leads to the deviation from the spinel ferrite stoichiometry.

The Seebeck voltage against temperature measurements for all doped spinel ferrites (Fig. 9) shows an initial fall in the negative charge carrier in the temperature range 325 to 450 K, and the number remains almost constant upto 580 K and then negative Seebeck voltage increases with increasing temperature. While Fe_{2.55}Ni_{0.12}□_{0.33}O₄ sample, the negative Seebeck voltage above 580 K becomes positive and its magnitude increases with increasing temperature upto 750K.

The Seebeck voltage for Ni_{0.6}Cu_{0.2}Zn_{0.2}Fe₂O₄, Co_{0.9}Cd_{0.1}Fe₂O₄, Al_{0.3}CoFe_{1.7}O₄, and CoRu_{0.04}Fe_{1.96}O₄ and

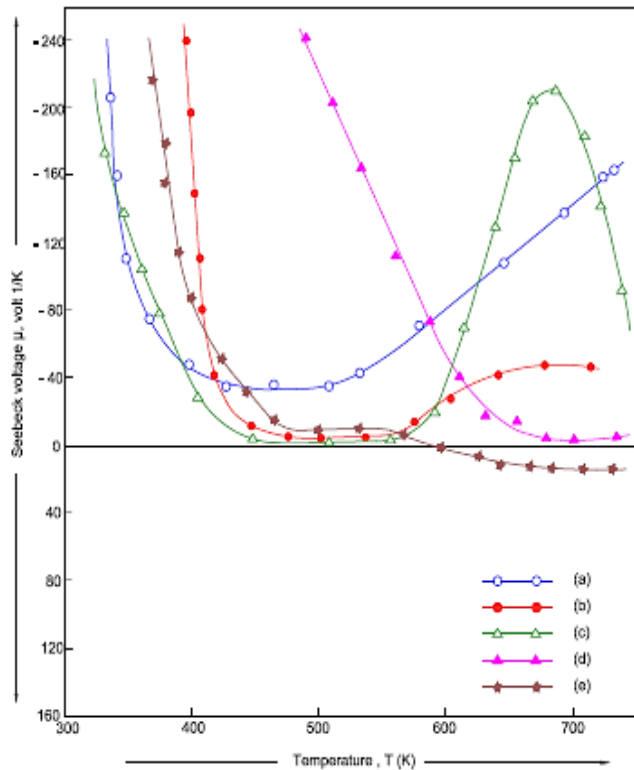


Fig. 9 Plot of Seebeck voltage, μ (volt K^{-1}) against temperature, T (K) for nanosized doped spinel ferrites. (a) $Ni_{0.6}Cu_{0.2}Zn_{0.2}Fe_2O_4$, (b) $Co_{0.9}Cd_{0.1}Fe_2O_4$, (c) $Al_{0.3}CoFe_{1.7}O_4$, (d) $CoRu_{0.04}Fe_{1.96}O_4$ (e) $Fe_{2.55}Ni_{0.12}\square_{0.33}O_4$.

$Fe_{2.55}Ni_{0.12}\square_{0.33}O_4$ samples are n-type semiconductivity. Verwey and deBoer^[39] have established that in oxide spinels containing one ion of variable valence, the conduction takes place by hopping via activation of state involving cation change valence as $Fe^{2+} \leftrightarrow Fe^{3+}$ and vice versa, which leads to electronic conduction of negative charge carrier for samples except for $Fe_{2.55}Ni_{0.12}\square_{0.33}O_4$ sample. In contrast for $Fe_{2.55}Ni_{0.12}\square_{0.33}O_4$ sample above 580 K, showed a hole-mediated conduction mechanism that seems to be dominant *i.e.* p-type semiconductivity. (the presence of an excess of oxygen in this sample provides Ni^{3+} sites which allow motion of holes between Ni^{2+} to Ni^{3+} ions by a thermally activated process in the system). So the low Seebeck values for $Fe_{2.55}Ni_{0.12}\square_{0.33}O_4$ sample may be due to electron-hole compensation.

These studies, also measured the Hall effect constantly in the magnetic field of 0.54 T at room temperature after passing current in nano Ampere. These results are listed in Table 3 for all doped samples except $Ni_{0.6}Cu_{0.2}Zn_{0.2}Fe_2O_4$, which do not show Hall constant values because of high resistivity. The high resistivity was found due to the small value of charge mobility and the increase in B – the site hopping length of this sample. The specific resistivity values were observed for all doped inverse spinel ferrites around 2.155×10^7 to 2.055×10^8 ohm-

cm at current passed from 10 to 20 nA. The variation in the observed specific resistivities is also reflected in mobility. The Hall coefficient at room temperature for all compounds is negative, indicating the electrons are the majority carriers. The observed Hall coefficient variations are also corresponding to mobility. This may suggest that the specific resistivity and Hall coefficient are mainly governed by the charge carrier mobility rather than a carrier.

3.2.4 Dielectric studies

The dielectric constant (ϵ') and dielectric loss ($\tan \delta$) against the log of frequency in the range 1-600 kHz were recorded at room temperature for doped spinel ferrites such as (a) $Ni_{0.6}Cu_{0.2}Zn_{0.2}Fe_2O_4$, (b) $Co_{0.9}Cd_{0.1}Fe_2O_4$, (c) $Al_{0.3}CoFe_{1.7}O_4$, (d) $CoRu_{0.04}Fe_{1.96}O_4$ (e) $Fe_{2.55}Ni_{0.12}\square_{0.33}O_4$ compounds. The representative of dielectric constant (ϵ') versus the log of frequencies of $Ni_{0.6}Cu_{0.2}Zn_{0.2}Fe_2O_4$ is shown in Fig. 10 (a). Similar nature of dielectric loss ($\tan \delta$) against the log of frequency is also observed for this doped spinel ferrite (see Fig. 10 (b)). The value of dielectric constant (ϵ') decreases with increasing frequency upto 110 kHz and then remains constant (see Fig. 10 (a)). The decrease of the dielectric constant (ϵ') with dopant ions can be explained based on the mechanism of the polarization process in ferrites. The whole polarization in ferrites is mainly contributed by the space charge polarization and hopping exchange of the charges between two localized states governed by the density of the localized state and the resultant displacement of charges with respect to the external field. The addition of substituents (dopants) reduces the iron ions on B – site, which is responsible for both space charge polarization and hopping exchange between the localized states. The decrease in dielectric constant (ϵ') with increasing frequency is attributed to the fact that the electron exchange between Fe^{2+} and Fe^{3+} ions cannot follow the change of the externally applied field beyond a certain frequency, *i.e.*, weak polarization.^[40] The value of the dielectric constant (ϵ') is very high at lower frequencies and decreases with increasing frequency up to 110 kHz and then remains constant up to 10×10^3 kHz. At this stage, domain wall motion occurs.

The values of dielectric loss ($\tan \delta$) decrease monotonically with an increase in log frequency for this sample. Generally, the dielectric loss in ferrites is considered to originate from two mechanisms: electron hopping and charged defect dipoles. The former contributes to dielectric loss in the low-frequency range, is due to electron hopping, while in the high-frequency range, dielectric loss main results from the response of the defect dipoles to the field. These dipoles in ferrites are formed due to changes in the cation state, such as Fe^{+3}/Fe^{2+} , during the sintering process. Relaxation of dipoles under an electric field

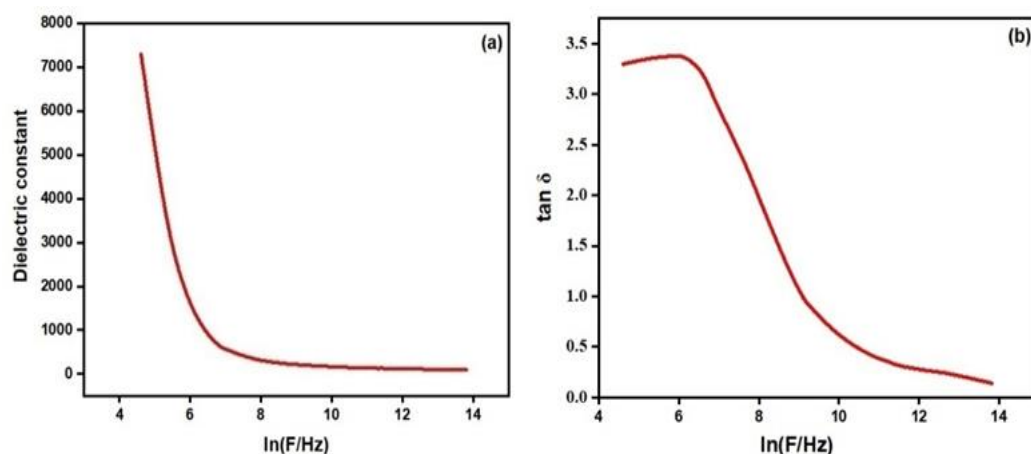


Fig. 10 (a) Plot of variation of dielectric constant (ϵ') and (b) dielectric loss ($\tan \delta$) with frequency for $\text{Ni}_{0.6}\text{Cu}_{0.2}\text{Zn}_{0.2}\text{Fe}_2\text{O}_4$.

is decreased with increasing frequency and ultimately results in a decrease in the dielectric loss in the high-frequency range.

3.2.5 Magnetic studies

Magnetization measurement of $\text{Ni}_{0.6}\text{Cu}_{0.2}\text{Zn}_{0.2}\text{Fe}_2\text{O}_4$, $\text{Co}_{0.9}\text{Cd}_{0.1}\text{Fe}_2\text{O}_4$, $\text{Al}_{0.3}\text{CoFe}_{1.7}\text{O}_4$, $\text{CoRu}_{0.04}\text{Fe}_{1.96}\text{O}_4$, and $\text{Fe}_{2.55}\text{Ni}_{0.12}\square_{0.33}\text{O}_4$ and respective undoped spinel ferrites (i.e. NiFe_2O_4 , CoFe_2O_4 and $\gamma\text{-Fe}_{2.67}\square_{0.33}\text{O}_4$) samples were carried out using a vibrating sample magnetometer (VSM) with the maximum applied field of 8 KOe at room temperature. The obtained hysteresis loops are shown in Fig. S3 of the supplementary information file and were found to be saturated with the available applied field. The representative hysteresis loop (i.e. magnetization versus applied field) for $\text{Fe}_{2.55}\text{Ni}_{0.12}\square_{0.33}\text{O}_4$ is shown here in Fig. 11. From the hysteresis loops, the magnetic parameters such as coercive force (H_c), saturation magnetization (M_s), a ratio of remanence to saturation magnetization (M_R/M_s) and magnetic moment (n_B) values have been calculated and are listed in Table 4. It can be seen that the observed magnetic parameters for respective undoped spinel ferrites are very close to the reported in the literature.^[11,12,17] However these magnetic parameters of undoped samples (such as NiFe_2O_4 , CoFe_2O_4 , and $\text{Fe}_{2.67}\square_{0.33}\text{O}_4$) are consistent with reports of S. Chakrabarti *et al.*^[20] They observed a decrease in the values of magnetic parameters of NiFe_2O_4 ($M_s = 61.3\text{ emu/g}$, $H_c = 53.0\text{ Oe}$), CoFe_2O_4 ($M_s = 63\text{ emu/g}$, $H_c = 2205\text{ Oe}$), and $\text{Fe}_{2.67}\square_{0.33}\text{O}_4$ ($M_s = 60\text{ emu/g}$, $H_c = 352\text{ Oe}$) are prepared by salt-assisted and Citrate gel autocombustion method, respectively, which depends on size, shape as well as a preparation method. In addition, the smaller grain size leads to a reduction in magnetic parameters for these samples.

The increase in observed coercivity (H_c) for all doped samples except $\text{Fe}_{2.55}\text{Ni}_{0.12}\square_{0.33}\text{O}_4$ sample as compared to respective undoped ferrites are indicative of

magnetocrystalline anisotropy (see Table 4). Coercivity is a structural-related extrinsic element. It is also known that when porosity is high, the average particle size would be smaller, and the value of coercivity (H_c) would be high. From Table 4, it is cleared that porosity increases due to which coercivity enhances.^[41] Another reason is that the defect formation in these spinel ferrites (in the form of point defects) also results in higher coercivity.^[42] According to Li *et al.*^[43], the longitudinal magnetic recording medium, which is the general type of magnetic recording medium used in industries, requires high enough coercivity (around 800 Oe). If coercivity is too high (above 1200 Oe), the material can be used for the perpendicular recording media, which is a developing new technology in magnetic recording media.^[43] In the present investigation, the coercivity is in the range of 72.87 - 811 Oe for all doped samples except $\text{CoRu}_{0.04}\text{Fe}_{1.96}\text{O}_4$ sample, so the material can be applied to longitudinal magnetic recording media. While the coercivity of $\text{CoRu}_{0.04}\text{Fe}_{1.96}\text{O}_4$ sample has 1218 Oe and therefore this material can be applied in the perpendicular magnetic recording media.^[43]

It can also be observed from Table 4 the saturation magnetization (M_s), and Remanence ratio (M_R/M_s) decrease for all doped ferrites as compared to the respective undoped spinel ferrite. The M_R/M_s ratio (i.e. squareness) below 0.5 signifies that the material has a multi-domain structure, while more than 0.5 indicate that the material has a single-domain structure.^[44] In the present investigation, the ratio of M_R/M_s is found between 0.11 to 0.47 indicating prepared samples such as $\text{Ni}_{0.6}\text{Cu}_{0.2}\text{Zn}_{0.2}\text{Fe}_2\text{O}_4$, $\text{Co}_{0.9}\text{Cd}_{0.1}\text{Fe}_2\text{O}_4$, $\text{Al}_{0.3}\text{CoFe}_{1.7}\text{O}_4$, and $\text{CoRu}_{0.04}\text{Fe}_{1.96}\text{O}_4$ possesses a multi-domain structure, while $\text{Fe}_{2.55}\text{Ni}_{0.12}\square_{0.33}\text{O}_4$ sample possesses M_R/M_s ratio 0.58, suggesting a single domain magnetic structure the values of squareness ratio M_R/M_s for undoped ferrites such as NiFe_2O_4 , CoFe_2O_4 , and $\gamma\text{-Fe}_{2.67}\square_{0.33}\text{O}_4$ are 0.55 0.65 and 0.68, respectively, which also confirms the single-domain structure.

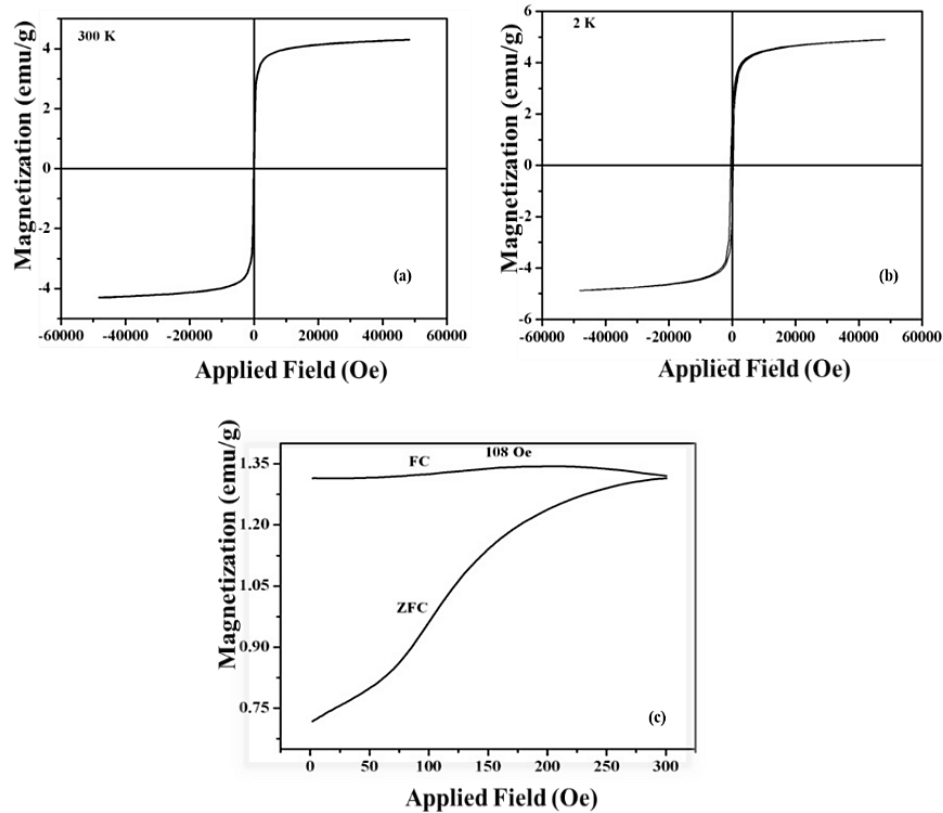


Fig. 11 Magnetization Vs Applied field and ZFC and FC magnetization against the temperature of nickel-doped gamma ferric oxide $Fe_{2.55}Ni_{0.12}□_{0.33}O_4$.

Table 4. Magnetic properties for nanosized doped spinel ferrites.

Compounds	Coercive force Hc ± 0.5 Oe	The saturation magnetization (Ms) ±2 emu / g	Ratio of M _R / M _s	Magnetic moment n _B ±0.1 μ _B	
				Observed	Calculated
Ni _{0.6} Cu _{0.2} Zn _{0.2} Fe ₂ O ₄	72.87	42.34	0.11	1.80	5.31
NiFe ₂ O ₄	72.01	63.00	0.55	2.21	2.83
Co _{0.9} Cd _{0.1} Fe ₂ O ₄	811.01	65.16	0.35	2.86	5.46
CoFe ₂ O ₄	680	91.8	0.65	3.85	3.87
Al _{0.3} CoFe _{1.7} O ₄	789.54	32.76	0.47	1.34	2.64
CoRu _{0.04} Fe _{1.96} O ₄	1218.1	54.78	0.47	2.31	3.87
Fe _{2.55} Ni _{0.12} □ _{0.33} O ₄	73.96	43.0	0.58	1.66	3.77
Fe _{2.67} □ _{0.33} O ₄	352	61.5	0.68	2.35	3.95

The larger the particle (grain) size, the greater the flow in the domain movement. The lesser particle size restricts domain movement leading to an increased coercive force (Hc) in the doped spinel compounds.^[45]

The variation of saturation magnetization (Ms) with different dopants can be estimated by exchange interaction among ions distributed in the octahedral (B) and tetrahedral (A) sites. Neel’s two sublattice models^[46] are applied to the magnetization at the B sub-lattice is higher than the A sublattice. This model is applied to understand the magnetic behavior of the samples. According to Neel’s two-sublattice model of ferrimagnetism, magnetic moment n_B is given by n_B = M_B – M_A. Where M_B and M_A are the B and A sub-lattice magnetic moments in μ_B. Using ionic magnetic moments of

Fe³⁺, Zn²⁺, Ni²⁺, Cu²⁺ and Co²⁺ as 5.92 μ_B, 0 μ_B, 2.83 μ_B, 1.38 μ_B, and 3.87 μ_B respectively, and using the above relation, Neel’s magnetic moment has been calculated. The experimental magnetic moment (n_B) is calculated from the saturation magnetization data using the following relations.

$$n_B = M_w \times M_s / 5585 \tag{6}$$

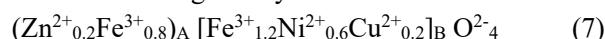
where M_w is the molecular weight of the doped spinel ferrites, and M_s is the saturation magnetization in emu/g. The saturation magnetization and the observed and calculated values of magneton numbers are listed in Table 4. It is evident from the table that there is a discrepancy in the observed and calculated values of the magneton number. This suggests that the structure is a non-collinear spin arrangement, i.e., the presence of a small canting of the B-site moment with respect

to the direction of the A-site moment of spinel.^[47] Furthermore, it is also possible to correlate the observed magnetic moment (n_B) to the porosity (P) of these samples (see Table 2). A pore is a sort of void or a gap, and this will break up the magnetic circuit between grains to the grain. If the number of pores is large, this may lead to the net reduction of magnetization in bulk.^[48] Another reason is that, as discussed in scanning electron microscopy (Fig. 4), the critical grain size decreases due to the displacement of the domain wall added to magnetic losses. This is because the existence of domain walls partly coincides with the grain boundaries. So the increase in grain boundaries with grain size decreases leads to the pinning of domain walls motion.^[49] As such, it is assumed that magnetic ordering can be broken up easily at nonmagnetic/magnetic (*i.e.*, dopants) grain boundaries, and then there is the presence of short-range magnetic exchange interaction. Therefore, in the range of applied field (H) for hysteresis measurement, the magnetization is not large enough to move the magnetic domain walls, *i.e.*, the contribution of the domain wall displacements in the magnetization process is small which, corresponds to nonmagnetic/magnetic (dopants) pores exist at the grain boundaries. Therefore, the magnetic moment (n_B), saturation magnetization (M_S) and remanence ratio (M_R/M_S) of doped spinel ferrite is less than that of undoped one.

(a) $Ni_{0.6}Cu_{0.2}Zn_{0.2}Fe_2O_4$ sample

The variation of magnetization for this sample could be explained based on cation distribution and exchange interaction between iron, zinc, and copper at tetrahedral A and octahedral B sites. K. S. Ramakrishna *et al.*^[50] in their studies for $Ni_xCu_{0.1}Zn_{0.9-x}Fe_2O_4$ ferrites ($X=0.5, 0.6, 0.7$) observed as Ni^{2+} concentration is being increased, their saturation magnetization (M_S) and coercive force (H_C) increases and then decreases. The highest value of $M_S = 38.36$ emu/g and $H_C = 66.77$ Oe is observed for $x = 0.6$. They observed that the substitution of Cu^{2+} in the place of Zn^{2+} greatly alters the cation distribution forcing more Ni^{2+} ions into A-site. It is well known that Zn^{2+} ions strongly prefer A sites (tetrahedral), Cu^{2+} and Ni^{2+} ions prefer B sites (octahedral), while Fe^{3+} ions occupy both A and B sites. The strong preference of Zn^{2+} ions for A sites displaces some Fe^{3+} ions from A to B site, which reduces the magnetic moment of the A-site, while the magnetic moment of B-site will increase. When Cu^{2+} ions are introduced, the Fe^{3+} ions are left at A-site, being small in number, the A-B interaction experienced by B-site Fe^{3+} ions decreases. Also, the increased number of Fe^{3+} ions at the B-site increases the B-B interaction, resulting in spin canting.^[51] Consequently, the magnetization of B sublattices is decreased. The reason for a decrease in magnetization may also be due to

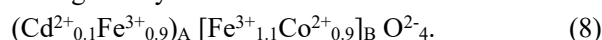
the Cu^{2+} content, the exchange interaction is weakened, and B spins are no longer held rigidity parallel to the few remaining A spins. The decrease in the B sublattice moment, interpreted as a spin departure from co-linearity, causes the effect known as canting. Therefore, the introduction of Ni^{2+} and Cu^{2+} ions, which have a strong preference for the spinel at the B-site and the cation distribution is given by



where the ions enclosed by the round bracket correspond to the tetrahedral A-site and the ions enclosed by the square bracket correspond to the octahedral B-site.

(b) $Co_{0.9}Cd_{0.1}Fe_2O_4$ sample

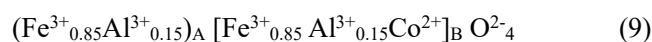
The saturation magnetization of this sample is in full agreement with the Neel theory of ferrimagnetism.^[46] The introduction of Co^{2+} ion, which has a strong preference for the spinel B-site, while Cd^{2+} ion prefers to A-site and the cation distribution is given by



The substitution of paramagnetic Co^{2+} ions at the B-site, then some Fe^{3+} ions started to migrate to the A-site hence strengthening the A-B interaction. When the Cd^{2+} ion is non-magnetic and occupies the Fe^{3+} site in the A-site sublattice, the magnetic bond $Fe^{3+}_A - O - Fe^{3+}_B$ decreases, and consequently, the magnetization at the B-site decreases. This decrease in the magnetization of the B-sub lattice, in turn, weakens the magnetic influence of the B-sublattice on the A-sublattice. This decreases the A – B interaction, which results in a decrease in the saturation magnetization.

(c) $Al_{0.3}CoFe_{1.7}O_4$ sample

Upon doping of the Fe ions with Al^{3+} (*i.e.*, non-magnetic ion), changes in the cation distribution take place, which affects the value of the magnetic moment per formula unit. It was found that Fe ions migrate from the octahedral B site to the tetrahedral A site as the concentration of Al ions. So that Fe and Al ions occupy both A and B sites in the spinel structure as

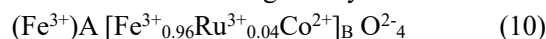


Therefore, the magnetic moment per formula unit decreases as the Al content is due to the doped of the magnetic Fe ion with non-magnetic Al ion and changes in cation distribution. Thus, shifting of magnetic Fe^{3+} ($5.92 \mu_B$) ion from the sublattice and the doped of the non-magnetic Al^{3+} (zero μ_B) ions in its place weakens the superexchange interactions. This tends to align neighboring magnetic dipole antiparallely, allowing a decrease in the magnetization due to enhanced spin nonlinearity. Therefore, on Al^{3+} doping, the saturation magnetization and M_R/M_S ratio decrease in the present sample

as compared to undoped CoFe_2O_4 .^[12] The more coercive force (see in Table 4) is due to enhanced magnetocrystalline anisotropy induced by the different cation distributions of this sample. P.P. Gauns Desai *et al.*^[52] observed the saturation magnetization (M_s) and Coercive force (H_c) decreases with an increase in nonmagnetic Al^{3+} concentration for $\text{Ni}_{0.7}\text{Zn}_{0.3}\text{Fe}_{2-x}\text{Al}_x\text{O}_4$ ferrite system (for $x = 0.0$ to 0.3 , $M_s = 65$ to 47 emu/g and $H_c = 80$ to 30 Oe respectively). It has been also observed that as the concentration Al^{3+} increases, the hysteresis loop becomes very narrow.

(d) $\text{CoRu}_{0.04}\text{Fe}_{1.96}\text{O}_4$ sample

The insertion of a small amount of Ru^{3+} cations into a cobalt ferrite here may have contributed to magnetization. Hence, in this compound, it may be reasonable that Ru^{3+} is considered magnetic at room temperature. Therefore, the effect of ruthenium (Ru) atoms in CoFe_2O_4 seems to be similar to the doping of magnetic atoms in the octahedral Fe sites of the spinel lattices. As the net magnetic moments in the ferromagnetic ferrites depends on the number of magnetic ions occupying the tetrahedral (A) and octahedral (B) sites, the reduction of magnetization (M_s) as Ru^{3+} content. This fact is evident as observed lower saturation magnetization value for Ru-doped cobalt ferrite having smaller crystallite size and average particle size (see Table 2) compound. The Ru^{3+} ions have a strong preference for the octahedral lattice (B) site of the spinel. The cation distribution is given by

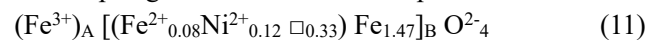


The large coercive force (H_c) of this sample may be due to the ruthenium ions (Ru^{3+}) usually having a strong spin-orbit coupling and thereby contribute to the anisotropy of a single-ion source when there located in the B-sites of spinel ferrites. In literature, the magnetization of Ru-doped NiFe_2O_4 increased with annealing temperature,^[53] and showed the narrow area of the hysteresis loop demonstrates soft magnetic nature which depends on the crystallinity dopant and particle size. The observed values of coercivity (H_c) = 47.02, 67.92, 99.26 Oe and saturation magnetization (M_s) = 3.25, 12.50, 34.92 emu/g increases as the annealed temperature at 300, 600 and 900°C increases respectively. They showed that lower magnetization at 300°C is due to smaller particle size where in a high surface disorder is expected. The coercivity rises with annealing temperatures is due to the grain boundaries can lead to increase pinning sites for spins and also, increases the strong exchange coupling as well growth of anisotropic properties.

(e) $\text{Fe}_{2.55}\text{Ni}_{0.12}\square_{0.33}\text{O}_4$ sample

The hysteresis loops of the as-synthesized Ni-doped gamma ferric oxide, $\text{Fe}_{2.55}\text{Ni}_{0.12}\square_{0.33}\text{O}_4$ sample at room temperature (300 K) is shown in Fig. 11 (a). This result indicates that all

particles are likely to have ferromagnetic properties at room temperature since the remanence ratio of the particles is equal to 0.19 and the coercivity is 73.96 Oe in the absence of an external magnetic field. It can be seen that the magnetic hysteresis loop obtained from the magnetization cycle is considerably small. The constant value or level in the horizontal region of the magnetization curve in the magnetic field, which seems to some extent to be out of ± 50 Koe range, may suggest that the nanoparticles have attained their saturated magnetization level, *i.e.*, 40 emu/g. This value is less than undoped gamma ferric oxide (see Table 4). Referring to the average grain size of the nanoparticles (20 nm) and the magnetic hysteresis loop, it could be claimed that magnetic nanoparticles are not superparamagnetic. Similar magnetization have has been observed in cobalt and gadolinium doped $\text{Fe}_{2.67}\square_{0.33}\text{O}_4$ (*i.e.* $\gamma\text{-Fe}_2\text{O}_3$) spinel ferrite.^[54] They reported that the saturation magnetization (M_s) = 56.8 and 46.0 emu/g, coercive force (H_c) = 387 and 346 Oe respectively for 1 wt% cobalt and gadolinium-doped gamma ferric oxide. These samples have been found to be single domains. The magnetization of this sample at a temperature of 2K is presented in Fig. 11 (b). The particles do have adequate thermal energy to attain complete thermal equilibrium with the applied field during the measurement time, and hence, hysteresis appears. It may be noted from Fig. 11 (b) that the hysteresis loop is open. The open hysteresis loop at 50 KOe and the ZFC/FC separation (Fig. 11 (c)) suggest high field irreversibility. In a manner similar to 300 K (*i.e.*, room temperature), the saturation magnetization of $\text{Fe}_{2.55}\text{Ni}_{0.12}\square_{0.33}\text{O}_4$ obtained at 2 K was estimated and found a good agreement with each other. This is indicative of the presence of ferromagnetic nanosized material. The ZFC – FC magnetization process at 100 Oe exhibit the typical features of an assembly of magnetic particles with a distribution of blocking temperature (see Fig. 11 (c)). In this sample, the ZFC and FC magnetization curves (Fig. 11 (c)) only collapse at the highest temperature measured (300 K), thus indicating that the blocking temperature is above room temperature. The observed irreversibility of the ZFC-FC curve indicative of ferromagnetism exists in this sample. According to Neel's two sublattice model of ferrimagnetism,^[46] the cation distribution for nickel-doped gamma ferric oxide sample can be written as



Although there is not much change in the bonding of iron atoms at the A-site, some change in bonding does take place at the octahedral B-site to nickel concentration. Therefore, nickel enters Fe vacant sites at the B-site of the spinel.

A thermogravimetric (TGA) method can be applied to the evaluation of the cationic *i.e.* Fe vacancy, (δ) in spinel ferrites.

This method correlates the Fe vacancy (δ) with the weight change due to oxygen evolution through the charge and mass balance in the spinel ferrite. From this data, the Fe vacancy (δ) at room temperature was calculated by using the following expression.^[55]

$$\delta = (\alpha - 3\theta) / m \quad (12)$$

Where δ = Fe (*i.e.* cationic) vacancy, α = initial mass (m_i) of the sample taken in mg, θ = molar fraction *i.e.* a certain amount of mass loss in mg, $\Delta m = m_i - m_f$ (where m_i and m_f are the initial and final mass of the sample) and $m = (4 + 3\alpha - \theta)$ called the cationic coefficient. These authors^[55] also discussed the change in Fe vacancy (δ) due to atmosphere changes are much more significant and these changes can be correlated to changes in the spinel ferrite magnetic properties. Further, they suggested that the values obtained for δ will not be altered by the presence of some electron hopping between Fe^{2+} and Fe^{3+} cations.

4. Conclusions

Five nanosized doped spinel ferrites such as $Ni_{0.6}Cu_{0.2}Zn_{0.2}Fe_2O_4$, $Co_{0.9}Cd_{0.1}Fe_2O_4$, $Al_{0.3}CoFe_{1.7}O_4$, $CoRu_{0.04}Fe_{1.96}O_4$, and $Fe_{2.55}Ni_{0.12} \square_{0.33}O_4$ samples are synthesized by soft chemical routes. The X-ray diffraction of these samples possesses a single-phase spinel structure with a slightly enlarged lattice constant as compared to respective undoped spinel ferrite samples. SEM and TEM images along with particle size distribution histograms confirmed the nano-size particle for these spinel ferrites. The electrical conductivity, Seebeck voltage and Hall effect measurements for all samples showed an n-type semiconductor. All doped samples show typical hysteresis behavior with a decrease in saturation magnetization (M_s), and the remanence ratio (M_R / M_s) due to the weak superexchange interaction and an increase in coercivity (H_c) as compared to respective undoped spinel ferrites. The observed and calculated values of magneton number (n_B) for all samples showed a significant canting spin exists at the octahedral B-site. A high value of coercivity (H_c) makes all synthesized materials except $CoRu_{0.04}Fe_{1.96}O_4$ sample is required for the applications in longitudinal recording media. While $CoRu_{0.04}Fe_{1.96}O_4$ sample will be suitable for application in perpendicular high-density recording media.

Acknowledgments

The authors thank the staff from TIFR, Mumbai for their technical support during the SEM-EDS and magnetization measurement experiment. They also thank DST-FIST Delhi, the staff from SAIF laboratories IIT Mumbai, for ICPEs and TEM-SAED experiment.

Conflict of Interest

There is no conflict of interest.

Supporting Information

Applicable.

References

- [1] S. Laurent, D. Forge, M. Port, A. Roch, C. Robic, L. Vander Elst, R. N. Muller, Magnetic iron oxide nanoparticles: synthesis, stabilization, vectorization, physicochemical characterizations, and biological applications, *Chemical Reviews*, 2008, **108**, 2064-2110, doi: 10.1021/cr068445e.
- [2] A Goldman, Modern Ferrite Technology, Springer-Verlay, PA, 2006 Pittsburgh.
- [3] S. Chakrabarty, M. Pal, A. Dutta, Structural, optical and electrical properties of chemically derived nickel substituted zinc ferrite nanocrystals, *Materials Chemistry and Physics*, 2015, **153**, 221-228, doi: 10.1016/j.matchemphys.2015.01.006.
- [4] K. E. Sickafus, J. M. Wills and N. W. Grimes, Structure of Spinel, *Journal of American Ceramic Society*, 1999, **82**, 3279-3292, doi: 10.1111/j.1151-2916.1999.tb02241.x.
- [5] D. V. Kurmude, R. S. Barkule, A. V. Raut, D. R. Shengule, K. M. Jadhav, X-ray diffraction and cation distribution studies in zinc-substituted nickel ferrite nanoparticles, *Journal of Superconductivity and Novel Magnetism*, 2014, **27**, 547-553, doi: 10.1007/s10948-013-2305-2.
- [6] A. T. Raghavender, R. G. Kulkarni, K. M. Jadhav, Magnetic Properties of Nanocrystalline Al Doped Nickel Ferrite Synthesized by the Sol-Gel Method, *Chinese Journal of Physics*, 2008, **46**, 366-375, doi: 10.6122/CJP.
- [7] W. Ying, K. X. Yu, Y. Xiong, W. Hui, EPR investigation of the site symmetry of Fe^{3+} ions in the spinel crystals, *Physica B: Condensed Matter*, 2006, **381**, 260-264, doi: 10.1016/j.physb.2006.01.495.
- [8] H. Bordeneuve, C. Tenailleau, S. Guillemin-Fritsch, R. Smit, E. Suard, A. Rousset, Structural variations and cation distributions in $Mn_{3-x}Co_xO_4$ ($0 \leq x \leq 3$) dense ceramics using neutron diffraction data, *Solid State Sciences*, 2010, **12**, 379-386, doi: 10.1016/j.solidstatesciences.2009.11.018.
- [9] K. Haneda, A. H. Morish, Noncollinear magnetic structure of $CoFe_2O_4$ small particles, *Journal of Applied Physics*, 1988, **63**, 4258-4260, doi: 10.1063/1.340197.
- [10] L. Lin, K. H. Hsu, J. G. Lin, Doping effects on the magnetic resonance of $ZnFe_2O_4$ and $NiFe_2O_4$, *Journal of Magnetism and Magnetic Materials*, 2006, **304**, 467-469, doi: 10.1016/j.jmmm.2006.02.069.
- [11] V. Rao, A. L. Shashimohan, A. B. Biswas, Studies on the formation of $-Fe_2O_3$ (maghemite) by thermal decomposition of ferrous oxalate dihydrate, *Journal of Materials Science*, 1974, **9**, 430-433, doi: 10.1007/bf00737843.
- [12] A. K. Nikumbh, A. V. Nagawade, V. B. Tadke, P. P. Bakare, Electrical, magnetic and Mössbauer properties of cadmium - cobalt ferrites prepared by the tartarate precursor method, *Journal of Materials Science*, 2001, **36**, 653-662, doi:

- 10.1023/A:1004872405266.
- [13] H. Kaur, A. Singh, V. Kumar, D. Singh Ahlawat, Structural, thermal and magnetic investigations of cobalt ferrite doped with Zn^{2+} and Cd^{2+} synthesized by auto combustion method, *Journal of Magnetism and Magnetic Materials*, 2019, **474**, 505-511, doi: 10.1016/j.jmmm.2018.11.010.
- [14] A. K. Nikumbh, R. A. Pawar, D. V. Nighot, G. S. Gugale, M. D. Sangale, M. B. Khanvilkar, A. V. Nagawade, Structural, electrical, magnetic and dielectric properties of rare-earth substituted cobalt ferrites nanoparticles synthesized by the coprecipitation method, *Journal of Magnetism and Magnetic Materials*, 2014, **355**, 201-209, doi: 10.1016/j.jmmm.2013.11.052.
- [15] L. Kumar, M. Kar, Influence of Al^{3+} ion concentration on the crystal structure and magnetic anisotropy of nanocrystalline spinel cobalt ferrite, *Journal of Magnetism and Magnetic Materials*, 2011, **323**, 2042-2048, doi: 10.1016/j.jmmm.2011.03.010.
- [16] A. Ghasemi, E. Ghasemi, E. Paimozd, Influence of copper cations on the magnetic properties of NiCuZn ferrite nanoparticles, *Journal of Magnetism and Magnetic Materials*, 2011, **323**, 1541-1545, doi: 10.1016/j.jmmm.2011.01.014.
- [17] A. K. Nikumbh, A. V. Nagawade, G. S. Gugale, M. G. Chaskar, P. P. Bakare, The formation, structural, electrical, magnetic and Mössbauer properties of ferrispinel, $Cd_{1-x}Ni_xFe_2O_4$, *Journal of Materials Science*, 2002, **37**, 637-647, doi: 10.1023/a: 1013790129045.
- [18] A. Tomitaka, T. Koshi, S. Hatsugai, T. Yanmada, Y. Takemura, Magnetic characterization of surface-coated magnetic nanoparticles for biomedical application, *Journal of Magnetism and Magnetic Materials*, 2011, **323**, 1398-1403, doi: 10.1016/j.jmmm.2010.11.054.
- [19] I. Desai, M. N. Nadagouda, M. Elovitz, M. Mill, B. Boulanger, Synthesis and characterization of magnetic manganese ferrites, *Materials Science for Energy Technologies*, 2019, **2**, 150-160, doi: 10.1016/j.mset.2019.01.009.
- [20] S. Chakrabarti, S. K. Mandal, S. Chaudhari, Cobalt doped γ - Fe_2O_3 nanoparticles: synthesis and magnetic properties, *Nanotechnology*, 2005, **16**, 506-511, doi: 10.1088/0957-4484/16/4/029.
- [21] S. Hamdy, M. B. Mohamed, S. S. Ata-Allah, Effect of Zn, Ga and Gd doping on structural and magnetic properties of nanonickel ferrite prepared by two different methods, *Journal of Superconductivity and Novel Magnetism*, 2019, **32**, 115, doi: 10.1007/s10948-018-4893-3.
- [22] R. Giovanoli, R. Brutsch, Dehydration of gamma- $FeOOH$ -direct observation of mechanism, *Chimia*, 1974, **28**, 188-191.
- [23] M. B. Khanvilkar, A. K. Nikumbh, R. A. Pawar, N. J. Karale, D. V. Nighot, G. S. Gugale, Synthesis and physicochemical properties of doped nano oxides-dilute magnetic semiconductors, *Journal of Materials Science: Materials in Electronics*, 2019, **30**, 13217-13222, doi: 10.1007/s10854-019-01685-3.
- [24] J. R. Allan, G. M. Baillie, N. D. Baird, The spectral and magnetic properties of some chloro and bromo transition metal complexes of isonicotinic acid, *Journal of Coordination Chemistry*, 1980, **10**, 171-175, doi: 10.1080/00958978008081012.
- [25] J. R. Allan, A. D. Paston, K. Turvey, H. J. Bowley, D. L. Gerrad, Thermal and electrical studies on pyrazine-2,3-dicarboxylic acid compounds of manganese(II), cobalt(II), nickel(II), copper(II) and zinc(II), *Thermochim Acta*, 1988, **124**, 345-357, doi: 10.1016/0040-6031(88)87037-0.
- [26] M. B. Khanvilkar, A. K. Nikumbh, R. A. Pawar, N. J. Karale, D. V. Nighot, R. C. Ambare, P. A. Nagawade, M. D. Sangale, G. S. Gugale, S. B. Misal, Preparation and Characterization of Nanosized Substituted Perovskite Compounds with Orthorhombic Structure, *Physics and Chemistry of Solid State*, 2021, **22**, 664-686. doi: 10.15330/pcss.22.4.664-686.
- [27] A. A. Ghani, A. A. Sattar, Composition dependence of magnetization in $Co_{1-x}Cd_xFe_2O_4$ ferrites, *Journal of Magnetism and Magnetic Materials*, 1991, **97**, 141-146 doi: 10.1016/0304-8853(91)90173-8.
- [28] M. A. Ahmed, M. M. EL-Sayyed, Magnetic characterization and thermoelectric power of $Ni_{1-y}Zn_y Cu_{0.3}Fe_{1.7}O_4$; $0.0 \leq y \leq 0.6$, *Journal of Magnetism and Magnetic Materials*, 2007, **308**, 40-45, doi: 10.1016/j.jmmm.2006.04.034.
- [29] T. Inoue, D. Kagaku, History of ECSJ Awards and Introduction of Award Winners in 2021, *Electrochemistry*, 1955, **23**, 24, doi: 10.5796/electrochemistry 21-00102.
- [30] J. Bernal, D. Dasgupta, A. Mackay, Oriented transformations in iron oxides and hydroxides, *Nature (London)*, 1957, **180**, 645-647, doi: 10.1038/180645a0.
- [31] A. M. EL-Sayyed, Influence of zinc content on some properties of Ni-Zn ferrites, *Ceramics International*, 2002, **28**, 363-367, doi: 10.1016/S0272-8842(01)00103-1.
- [32] B. D. Cullity, Elements of X-ray diffraction and Addison Wesley Publication Company Inc. Indiana, U.S.A. 1959.
- [33] T. Abbas, M. U. Islam, M. A. Chaudhary, Study of sintering behavior and electrical properties of Cu-Zn-Fe-O system *Modern Physics Letters B*, 1995, **22**, 1419-1426, doi: 10.1142/S0217984995001418.
- [34] P. Singh, V. K. babbar, A. Razdan, S. L. Srivastava, V. K. Agrawal, T. C. Goel, Dielectric constant, magnetic permeability and microwave absorption studies of hot-pressed Ba-CoTi hexaferrite composites in X-band, *Journal of Materials Science*, 2006, **41**, 7190-7196, doi: 10.1007/s10853-006-0921-y.
- [35] K. Ravichandan, D. Nedumaran, *International Journal of Mechanical and Materials Engineering*, 2011, **4**, 25-30, doi: ISSN-2198-2791(electronic).
- [36] O. S. Josyulu, J. Sobhanadri, The far-infrared spectra of some mixed cobalt zinc and magnesium zinc ferrites, *Physica Status Solidi (a)*, 1981, **65**, 479-483, doi: 10.1002/pssa.2210650209.
- [37] B. J. Evans, O. K. Hang Nam, Collective electron states in $Zn_xFe_{3-x}O_4$ and $Cd_xFe_{3-x}O_4$ for $0 \leq x \leq 0.3$, *Physica B+C*, 1977, **86-88**, 931-933, doi: 10.1016/0378-4363 (77) 90747-1.
- [38] M. Mogensen, N. M. Sammes, G. A. Tom, Effect of surface modifications on the layered solid solution cathodes $(1 - z) Li[Li_{1/3}Mn_{2/3}]O_2 - (z) Li[Mn_{0.5} - yNi_{0.5} - yCo^{2y}]O_2$, *Solid State Ionics*, 2009, **180**, 63-72, doi: 10.1016/j.ssi.2008.11.002.

- [39] E. J. W. Verway, *Semiconducting Materials*, (H. K. Henisch, Edition) Butterworths, 1951, page 151, London.
- [40] A.M. Abo El Ata, S.M. Attia, T.M. Meaz, AC conductivity and dielectric behavior of $\text{CoAl}_x\text{Fe}_{2-x}\text{O}_4$, *Solid State Sciences*, 2004, **6**, 61-69, doi: 10.1016/j.solidstatesciences.2003.10.006.
- [41] M. I. Iqbal, R. A. Khan, S. Takeda, S. M. Zukami, T. Miyazaki, W-type hexaferrite nanoparticles: A consideration for microwave attenuation at wide frequency band of 0.5–10 GHz, *Journal of Alloys and Compounds*, 2011, **509**, 7618-7624, doi: 10.1016/j.jallcom.2011.04.103.
- [42] J. Gao, Y. Cui, Z. Yang, The magnetic properties of $\text{Ni}_x\text{Zn}_{1-x}\text{Fe}_2\text{O}_4$ films fabricated by alternative sputtering technology, *Materials Science and Engineering: B*, 2004, **110**, 111-114, doi: 10.1016/j.mseb.2003.10.111.
- [43] Y. Li, R. Liu, Z. Zhang, C. Xiang, Synthesis and characterization of nanocrystalline $\text{BaF}_{0.6}\text{Zr}_{0.8}\text{Co}_{0.8}\text{Ti}_{0.8}\text{Mn}_{0.8}\text{O}_{19}$ particles, *Materials Chemistry and Physics*, 2000, **64**, 256-259, doi: 10.1016/S0254-0584(99)00218-7.
- [44] H. N. Chaudhari, P. N. Dhruv, C. Singh, S. Singh Meena, S. Kavita, R. B. Jotania, Effect of heating temperature on structural, magnetic, and dielectric properties of Magnesium ferrites prepared in the presence of Solanum Lycopersicum fruit extract, *Journal of Materials Science: Materials in Electronics*, 2020, **31**, 18445, doi:10.1007/s10854-020-04389-1.
- [45] C. N. Chinnasamy, B. Jeyadevan, K. Shinoda, K. Tohji, D. J. Djayaprawira, M. Takahashi, R. Justin Joseyphus, A. Narayanasamy, Unusually high coercivity and critical single-domain size of nearly monodispersed CoFe_2O_4 Nanoparticles, *Applied Physics Letters*, 2003, **83**, 2862, doi: 10.1063/1.1616655.
- [46] M. Louis Neel, Magnetic properties of ferrites; ferrimagnetism and antiferromagnetism, *Annals of Physics*, 1948, **12**, 137-198, ISSN: 003-4169, eISSN:1286-4838.
- [47] Y. Yafet, C. Kittel, Antiferromagnetic Arrangements in Ferrites, *Physics Review*, 1952, **87**, 290-294, doi: 10.1103/PhysRev.87.290.
- [48] H. Rikukawa, Relationship between microstructures and magnetic properties of ferrites containing closed pores, *IEEE Transactions on Magnetics*, 1982, **18**, 1535-1537, doi: 10.1109/TMAG.1982.1062065.
- [49] S. B. Ren, C. J. Lu, H. M. Shen, Y. N. Wang, In situ study of the evolution of domain structure in free-standing polycrystalline PbTiO_3 thin films under external stress, *Physical Review B*, 1997, **55**, 3485-3489, doi: 10.1103/PhysRevB.55.3485.
- [50] K. S. Ramakrishna, C. Srinivas, S. S. Meena, B. V. Tirupanyam, P. Bhatt, S. M. Yusuf, C. L. Prajapat, D. M. Potukuchi, D. L. Sastry, *Ceramics International*, 2017, **43**, 7984-7991, doi: 10.1016/j.ceramint.2017.03.078.
- [51] S. E. Shrisath, B. G. Toksha, R.H. Kadam, S. M. Patange, D.R. Mane, G. S. Jangam, A. Ghasemi, Doping effect of Mn^{2+} on the magnetic behavior in Ni–Zn ferrite nanoparticles prepared by sol–gel auto-combustion, *Journal of Physics and Chemistry of Solids*, 2010, **71**, 1669-1675. doi: 10.1016/j.jpics.2010.08.016.
- [52] P. P. Gauns Dessai, S. S. Meena, V. M. S. Verenkar, Influence of addition of Al^{3+} on the structural and solid state properties of nanosized Ni–Zn ferrites synthesized using malic acid as a novel fuel, *Journal of Alloys and Compounds*, 2020, **842**, 155855, doi: 10.1016/j.jallcom.2020.155855.
- [53] V. Manikandan, A. Mizzaei, S. Vigneselvan, S. Kavita, R.S. Mane, S. S. Kim, J. Chandrasekaran, Role of ruthenium in the dielectric, magnetic properties of nickel ferrite ($\text{Ru–NiFe}_2\text{O}_4$) Nanoparticles and their application in hydrogen sensors, *ACS Omega*, 2019, **4**, 12919-12926, doi:10.1021/acsomega.9b01562.
- [54] A. K. Nikumbh, Magnetic properties and Mössbauer spectra of gamma ferric oxide and doped gamma ferric oxide, *Journal of Materials Science*, 1990, **25**, 3773-3779, doi:10.1007/BF00575417.
- [55] A. Gonzalez Arias, A. delCueto, J. M. Munoz, C. de Francisco, Deposition of nanostructured CdS thin films by thermal evaporation method: effect of substrate temperature, *Materials*, 1998, **37**, 187-191, doi: 10.1016/S0167-577X(98)00089-5.

Author Information



Mahesh B. Khanvilkar is working as Professor of Chemistry at K. M. C. College, Khopoli since 1988. He has completed his Ph.D. from Savitribai Phule Pune University, Pune in 2014. He is working as ex-Incharge Principal and Head, in the same institute. He is working in the area of Material science, heterogeneous catalysis, nanomaterials etc. He has published 12 research papers in various reputed international journals and published 02 book chapters. He has been awarded the 'Best NSS Programmer Officer' by University of Mumbai, Mumbai, India in 2006 for his excellent contribution in extension activities.



Arvind K. Nikumbh is an ex-Professor of Inorganic Chemistry in the Department of Chemistry, Savitribai Phule Pune University (Formerly University of Pune) Pune-411007, India. He received his master's degree in Inorganic Chemistry in 1976 and his Ph. D in 1982 from the Department of Chemistry, University of Pune. During 1986-1988 he was a postdoctoral fellow at Karsruhe, Germany under DAAD Fellowship. His current research interest include electrothermal analysis of metal (II) dicarboxylates, slip casting of ceramic oxide, nanomaterials such as mixed ferrites, substituted perovskite and pyrochlore oxides and photocatalysis. He has several publications in peer review International journals. He is also a reviewer of many International journals of his research area.



Ramdas A. Pawar is Professor of Chemistry working in the Department of Chemistry, Prof. Ramkrishna More ACS College, Akurdi, Pune. He received master degree in Inorganic Chemistry in 1993 and his Ph. D. in 2006 from Department of Chemistry, Savitribai Phule Pune University, Pune. His current research interest includes Nanomaterials, heterogeneous catalysis and sensors. He has published several research papers in the journals of international repute with total citation-348, with h-index-08 and i-10 index-07. Two students completed their Ph. D. research under his supervision. He is able to grab research funding of about 6.5 lakh from UGC and BCUD, SPPU, Pune. He has been awarded the 'NSS Best Programmer Officer' by Mahajana Education Society, Mysore, and Karnataka, India in 2003 for his excellent contribution in extension activities.



Neeta J. Karale is working as an Assistant Professor at Fergusson College, Pune since 2006. She has completed her Ph.D. at Savitribai Phule Pune University, Pune in 2016. Her area of research is in the field of Material Science. She has published 09 research papers in various Journals.



Pratik A. Nagwade has completed his Ph.D. degree in the year 2017 from Savitribai Phule Pune University, Pune in the area of materials science. Presently he is working as Assistant Professor and Ph.D. guide in Chemistry at Shri Anand College, Pathardi, Dist. Ahmednagar. He has published 12 research papers in various journals.



Deepak V. Nighot is presently working as Associate Professor in the Department of Engineering Science, AISSMS College of Engineering, Pune since 1999. He has received his Ph. D. from Savitribai Phule Pune University, Pune (SPPU). His research interest is in material science particularly electrothermal analysis, synthesis and characterization of the mixed metal dicarboxylato complexes route to convert novel semiconductor nanomaterials. He has received Ph. D. guide recognition in Chemistry from SPPU, Pune. He has published 12 research articles in the reputed international journals and published 4 book chapters.



Gulab S. Gugale received his master degree and Ph.D. in Inorganic Chemistry from Savitribai Phule Pune University (earlier University of Pune), Pune, India. He is working as Head, Department of chemistry in The Poona Gujrati Kelvani

Mandal's Haribhai V. Desai College, Pune from 1993. Now he is working as Professor in the same institute. He is working in the area of Material science, organic and inorganic semiconductors, photocatalysis, spinel ferrite nanomaterials etc. More than 20 research papers are in his credit. He has published 78 book chapters in the Chemistry subject.



Mohan D. Sangale is presently working as a Professor in Chemistry at S.S.G.M. College Kopargaon District Ahmednagar (Maharashtra) India. He is research supervisor in S. P. P. University, Pune. His area of interest are Material Science. He has Published 25 research Papers and presented more than 50 papers in national and international conferences (that is Germany, Bangkok, Thailand). He has published 10 book chapters in Chemistry subject.



Sham B. Misal received his master's degree in Inorganic Chemistry, M. Phil. Degree in Chemistry and Ph.D. degree in Chemistry from the Savitribai Phule Pune University, Pune. The title of his thesis at M. Phil. degree is Synthesis and Characterization of Substituted M-type Hexaferrite by Tartrate Coprecipitation. The title of his Ph.D. thesis is Preparation and Properties of Substituted Hard and Soft Ferrites. He has published several research papers in peer-reviewed international journals. Presently he is working as an Assistant Professor in Rayat Shikshan Sanstha's Annasaheb Awate Arts, Commerce & Hutatma Babu Genu Science College, Manchar, Pune. He received Ph. D. guide recognition from Savitribai Phule Pune University, Pune. His area of research is mixed metal oxides, ferrite nanomaterials. Presently he is working on Lanthanum substituted mixed metal oxides.



Sharad P. Panchgalle, did his post-graduation in Chemistry from Swami Ramanand Teerth Marathwada University, Nanded in 2001 with second rank in merit order. He received Ph. D. degree from Savitribai Phule Pune University in 2010. In 2010-11, he had worked as post-doctoral researcher with Prof. Alfred Hassner at Bar-Ilan University, Ramat Gan, Israel. Presently, he is working as Assistant Professor in Department of Chemistry, KMC College Khopoli (affiliated to University of Mumbai) since 2012. His area of interest is organocatalysis, total synthesis, chemical biology, heterocycle synthesis through multi-component reactions, etc.

Publisher's Note: Engineered Science Publisher remains neutral with regard to jurisdictional claims in published maps and institutional affiliations.

Exploring the Role of Social Connectedness and Health Anxiety in Predicting Psychological Well-being

Ezaz Shaikh^{1*}, Petare Pratika²

ABSTRACT

Background: Due to COVID-19 pandemic, social distancing was taken as one of the precautionary measure in India. Uncertainty about signs and symptoms, modes of transmission, and lack of definite treatment of COVID-19 have put the mental health of people in India at risk. This study was carried out to explore the role of connectedness, affiliation, and companionship factors of social connectedness and health anxiety in predicting psychological well-being and its components. **Method:** This study was carried out on 317 Indian adults recruited through convenience sampling method during July 2020 to November 2020. Hypotheses were tested using linear regression methods. **Results:** Companionship predicted 1.9% and 7.7% of variance in autonomy and environmental mastery, respectively. Affiliation predicted 6.7% variance in personal growth. Connectedness and companionship explained 26.8% variance of positive relationships with others and 16.1% of self-acceptance. Health anxiety predicted 6.3%, 6.8, 6.7%, 8.3%, and 9% variance of autonomy, environmental mastery, personal growth, positive relationship with others, and self-acceptance, respectively. **Conclusion:** "Connectedness" and "companionship" were the significant predictors of "positive relationships with others" and "self-acceptance." "Companionship" predicted "autonomy" and "environmental mastery," whereas "personal growth" was predicted by "affiliation." Health anxiety predicted all domains of psychological well-being except purpose of life.

Keywords: Companionship, Connectedness, COVID-19, Health anxiety, Psychological well-being

Asian Pac. J. Health Sci., (2022); DOI: 10.21276/apjhs.2022.9.4S1.18

INTRODUCTION

In the year 2020, the highly contaminating COVID-19 virus affected the humans across the globe. In the absence of definite treatment, preventive measures such as hand sanitization, wearing face mask, social distancing, home isolation, and work from home were recommended^[1] which resulted in social disconnectedness.^[2] Even though people were connected digitally, the affiliation needs were compromised. Students from Italian universities attributed their psychological distress to inability to see friends, family, uncertainty, and inability to perform physical activities during lock down.^[3] Due to prolonged social disconnectedness, people reported experience of stress, anxiety, depression, sleep disturbances, and emotional exhaustion which affected psychological well-being.^[4,5]

This uncertain conditions put the individuals with high health anxiety at high risk as they are more likely to be preoccupied with the "fear of illnesses." They pay excessive attention to bodily changes and misinterpret normal cough or cold or fever as the signs of COVID-19^[6,7] which further increase their anxiety that may lead to PTSD and depression.^[8] Social connectedness work as a protective factor against the health anxiety as it helps in reducing the physiological arousal^[9] and preoccupation with bodily sensations.^[10]

Researchers found that better social connectedness leads to better quality of life,^[11] psychological well-being,^[12] and reduced occurrence of depression.^[13] Especially, the quality and quantity of the relationships are positively related with personal meaning, life satisfaction, and positive affect.^[14,15] Whereas poor social connectedness leads to early mortality, depression, low life satisfaction, increased maladaptive behavior, and less purposeful relationships.^[16]

Since the past few decades, humans were exposed to pandemics due to different contagious diseases which threatened their psychological well-being. However, there is paucity of research exploring how different factors of social connectedness affect different domains of psychological well-being. Thus, the present

¹Department of Psychology, Radhabai Kale Mahila Mahavidyalaya, Ahmednagar, Maharashtra, India

²Department of Psychology, Karmaveer Bhaurao Patil College (Autonomous), Vashi, Maharashtra, India

Corresponding Author: Dr. Ezaz Shaikh, Department of Psychology, Radhabai Kale Mahila Mahavidyalaya, Ahmednagar - 414 001, Maharashtra, India. E-mail: ezazpsychologist@gmail.com

How to cite this article: Shaikh E, Pratika P, Exploring the Role of Social Connectedness and Health Anxiety in Predicting Psychological Well-being. *Asian Pac. J. Health Sci.*, 2022;9(4S1):112-116.

Source of support: Nil

Conflicts of interest: None

Received: 01/04/2022 **Revised:** 23/05/2022 **Accepted:** 19/06/2022

study was planned to fill the gap in the relationship between social connectedness and psychological well-being. Further, the role of health anxiety in predicting different domains of psychological well-being was also explored. The findings of this study are expected to use for planning the interventions to reduce the occurrence of health anxiety and promotion of psychological well-being.

MATERIALS AND METHODS

Objectives

The aim of the study was to explore the role of social connectedness and health anxiety in predicting psychological well-being.

Hypotheses

1. Connectedness, affiliation, and companionship factors of social disconnectedness will predict psychological well-being and its different components.

2. Health anxiety will predict psychological well-being and its components.

Sample

Three hundred and seventeen Indian adults were recruited through convenient sampling method, out of which 80.44% females (n = 255). The data were collected through an online survey method from July 2020 to November 2020.

Tools

Social connectedness scale

This eight-item, 5-point Likert scale is developed by Lee and Robbins.^[17] It is used to measure connectedness, affiliation, and companionship. The Cronbach alpha of the scale is.993.

Short health anxiety inventory

This is an 18-items inventory designed by Salkovskis, Rimes, Warwick, and Clark in 2002 to measure the health anxiety among adults.^[18] The respondents are expected to select any one alternative out of four, based on their experience in the past 6 months.

Ryff's psychological well-being scale

This is a 42-items scale measures six components of psychological well-being; namely, autonomy, environmental mastery, personal growth, positive relations, purpose of life, and self-acceptance.^[19]

[Table 1]. Before the regression analysis, outliers were identified using t-residual distributions and Pearson's correlations were conducted between social connectedness variables, health anxiety, and domains of psychological well-being [Table 2].

Hypothesis 1: Connectedness, Affiliation, and Companionship Factors of Social Disconnectedness will Predict Psychological Well-being and its Different Components

The first hypothesis was partially accepted as "companionship" was the only factor that contributed to the variance of the "autonomy" [Table 3]. This may be because people with high companionship do get more social support which increases their perceived control over life. Further, "companionship" was the only predictor of "environmental mastery" as the increased social and emotional support received from the companion helps them to manage challenges resulting from uncertainty and meet the demands resulting from lockdown.

In this study, "affiliation" was found to be the predictor of "personal growth" which states that being affiliated with others can promote personal growth. People who have good relationships not only receive feedback about their strengths but also get the encouragement to pursue their goals. The "positive relationship with others" was successfully predicted by "connectedness" and "companionship." Being connectedness with others makes the relationships more meaningful^[14] and the resulting support received in adverse conditions promotes psychological well-being in people with high connectedness.^[12] "Connectedness" and "companionship" were also the significant predictors of "self-acceptance." Self-acceptance depends on what friends, family, and society think about us. People with high connectedness with others feel that others have accepted them and meaningful relationships with others provide cues that people like us which, in turn, increase the self-acceptance in people with high companionship.^[17]

RESULTS AND DISCUSSION

All analyses were performed using IBM SPSS 23. The data were scrutinized for normality using statistical and graphical methods

Table 1: Descriptive statistics for social connectedness, health anxiety, and psychological well-being variables (n=317)

Variable	Mean	SD	Std. Error	Skewness	Kurtosis	Kolmogorov-Smirnov		
						Statistic	df	Sig.
Connectedness	11.0158	4.04989	0.22746	0.120	-0.902	0.098	317	0.000***
Affiliation	12.6215	3.68738	0.20710	-0.276	-0.621	0.130	317	0.000***
Companionship	7.6782	2.70909	0.15216	-0.065	-0.839	0.137	317	0.000***
Social connectedness	31.3155	9.41189	0.52862	0.001	-0.706	0.053	317	0.035*
Health anxiety	13.9338	8.28557	0.46536	0.731	-0.033	0.093	317	0.000***
Autonomy	14.9527	3.05658	0.17167	-0.274	0.642	0.125	317	0.000***
Environmental mastery	14.6025	3.20202	0.17984	-0.537	0.804	0.125	317	0.000***
Personal growth	17.0032	3.18074	0.17865	-0.590	0.315	0.114	317	0.000***
Positive relationship with others	13.5868	4.15707	0.23348	0.198	-1.003	0.109	317	0.000***
Purpose of life	13.5363	3.50083	0.19663	0.153	-0.503	0.089	317	0.000***
Self-acceptance	15.7981	3.43800	0.19310	-0.576	0.468	0.105	317	0.000***
Psychological well-being	89.4795	13.32566	0.74844	0.191	-0.259	0.060	317	0.007**

P<0.01, *P<0.001

Table 2: Correlation of components of social connectedness and health anxiety with domains of psychological well-being (n=317)

Variables	Connectedness	Affiliation	Companionship	Social connectedness	Health anxiety
Autonomy	0.098	0.104	0.165**	0.130*	-0.257**
Environmental Mastery	0.267**	0.192*	0.274**	0.269**	-0.261**
Personal Growth	0.238**	0.263**	0.232**	0.272**	-0.265**
Positive Relationship with Others	0.463**	0.441**	0.50**	0.516**	-0.293**
Purpose of Life	0.113*	0.180**	0.165**	0.166**	-0.057
Self-Acceptance	0.372**	0.278**	0.391**	0.382**	-0.305**
Psychological Well-being	0.413**	0.389**	0.459**	0.463**	-0.370**

*P<0.05, **P<0.01

Table 3: Beta coefficient for connectedness, affiliation, and companionship when psychological well-being and its components were dependent variables

Variations	Dependent Variables	Unstandardized coefficients		Standardized coefficients	t	Adjusted R ²
		B	Std. Error	Beta		
(Constant)	Autonomy	13.652	0.616		22.151	0.019
Connectedness		-0.042	0.068	-0.055	-0.617	
Affiliation		-0.005	0.070	-0.006	-0.075	
Companionship		0.238	0.103	0.211	2.318*	0.077
(Constant)	Environmental	12.066	0.627		19.258	
Connectedness	Mastery	0.130	0.069	0.164	1.887	
Affiliation		-0.051	0.071	-0.058	-0.713	0.067
Companionship		0.228	0.104	0.193	2.180*	
(Constant)	Personal Growth	13.984	0.626		22.356	
Connectedness		0.064	0.069	0.082	0.937	0.268
Affiliation		0.147	0.071	0.170	2.069*	
Companionship		0.060	0.104	0.051	0.575	
(Constant)	Positive Relationship with Others	6.574	0.724		9.077	0.028
Connectedness		0.159	0.079	0.155	2.008*	
Affiliation		0.139	0.082	0.124	1.698	
Companionship		0.456	0.121	0.297	3.775**	0.161
(Constant)	Purpose of Life	11.311	0.703		16.098	
Connectedness		-0.070	0.077	-0.081	-0.912	
Affiliation		0.145	0.080	0.153	1.823	0.218
Companionship		0.152	0.117	0.118	1.300	
(Constant)	Self-Acceptances	11.878	0.641		18.524	
Connectedness		0.175	0.070	0.206	2.490*	0.063
Affiliation		-0.060	0.073	-0.064	-0.825	
Companionship		0.358	0.107	0.282	3.350**	
(Constant)	Psychological Well-being	69.464	2.399		28.952	0.134
Connectedness		0.417	0.263	0.127	1.583	
Affiliation		0.315	0.272	0.087	1.159	
Companionship		1.491	0.400	0.303	3.730***	

*P<0.05, **P<0.01, ***P<0.001

Table 4: Beta coefficient for health anxiety when psychological well-being components were dependent variables

Variations	Dependent variables	Unstandardized coefficients		Standardized coefficients	t	Adjusted R ²
		B	Std. Error	Beta		
(Constant)	Autonomy	16.271	0.326		49.982	0.063
Health Anxiety		-0.095	0.020	-0.257	-2.711***	
(Constant)	Environmental	16.009	0.341		47.002	0.068
Health Anxiety	Mastery	-0.101	0.021	-0.261	-4.801***	
(Constant)	Personal Growth	18.421	0.338		54.508	0.067
Health Anxiety		-0.102	0.021	-0.265	-4.880***	
(Constant)	Positive Relationship with Others	15.635	0.438		35.70	0.083
Health Anxiety		-0.147	0.027	-0.293	-5.44***	
(Constant)	Purpose of Life	13.872	0.385		36.018	0.000
Health Anxiety		-0.024	0.024	-0.057	-1.014	
(Constant)	Self-Acceptances	17.560	0.361		48.667	0.090
Health Anxiety		-0.126	0.022	-0.305	-5.679***	
(Constant)	Psychological Well-being	97.769	1.364		71.665	0.134
Health Anxiety		-0.595	0.084	-0.370	-7.066***	

**P<0.001

In this study, the domains of social connectedness did not found to predict "purpose of life." This result was contradicted with the findings reported by Eraslan-Capan^[14] and Kaminski *et al.*^[20] which states that people with high social connectedness have good psychological well-being as it makes the relationship meaningful and purposeful.

Companionship was the only factor that played a significant role in predicting overall psychological well-being of the participants. The results of this study were supported by the findings stating that social connectedness leads to better psychological outcomes, quality of life, and psychological well-being.^[11,21]

Hypothesis 2: Health Anxiety will Predict Psychological Well-being and its Components

The second hypothesis was partially accepted as health anxiety was found to be a significant predictor of all components of psychological well-being except purpose of life [Table 4]. It was found that increased health anxiety reduces the "autonomy" due to difficulties in taking decisions and acting on them during pandemic. Because of the restrictions imposed on the movements outside one's own house, except emergencies and medical reasons, to prevent the spread of COVID-19, people with high

health anxiety were unable to meet health professional to seek reassurance regarding their health status. In pandemic, individuals with high health anxiety experienced low mastery over their immediate environment. This is due to their perceived lack of control over the amount and type of information shared on social media regarding COVID-19 which was the source of their increased anxiety.^[22,23]

In pandemic, the priority of the people was to survival rather than self-growth. It is especially true for people with high health anxiety. Due to their intense survival instinct, they focused more on their internal body changes to detect early signs and symptoms of COVID-19 and prevent its adverse consequences than personal goals and aspirations. With the excessive engagement with their health, they had less time to think and plan about their goals.^[5]

In the first and the second wave of COVID-19, uncertainty about signs and symptoms, its changing nature, and modes of spreading had increased fear in people. The condition was worst for people with high health anxiety. In their efforts to protect themselves from the infection, they start perceiving every individual as a carrier or spreader of COVID-19. They had adopted an extreme level of self-isolation and preferred to avoid going into the public gatherings, funerals, and marriage ceremonies of their relatives. This had affected the quality of relationships with others and this in turn reduced the psychological well-being in people with higher health anxiety.^[2]

The health anxiety had reduced the "self-acceptance" in participants as they prone to pay more attention to their weaknesses than strengths and they also had low self-confidence due to inability to control fear of being infected.^[5]

CONCLUSIONS

1. Companionship predicted autonomy and environmental mastery.
2. Affiliation predicted personal growth.
3. Positive relationships with others and self-acceptance were predicted by connectedness and companionship.
4. Health anxiety was the significant predictor of autonomy, environmental mastery, personal growth, positive relationship with others, and self-acceptance.

Limitations

The results drawn from the study could be compromised due to its limitations such as: Use of self-report measures and online survey methods for collection of data. The finding is also limited due to the use of convenience sampling methods and overrepresentation of female participants. This study did not examine the positive outcomes resulting from the health anxiety during the pandemic such as protecting one's health from highly infectious illness. Mediating or moderating role of social connectedness in predicting the relationship of health anxiety and psychological well-being was not explored.

Recommendations

Qualitative methods such as structured interviews can provide more detailed information regarding the nature of social connectedness, health anxiety, and psychological well-being as experienced by the participants. Longitudinal research can

provide more fruitful information regarding changes in social connectedness, health anxiety, and psychological well-being and changes in their interrelationships during the different stages of pandemic. The research can be conducted to evaluate the protective role of health anxiety during pandemic conditions.

REFERENCES

1. World Health Organization. Coronavirus Disease. COVID-2019 Situation Reports. Geneva: World Health Organization. Available from: <https://www.who.int/emergencies/diseases/novel-coronavirus-2019/situation-reports> [Last accessed on 2019 Mar 27].
2. Matias T, Dominski FH, Marks DF. Human needs in COVID-19 isolation. *J Health Psychol* 2020;25:871-82.
3. Villani L, Pastorino R, Molinari E, Anelli F, Ricciardi W, Graffigna G, *et al.* Impact of the COVID-19 pandemic on psychological well-being of students in an Italian university: A web-based cross-sectional survey. *Global Health* 2021;17:39.
4. Singh R, Bajpai R, Kaswan P. COVID-19 pandemic and psychological wellbeing among health care workers and general population: A systematic-review and meta-analysis of the current evidence from India. *Clin Epidemiol Glob Health* 2021;11:100737.
5. Brooks SK, Webster RK, Smith LE, Woodland L, Wessely S, Greenberg N, *et al.* The psychological impact of quarantine and how to reduce it: Rapid review of the evidence. *Lancet* 2020;395:912-20.
6. Asmundson GJ Taylor S. How health anxiety influences responses to viral outbreaks like COVID-19: What all decision-makers, health authorities, and health care professionals need to know. *J Anxiety Disord* 2020;71:102211.
7. Rajkumar RP. COVID-19 and mental health: A review of the existing literature. *Asian J Psychiatr* 2020;52:102066.
8. Ahorsu DK, Lin CY, Imani V, Saffari M, Griffiths MD, Pakpour AH. The fear of COVID-19 Scale: Development and initial validation. *Int J Ment Health Addict* 2022;20:1537-45.
9. Cohen S, Wills TA. Stress social support, and the buffering hypothesis. *Psychol Bull* 1985;98:310-57.
10. Jetten J, Haslam SA, Cruwys T, Greenaway KH, Haslam C, Steffens NK. Advancing the social identity approach to health and well-being: Progressing the social cure research agenda. *Eur J Social Psychol* 2017;47:789-802.
11. Gillison F, Standage M, Skevington S. Changes in quality of life and psychological need satisfaction following the transition to secondary school. *Br J Educ Psychol* 2008;78:149-62.
12. Horn R. Exploring Psychosocial Well-Being and Social Connectedness in Northern Uganda. *Logica Working Paper Series*; no. 2. Washington, DC: World Bank; 2013.
13. Cruwys T, Dingle GA, Haslam C, Haslam SA, Jetten J, Morton TA. Social group memberships protect against future depression, alleviate depression symptoms and prevent depression relapse. *Soc Sci Med* 2013;98:179-86.
14. Eraslan-Capan B. Social connectedness and flourishing: The mediating role of hopelessness. *Univ J Educ Res* 2016;4:933-40.
15. Jose P, Ryan N, Pryor J. Does social connectedness promote a greater sense of well-being in adolescent over time? *J Res Adolesc* 2012;22:235-51.
16. Patterson AC, Veenstra G. Loneliness and risk of mortality: A longitudinal investigation in Alameda county, California. *Soc Sci Med* 2010;71:181-6.
17. Lee R, Robbins S. Measuring belongingness: The social connectedness and the social assurance scale. *J Couns Psychol* 1995;42:232-41.
18. Salkovskis PM, Rimes KA, Warwick HM, Clark DM. The health anxiety inventory: Development and validation of scales for the measurement of health anxiety and hypochondriasis. *Psychol Med* 2002;32:843-53.
19. Ryff CD. Psychological well-being in adult life. *Curr Dir Psychol Sci* 1995;4:99-104.

20. Kaminski JW, Puddy RW, Hall DM, Cashman SY, Crosby AE, Ortega LA. The relative influence of different domains of social connectedness on self-directed violence in adolescent. *J Youth Adolesc* 2010;39:460-73.
21. Tuason MT, Güss CD, Boyd L. Thriving during COVID-19: Predictors of psychological well-being and ways of coping. *PLoS One* 2021;16:e0248591.
22. Gao J, Zheng P, Jia Y, Chen H, Mao Y, Chen S, *et al.* Mental health problems and social media exposure during COVID-19 outbreak. *PLoS One* 2020;15:e0231924.
23. Garfin DR, Silver RC, Holman EA. The novel coronavirus (COVID-2019) outbreak: Amplification of public health consequences by media exposure. *Health Psychol* 2020;39:355-7.

Development and Validation of Attitudes and Concerns toward COVID-19 Vaccination Scale

Ezaz Shaikh^{1*}, Petare Pratika²

ABSTRACT

Background: COVID-19 vaccines are one of the fastest developed vaccines to date. People have different views and opinions about it. A positive attitude can strengthen the vaccination program, whereas a negative attitude will be an obstacle for a healthy and safe nation. This study aimed at developing and validating the Attitudes and Concerns toward the COVID-19 vaccination. **Methods:** Initial draft of 48 items was developed based on literature review and interview of experts. After content validation with four experts and semantic validation with 20 respondents, 32 items were retained and administered to 607 Indian adults aged 18–60 years. **Results:** Data were analyzed by IBM-SPSS Version-23 with AMOS. Exploratory factor analysis supported the two-factor structure for the attitude toward COVID-19 vaccination and three factors structure for the concern domain. Cronbach alpha for “Vaccine Acceptance” and “Vaccine Hesitance” was .825 and .721. The reliability of religious concerns ($\alpha = 0.785$), social concerns ($\alpha = 0.714$), and health concern ($\alpha = 0.699$) subscales was acceptable. The confirmatory factor analysis results verified two-factor model of attitude and three-factor model of concerns as the model indices were close to 1; RMSEA was 0.000 and PCLOSE values were 0.861 and 0.927, respectively, for Parts I and II. **Conclusion:** This is 12-item scale that measures vaccine acceptance, vaccine hesitance, religious concerns, social concerns, and health concerns related to COVID-19 vaccination.

Keywords: Attitude, Concerns, COVID-19, Scale, Vaccination

Asian Pac. J. Health Sci., (2022); DOI: 10.21276/apjhs.2022.9.451.17

INTRODUCTION

Vaccination is an important tool in the prevention of infectious diseases. Although vaccine development requires years of research; due to the highly contaminating nature of COVID-19, it was taken at the war front priority to develop herd immunity. COVID-19 vaccines are one of the fastest developed vaccines till date. However, the control of COVID-19 depends on effective implementation of vaccination programs, especially, in India, due to its large population, sociocultural and economic diversity, educational backwardness, and inequality in the access to health care services.^[1] In addition, the attitude of people is also hindering factor in the effective implementation of vaccination program.

Although scientists are certain about the benefits of COVID-19 vaccines, people at large have found to hold different views and opinions about it. The positive attitude toward the vaccine facilitates the government's initiative of effective implementation of the vaccination program for prevention and control of COVID-19 spread; whereas the unfavorable attitude toward vaccines, known as “vaccine reluctance” or “vaccine refusal,” is an obstacle in meeting the goal of a healthy and safe nation. The WHO had also listed the vaccine hesitancy as one of the ten threats to global health in 2019.^[2]

Researchers have used unstandardized questionnaires and semi-structured interviews to study “what people think about COVID-19 vaccination?” However, they focused on average acceptance rate of COVID-19 vaccines and the age, knowledge, and employment status wise differences in vaccine acceptance and vaccine hesitancy. A study conducted in America before the introduction of COVID-19 vaccine reported that 30% participants were unsure about the vaccination and 10% participants did not intend to get vaccinated.^[3] Other studies found higher acceptance rate (61%) for adults, but unacceptance of vaccination for the children attending school (38.4%) in their respondents.^[4,5] In a study of 3100 participants from Jordan, only 37% showed willingness to get vaccinated.^[6]

¹Department of Psychology, Radhabai Kale Mahila Mahavidyalaya, Ahmednagar, Maharashtra, India

²Department of Psychology, Karmaveer Bhaurao Patil College (Autonomous), Vashi, Maharashtra, India

Corresponding Author: Dr. Ezaz Shaikh, Department of Psychology, Radhabai Kale Mahila Mahavidyalaya, Ahmednagar - 414 001, Maharashtra, India E-mail: ezazpsychologist@gmail.com

How to cite this article: Shaikh E, Pratika P. Development and Validation of Attitudes and Concerns toward COVID-19 Vaccination Scale. *Asian Pac. J. Health Sci.*, 2022;9(451):107-111.

Source of support: Nil

Conflicts of interest: None

Received: 01/04/2022 **Revised:** 18/05/2022 **Accepted:** 20/06/2022

In India, the vaccine acceptance rate was ranged from 35% to 69% and the vaccine hesitancy ranged from 3.4% to 10%.^[7-10] These studies reported lower vaccine hesitancy compared with other countries. A study of 944 Indians found 69% acceptance rate and 3.4% vaccine hesitancy among their participants.^[7,8] Another study reported that 70% participants had concerns regarding COVID-19 vaccine, 10% refuse to take vaccine, and 27% were not sure if they would get the vaccine.^[9] Praveen, Ittamalla, and Deepak found positive attitudes toward vaccination in 35% participants.^[10] However, the findings of these studies are not directly comparable due to the differences in their research methodology, sample size and characteristics, and tools used to assess vaccine acceptance and refusal.

Eniola and Sykes reported four reasons of vaccine hesitancy among health-care workers, namely, (a) safety and efficacy concerns, (b) preference for physiological immunity, (c) distrust in government and health organizations, and (d) autonomy and personal freedom.^[11] Other studies showed that fear of ill health, lack of trust, less information on vaccine, and allergic reactions

were most commonly cited reasons for negative attitudes.^[4,7,8] Similarly, demographic, social, and contextual constructs were also associated with intention to vaccinate among the adult population.^[3,5]

Thus, in the background of highly contaminating and mutating COVID-19 virus and the unavailability of standardized tool to measure the attitude and concerns of Indian adults toward COVID-19 vaccination, the present study was undertaken to develop a short, standardized, and valid tool to assess the individual's attitudes and concerns toward COVID-19 vaccination among Indian adults. In India, this scale can be used to identify the attitude as well as concerns of Indian adults toward COVID-19 vaccination. The results of the future studies based on this scale can be useful in planning the vaccination programs and development of intervention programs addressing the specific concerns of people.

MATERIALS AND METHODS

Item Generation

Literature review was conducted through Google scholar, Research Gate, PubMed, and Directory of Open Access Journals using "vaccine attitude," "COVID-19 scale," and "vaccination scale" as keywords. In addition, individual interviews of two medical professionals, two psychologists, and three people from the community were conducted. Based on the themes identified, the initial item pool consists of 48 items, which was created to measure vaccine acceptance, vaccine hesitancy, social concerns, physical health concerns, psychological health concerns, financial concerns, and religious concerns. Response for each item is ranged on five-point Likert scale from "strongly disagree" to "strongly agree."

Content Validation

Four experienced experts in the field of Psychology with master or doctoral degrees assessed each on a four-point Likert scale regarding the relevance of item to each domain and provided feedback for omission of item, adding the item and rephrasing the item to improve the respondents understanding. Sixteen items with $i\text{-CVI} < 0.70$ were omitted and four items were revised.

Semantic Validation

To identify the difficulties of the respondents in understanding the meaning of the statements/items due to their educational, cultural, and religious background, the draft of 32 items was shared with 20 respondents.^[12] Based on their feedback, three statements were rephrased. The participants involved in the semantic validation procedure were excluded from the final data collection phase.

Scale Description

The 32 items were divided into two parts; ten items in first part measure attitudes toward COVID-19 vaccination; and 22 items from the second part were measuring five concerns related to COVID-19 vaccination, that is, social, physical health, psychological health, financial, and religious concerns. Statements were both positively and negatively framed for different domains and arranged randomly to prevent rating errors. Items seeking

information about demographic characteristics were placed at the end to avoid the effect of social desirability.

Ethical Consideration

The study was approved by the Institutional Ethics and Research Promotion Committee. The consent for the participation was obtained from all participants before the start of this study. They were informed that their participation in the study is voluntary and they can withdraw from the study at any point of time. They were also informed that the participation in this study does not cause physical or psychological harm. Participants did not receive direct or indirect monetary benefits. They were assured that confidentiality of their responses and its uses.

Data Collection

The data were collected during the second wave of COVID-19 between June 1, 2021, and July 30, 2021, from 607 Indian adults aged 18–60 years [Table 1]. The participants were selected from the community by the Snowball sampling method. To reduce the possibility of giving socially desirable responses and increase the reliability of responses, the data were collected anonymously.

RESULTS

The obtained data were closely scrutinized to check the random responding and missing data. Few items were reverse coded before calculating the item score and scale score. The data were analyzed using IBM SPSS version 23 with AMOS. The respondents were randomly split into two groups;^[12] the first group of 302 respondents was used to perform the Exploratory Factor Analysis (EFA) and the second group of 305 respondents was used to validate the results of the EFA by performing Confirmatory Factor Analysis (CFA).

Two EFA was performed separately for *part-I*, general attitude toward COVID-19 Vaccine and *part-II*, concern toward COVID-19 vaccine using Principal Axis Factoring (PAF) method of factor extraction^[13] and Varimax rotation method. The sample was much higher than recommended sample size.^[14-17] The items with Pearson r correlation coefficient > 0.7 (to avoid redundant

Table 1: Demographic characteristics of the participants ($n=607$)

Gender	
Female	452 (74.5%)
Male	155 (25.5%)
Marital status	
Unmarried	509 (83.85%)
Married	96 (15.82%)
Widow/Widower	02 (0.33)
Religion	
Hindu	431 (71%)
Islam	84 (13.84%)
Christian	34 (5.60%)
Buddhism	30 (4.94%)
Jain	09 (1.48%)
Atheist	09 (1.48%)
Sikh	07 (1.15%)
Other	03 (0.49%)
Status related to COVID-19	
I never suffered from COVID-19	482 (79.4%)
I had suffered from COVID-19	67 (11.04%)
I Did not get diagnosed but had symptoms of COVID-19 (testing was not done)	58 (9.56%)

Table 2: Factor loadings, communalities, and internal consistency results for attitude towards COVID-19 vaccination

Items	F1	F2	Communality	Factor Name	Mean (SD)	Cronbach's α
I would recommend my family members and friends to get a vaccine for COVID-19.	0.743		0.507	Vaccine Acceptance	3.76 (1.03)	0.825
If I get the chance, I will get a vaccine to prevent COVID-19 infection.	0.693		0.483			
COVID-19 Vaccine strengthens immune system response against COVID-19.	0.691		0.408			
I'm happy to hear that scientist have developed a vaccine for COVID-19.	0.616		0.344			
COVID-19 Vaccination can protect me and my family from COVID-19 infection.	0.610		0.404			
I'm disappointed by the effects of COVID-19 vaccine.		0.702	0.326	Vaccine Hesitance	4.19 (0.885)	0.721
Even if it is free, I will not take COVID-19 vaccine.		0.647	0.399			
COVID-19 vaccine is causing serious side effects.		0.612	0.273			

Table 3: Factor loadings, communalities, and internal consistency results for Attitude towards COVID-19 vaccination

Item	Vaccine acceptance	Vaccine hesitance	Communality	Mean (SD)
COVID-19 Vaccine strengthens immune system response against COVID-19.	0.794		0.643	4.14 (0.836)
I would recommend my family members and friends to get vaccine for COVID-19.	0.743		0.628	
COVID-19 Vaccination can protect me and my family from COVID-19 infection.	0.723		0.555	
COVID-19 vaccine is causing serious side effects.		0.836	0.719	3.542 (1.05)
I'm disappointed by the effects of COVID-19 vaccine.		0.825	0.702	

Table 4: The goodness of fit indexes of confirmatory factor analysis

χ^2	GFI	AGFI	NFI	CFI	RFI	IFI	RMSEA	PCLOSE
2.568	0.997	0.987	0.990	1.00	0.974	1.00	0.000	0.861

items), factor loading <0.60, and cross loading of >0.30 on other factor/s were omitted. The criterion for factor extraction was the Eigenvalue >1, Scree plot, and parallel analysis.

Part I: Attitudes toward COVID-19 Vaccination

EFA

The result of Kaiser–Meyer–Olkin (KMO) was.838 (meritorious)^[12] and the Bartlett’s test was also significant ($\chi^2 = 774.450, P = 0.000$). Statements with low factor loading (<0.40) were omitted, that is, “Vaccine is the only protective shield available against COVID-19” and “I will prefer alternative ways rather than getting vaccine for COVID-19” [Table 2].

The PAF method revealed the two factors with Eigenvalue higher >1, that is, positive attitude and negative attitude. They explained 30.04% and 18.74% of variance, respectively, and 48.774% total variance. Five statements had higher loading on factor 1 and three statements had higher loading on factor 2. After analyzing the meaning of the statements, the factors were named as “Vaccine Acceptance” and “Vaccine Hesitance.” The reliability of internal consistency for “Vaccine Acceptance” subscale was good, that is, .825 and “Vaccine Hesitance” subscale was acceptable, that is, 0.721. The overall scale had good internal consistency ($\alpha = 0.819$).

Confirmatory factor analysis

The validity of two-factor model of attitudes toward COVID-19 vaccination, that is, “Vaccine Acceptance” and “Vaccine Hesitance” was tested with CFA performed in AMOS ($n = 305$). The results

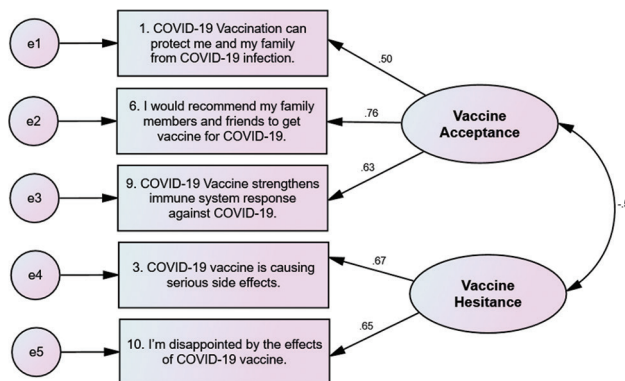


Figure 1: Standardized factor loadings and correlations among vaccine acceptance and vaccine hesitance

revealed that KMO test was 0.717, that is, middling^[18] Bartlett’s test that was also significant ($\chi = 0.248, P = 0.000$). Statement “Even if it is free, I will not take COVID-19 vaccine” was omitted due to higher cross-loading. Statements such as “If I get the chance, I will get a vaccine to prevent COVID-19 infection” and “I’m happy to hear that scientist has developed a vaccine for COVID-19” were deleted, because their >1 standardized residual covariance. Remaining five statements were retained in final model; three statements contributing to “vaccine acceptance” and two statements loading on “vaccine hesitance.” Vaccine acceptance had explained 44.79% variance and vaccine hesitance explained 20.17% variance. These two factors had explained 64.96% of total variance. The result of model fit indices revealed that values of GFI, AGFI, NFI, and RFI were more than 0.97. The values of CFI and IFI were exactly 1.00. Further, RMSEA was <0.05, that is, 0.000 and PCLOSE value was 0.861 [Tables 3 and 4] [Figure 1].

Table 5: Factor loadings, communalities, and internal consistency results for concerns related to COVID-19 vaccine

Items	F1	F2	F3	Communality	Factor Name	Mean (SD)	Cronbach's α
COVID-19 vaccine contain the ingredient that are not permitted in my religion	0.748			0.408	Religious Concerns	1.863 (1.025)	0.785
Religious rituals may protect me from COVID-19 infection than the vaccine.	0.680			0.581			
After COVID-19 vaccination, I won't be able to perform my routine religious rituals.	0.650			0.512			
My religious beliefs don't permit me to take vaccine.	0.607			0.489	Social Concerns	2.456 (1.024)	0.714
COVID-19 vaccine will bring my social life back to its earlier state.		0.728		0.415			
COVID-19 vaccine will help me enjoy social gatherings.		0.641		0.550			
COVID-19 vaccine will make me more connected with people around me.		0.640		0.414			
COVID-19 vaccine may increase the risk of heart disease.			0.705	0.496	Health Concerns	2.258 (0.882)	0.699
COVID-19 vaccine may cause diabetes.			0.655	0.580			

Table 6: Factor loadings, communalities, and internal consistency results for concerns related to COVID-19 vaccine

Items	F1	F2	F3	Communality	Factor Name	Mean (SD)
COVID-19 vaccine contain the ingredient that are not permitted in my religion	0.750			0.602	Religious Concerns	1.884 (0.996)
After COVID-19 vaccination, I won't be able to perform my routine religious rituals.	0.693			0.603		
COVID-19 vaccine will bring my social life back to its earlier state.		0.716		0.418	Social Concerns	2.46 (0.990)
COVID-19 vaccine will help me enjoy social gatherings.		0.641		0.519		
COVID-19 vaccine will make me more connected with people around me.		0.625		0.397		
COVID-19 vaccine may increase the risk of heart disease.			0.761	0.617	Health Concerns	2.29 (0.856)
COVID-19 vaccine may cause diabetes.			0.637	0.474		

Table 7: The goodness of fit indexes for concerns related to COVID-19 vaccine

χ^2	GFI	AGFI	NFI	CFI	RFI	IFI	RMSEA	PCLOSE
9.685	0.991	0.978	0.977	1.00	0.957	1.00	0.000	0.927

with each other (r 's ranging from 0.239 to 0.529) indicate that concerns are unaffected by each other [Table 5].

The reliability of religious concerns ($\alpha = 0.785$), social concerns ($\alpha = 0.714$) and health concern ($\alpha = 0.699$) subscales was acceptable and the alpha coefficient of the overall test was 0.728.

Part II: Concerns toward COVID-19 Vaccination

EFA

For the Second Part of the Scale, KMO test value was middling, that is, 0.759^[18] and Bartlett's test was also significant ($\chi^2 = 703.50, P = 0.000$). "COVID-19 vaccine will make me impotent/infertile" was omitted due to loading on the wrong dimension. "COVID-19 vaccine may reduce my life expectancy" and "COVID-19 vaccine may increase the risk of being infected with COVID-19 virus" were deleted due to high cross loading. Further, eight items designed to measure economic and psychological concerns were also omitted due to very low factor loading. There were three factors with Eigenvalues >1 as shown in scree plot and those exceeded their parallel factors' average eigenvalues. The PAF method revealed the three factors explained 27.70, 15.76%, and 5.93% of variance and 49.39% of total variance. After examining the content of the items, first factor (F1) was named as the "religious concerns," second factor (F2) as the "social concerns," and third factor (F3) as "health concerns." The items best reflected underlying subscales were retained regardless of the direction of their wording. The association among the subscales was examined and it was found that they had weak to moderate correlation

Confirmatory factor analysis

The CFA was conducted in AMOS to validate three factor structures about concerns related to COVID-19 vaccination. The KMO test results (0.767, i.e., middling) supported the adequacy of the sample size^[16] and Bartlett's test ($\chi = 0.758.623, P = 0.000$) was significant too. Statements such as "My religious beliefs don't permit me to take vaccine" and "Religious rituals may protect me from COVID-19 infection than the vaccine" were omitted from the model before assessing the model fit, because >1 standardized residual covariance. Inter correlation between the factors was <0.50. The religious concerns explained highest, that is, 28.49% variance, followed by social concern (15.75%) and health concern (7.43%). The total variance explained by these three factors was 51.66%. The model fit indices revealed that the values of GFI, AGFI, NFI, and RFI are more than 0.95. The values of CFI and IFI are exactly 1.00. Further, RMSEA is <0.05, that is, 0.000 and PCLOSE value is 0.927 [Tables 6 and 7].

Figure 2 denotes the graphical representation of the standardized factor loadings and correlations among religious, social, and health concern. The figure indicated that all the loadings were positive and higher than 0.60. The correlation between the religious concerns and health concern was moderately positive ($r = 0.51$) and significant ($P = 0.05$) and the relationship between

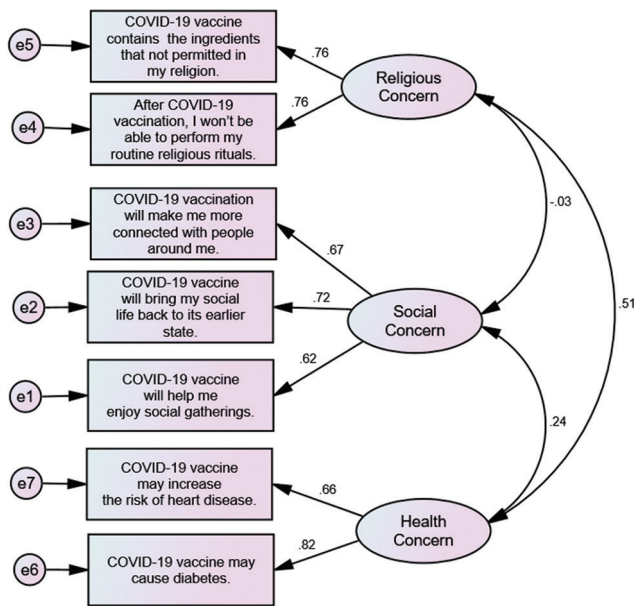


Figure 2: Standardized factor loadings and correlations among religious, social, and health concern

social concern and health concern ($r = 0.24$) was also significant at 0.05.

CONCLUSION

This 12-item scale is a short, simple, valid, reliable, and easy to administer measure of attitudes and concerns toward COVID-19 vaccination. The scale measures vaccine acceptance, vaccine hesitancy, religious, social, and health concerns related COVID-19 vaccination.

Approval for the Study

The Institutional Research Advisory and Ethics Committee of Radhabai Kale Mahila Mahavidyalaya, Ahmednagar has provided permission to carry out this study.

ACKNOWLEDGMENT

We are thankful to the experts for their evaluation contribution in item development and content validation phase. We are also thankful to the participants for their valuable feedback during semantic validation phase.

REFERENCES

1. Acquilla S, Sibal B, Shukla H, Mathews S, Rai GK, Lakhanpaul M. SARS-CoV-2 (COVID-19) and the lessons learned from global pandemic. *Indian J Public Health* 2021;65:215-7.
2. World Health Organization. Ten Threats to Global Health in 2019. Geneva: World Health Organization. Available from: <https://www.who.int/news-room/spotlight/ten-threats-to-global-health-in-2019> [Last accessed on 2021 Dec 28].
3. AlShurman BA, Khan AF, Mac C, Majeed M, Butt ZA. What demographic, social, and contextual factors influence the intention to use COVID-19 vaccines: A scoping review. *Int J Environ Res Public Health* 2019;18:9342.
4. Fisher KA, Bloomstone SJ, Walder J, Crawford S, Fouayzi H, Mazor KM. Attitudes toward a potential SARS-CoV-2 vaccine: A survey of U.S. adults. *Ann Intern Med* 2020;173:964-73.
5. Largent EA, Persad G, Sangenito S, Glickman A, Boyle C, Emanuel EJ. US public attitudes toward COVID-19 vaccine mandates. *JAMA Netw Open* 2020;3:e2033324.
6. El-Elimat T, AbuAlSamen MM, Almomani BA, Al-Sawalha NA, Alali FQ. Acceptance and attitudes toward COVID-19 vaccines: A cross-sectional study from Jordan. *PLoS One* 2021;16:e0250555.
7. Dasgupta R, Mishra P, Yadav K. COVID-19 vaccination and the power of rumors: Why we must "Tune in". *Indian J Public Health* 2021;65:206-8.
8. Garg SR, Singh G, Tailor SK, Yadav C. Acceptance and attitude toward covid-19 vaccination: A cross-sectional study from Udaipur district. *Int J Adv Res* 2021;9:621-8.
9. Chandani S, Jani D, Sahu PK, Kataria U, Suryawanshi S, Khubchandani J, et al. COVID-19 vaccination hesitancy in India: State of the nation and priorities for research. *Brain Behav Immun Health* 2021;18:100375.
10. Praveen SV, Ittamalla R, Deepak G. Analyzing the attitude of Indian citizens towards COVID-19 vaccine-a text analytics study. *Diabetes Metab Syndr* 2021;15:595-9.
11. Eniola K, Sykes J. Four Reasons for COVID-19 Vaccine Hesitancy among Health Care Workers, and Ways to Counter Them. *FPM J*. Available from https://www.aafp.org/journals/fpm/blogs/inpractice/entry/countering_vaccine_hesitancy.html. [Last accessed on 2021 December 29].
12. Hair JF Jr., Gabriel M, Da Silva D, Junior SB. Development and validation of attitudes measurement scales: Fundamental and practical aspects. *RAUSP Manag J* 2019;54:490-507.
13. Fabrigar LR, Wegener DT, MacCallum RC, Strahan EJ. Evaluating the use of exploratory factor analysis in psychological research. *Psychol Methods* 1999;4:272-99.
14. Hair JF, Black, WC, Babin, BJ, Anderson RE. *Multivariate Data Analysis*. 8th ed. Hampshire: Cengage Learning; 2018.
15. Gorsuch RL. *Factor Analysis*. 2nd ed. Hillsdale, NJ: Lawrence Erlbaum; 1983.
16. Henson RK, Robert JK. Use of explorative factor analysis in published research: Common errors and some comment on improved practice. *Educ Psychol Meas* 2006;66:393-416.
17. Comrey AL, Lee HB. *A First Course in Factor Analysis*. Hillsdale, NJ: Lawrence Erlbaum Associates; 1992.
18. Kaiser HF, Rice J. Little Jiffy, Mark Iv. *Educ Psychol Meas* 1974;34:111-7.

PARADIGM SHIFT DUE TO PANDEMIC IN EMPLOYEE ENGAGEMENT

Dr. Nikam Vijay Balkrishna

Assistant Professor and Vice Principal, Department of Commerce and Management
S.S.G.M. College Kopergaon, Email. :- nikamvb23382@gmail.com

Dr. Teltumbade Ganesh Ramesh

Associate Professor, I/c Director, MGV's Institute of Management and Research, Panchavati,
Nashik, Email. :- teltumbadeganesh@gmail.com

Dr Chavan Vishal Dilip

Associate Professor Sanjivani College of Engineering (MBA) , Kopergaon
Email- yeshwishall123@gmail.com

Abstract:-

Worldwide COVID and pandemic affect on various sectors and segment. Some sectors and industries are totally changed due to pandemic and lockdown situation. Industries like education, constructions, tourism and unorganised sectors affect badly due to lockdown and COVID. Whereas paradigm shift observed in healthcare sector which create huge demand in the form of revenue and employment.

But various industries & sectors were faced difficulties in Employee engagement at their end during pandemic and lockdown period. Manufacturing industries suffer more in the same duration in Employee engagement. As per research it is found that only 17% of employees are engaged with their work in manufacturing industries.

In this research study researcher would like to analyze the contemporary issues in employee engagement practices in manufacturing industries of Nashik Districts. Also researcher tried to focus on key tools to improve employee engagement in manufacturing industries of Nashik districts.

Keywords- Employee Engagement, Pandemic, & COVID19

• Introduction

Success of any sector or industry is totally upon their workforce and personnel; one can increase the productivity & performance of business by giving motivation to employee. Indirectly employee is human capital of any organisation that can lead and sustain the business in any conditions. One should nourish & nurture these human capitals by providing them training, education, skills, healthy environment, intelligence and power which creates corporate values among them to be loyal and punctual towards their duties and responsibilities.

Employee engagement is affected by many factors which broadly categorised in emotional and rational factors both are based upon work experience and current work status. According to study conducted in 2003 by Perrin's Global Workforce employee engagement means "employees' willingness and ability to help their company succeed, largely by providing discretionary effort on a sustainable basis." Robinson et al. (2004) define employee engagement as "a positive attitude held by the employee towards the organization and its value. An engaged employee is aware of business context, and works with colleagues to improve performance within the job for the benefit of the

organization. The organization must work to develop and nurture engagement, which requires a two-way relationship between employer and employee.”

Few author said that employee engagement is closely related with employee satisfaction & Job satisfaction. No doubt job satisfaction can help in the employee engagement, but these two are different concepts. Fernandez (2007) shows the distinction between job satisfaction, the well-known construct in management, and engagement contending that employee satisfaction is not the same as employee engagement and since managers cannot rely on employee satisfaction to help retain the best and the brightest, employee engagement becomes a critical concept. In short employee engagement is about to employee’s commitments & willingness to engage self to work for organisation and team to create it more profitable than earlier.

As per the risk assessment report of World Health Organisation (WHO) COVID19 is extraordinarily virus and it is high risky communicable diseases which create serious illness worldwide. Millions of families suffer from COVID19 during the peak time of phase one and phase two. Some many lost their loving ones in pandemic, whereas some faced financial and emotional harassments.

- **Objective of Study-**

In this study researcher wants to identify current status of employee engagement in manufacturing districts. As pandemic affect on rational and emotional thinking of employee and employer so how this pandemic and lockdown affect on the practices of employee engagement.

- **Methodology & Data analysis**

Data collection was done through primary and secondary collection methods. Detailed questionnaire and schedules designed for employee and employer of selected manufacturing industries of Nashik Districts. Questionnaire was circulated through Google form. Secondary data was collected through various research study, research article and website.

- **Analysis & Discussion-**

- **Employee Engagement scenario during pandemic**

Employee engagement is important during tough time, as everyone in pandemic faced lots of issues and problem all of sudden arises due to lockdown and social distancing to maintain employee engaged is too difficult. Companies allowed worked from home but initially it was very tough to digest. Its hard to work online in manufacturing industries as its required physical production. In the difficult time company or organisation should take special efforts to enhance employee engagement as it crates special image in the mindset of employee and other stakeholders. Innovative leadership practices and effective communication helped a lot to enhance engagement of employees. Manufacturing companies of Nashik came up with innovative solution to connect with their employees in the pandemic era. They used e-platform zoom, webX, Google meet, Skype, Google classroom, MOOCs and virtual meet, training modules, webinars, simulations, e-conferences to engage their employees. Same platform were used to communication and delegation of work in the pandemic.

Training is one of the best employee engagement activities conducted in Nashik manufacturing companies. Special training sessions were organised for various levels of employee, to handle stress and insecurities during the lockdowns and pandemic. Along with this special sessions such as metal peace, yoga, wellbeing through meditations and how to take diet conducted by various organisations in addition to their domain training few companies arranged e-get to gather and cultural events where family member of employee accommodated and participated.

Companies also supported families of employee during the pandemic and COVID by providing them various emotional and physical helps. Few companies allowed special financial allowance whereas few organisations organized virtual counselling sessions, social interactions, online meditations and exercise etc.

Challenges in front of HRM for Employee engagement 2022 in front of HRM

1. Resources planning after pandemic
2. Rescheduling workloads as per pre pandemic.
3. Vaccination of all employees
4. Countering the psychological effect COVID on employees mind.
5. Increasing work speed of employees as per pre pandemic.
6. Providing secured and hygiene work environment after Pandemic situation.
7. Providing medical facility with consideration of COVID and its variants
8. Managing Medical leaves during COVID & pandemic to employees
9. Managing various overheads and costs during and after pandemic

• Conclusion-

Employee is core part of any organisation, they are the backbone of entire organisation. To be a successful in the ruthless competition Employee should be nourish and nurture in a systematic way. Employee can be motivated by adopting various engagement practices but it's too hard and difficult in tough time like pandemic and lockdown. To maintain employee's emotional and mental health during the pandemic is major issue to every organisation and company. Still to cope with the challenges companies and organisations engage their employee adopted innovative and creative practices. Companies conducted lots of efforts for employee engagement during the pandemic they used e-platform such as zoom, webx, Skype, training modules, e-conferences, webinars, e-workshops, sessions on yoga, mental health, metal peace, brainstorming session, online quizzes, virtual get together and cultural events. All of this shift the paradigm of employee engagement. Which ultimately boost the morale of employee and creates the self belief and faith on the organisational affairs, enhance the productivity and profitability .

• References -

Bhardwaj, D. (2020). CARS24 is raising the bar of employee engagement as they work from home. CARS24. Retrieved from <https://www.cars24.com/blog/cars24-is-raising-the-bar-with-their-work-from-home-initiative/>

Chanana N, Sangeeta. Employee engagement practices during COVID-19 lockdown. J Public Affairs. 2020;e2508. <https://doi.org/10.1002/pa.2508>

Fallon, N. (2020, March 19). Managing from home? Here's how to keep your team engaged during coronavirus. U.S. Chamber of Commerce. Retrieved from <https://www.uschamber.com/co/run/human-resources/keeping-remote-employees-engaged>

Fernandez. C.P. (2007). Employee engagement. Journal of Public Health Management and Practice. [Online] Available: <http://find.galegroup.com>.

Masson, M. (2009, May 6). Employee engagement in tough times. Workforce. com. <https://www.workforce.com/news/employee-engagement-in-tough-times-part-two>

Matkin, J. (2016, December 19). Keeping employees engaged during tough times. LinkedIn. Retrieved from <https://www.linkedin.com/pulse/keeping-employees-engaged-during-tough-times-jo-matkin/>

Perrin T. (2003). Working Today: Understanding What Drives Employee Engagement The 2003 Towers Perrin Talent Report U.S Report. [Online] Available: http://www.towersperrin.com/tp/getwebcachedoc?Webc=HRS/USA/2003/200309/Talent_2003.pdf

Robinson D., Perryman S., and Hayday S. (2004). The Drivers of Employee Engagement Report 408, Institute for Employment Studies, UK

Vance, R. J. (2006). Employee engagement and commitment (pp. 1–53). Alexandria, Virginia: SHRM Foundation Retrieved from <https://www.shrm.org/foundation/ourwork/initiatives/resources-from-pastinitiatives/Documents/Employee%20Engagement%20and%20Commitment.pdf>

World Health Organization. (2020c). Coronavirus disease 2019 (COVID-19) outbreak. Retrieved from https://www.who.int/health-topics/coronavirus#tab=tab_1

Dr. Vishal Dilip Chavan (Associate Professor)
Sanjivani College of Engineering,
Department of MBA,
Kopargaon, Ahmednagar, Maharashtra

ATISHAY KALIT
Vol. 9, Pt. A
Sr. 15, 2022
ISSN: 2277-419X

Dr. Vijay Nikam (Vice-Principal)
Shri Sadguru Gangageer Maharaj Science,
Gautam Arts and Sanjivani Commerce College,
Kopargaon, Dist. Ahmednagar 423601 (Maharashtra)

Dr. Niraj C. Chaudhari (Assistant Professor)
Sanjivani College of Engineering, Department of MBA ,
Kopargaon, Ahmednagar, Maharashtra

Rising Inflation, Retirement Planning, Savings and Investments Decisions Study conducted for Nasik Region

ABSTRACT

Saving and Investing for Uncertainty is everyone's need. Many people invest their hard earned money in various investment options, starting from Bank account, FD's, Insurance, Gold, Share Market, Government Security Bonds and finally real estate. Due to national and international turmoil due to Covid-19, Shift in Economic Power, Changes in Leadership and decisions, Disputes between country and regions fuelling the accelerator of Inflation.

Key Words: Investment decisions, Inflation, Investment Options. Global Instability

INTRODUCTION

- **Savings** is best defined as the: portion of current income not spent on consumption. Investing is best defined as the: purchase of assets with the goal of increasing future income or wealth.
- **Investment** definition is an asset acquired or invested in to build wealth and save money from the hard earned income or appreciation. Investment meaning is primarily to obtain an

additional source of income or gain profit from the investment over a specific period of time.

- **Retirement** refers to the time of life when one chooses to permanently leave the workforce behind. The traditional retirement age is 65 in the United States and most other developed countries, many of which have some kind of national pension or benefits system in place to supplement retirees' incomes.
- **Inflation** is the decline of purchasing power of a given currency over time. A quantitative estimate of the rate at which the decline in purchasing power occurs can be reflected in the increase of an average price level of a basket of selected goods and services in an economy over some period of time.
- **Investment assets** can be generated through Financial Assets and Non-Financial Assets. Financial assets can be divided into market-linked products (such as stocks and mutual fund) and fixed income products (like Public Provident Fund, bank fixed deposits). Non-financial assets - many Indians invest via this mode - are the likes of physical gold and real estate. Due to national and international turmoil due to Covid-19, Shift in Economic Power, Changes in Leadership and decisions, Disputes between country and regions fuelling the accelerator of Inflation.

REVIEW OF LITERATURE

- ❖ **Z. Bodie (1999):** Thoughts Investment Management and Technology: Past, Present and Future: This paper talks about 45 years of analysis and development in various investment products due to progress in technology, innovation in market and advances in finance theory. This paper also talks about radical changes in new products from 'pay as you go' social security products to self-directed retirement products of insurance & investment which are customized, integrated.

- ❖ **P. Booth, Y. Yakoubov (2000):** Investment Policy for Defined-Contribution Pension Scheme Members Close to Retirement: This paper considers the investment decision facing a defined-contribution pension scheme investor close to retirement. Specifically, it investigates the lifestyle strategy whereby investors automatically switch investment policy in the years before retirement. The argument for switching is that investors may become more risk averse as they approach retirement and will wish to prevent unnecessary volatility of their fund.
- ❖ **Z. Bodie (2003):** Thoughts on the Future: Life-Cycle Investing in Theory and Practice: This paper talks about various investment products and Life-Cycle stages in investment decision. This paper also talks about bundling of insurance and investment products for providing right mix of security and saving.
- ❖ **Eduardo Rodríguez-Monte mayor (2014):** Investment Choice in Defined-Contribution Pension Schemes: International Experience and Policy Issue: This paper reviews how investment choice in DC pension schemes is regulated across different countries and also reviews actual country experiences in terms of individual active choice.

STATEMENT OF PROBLEM

Literature review and various studies show that, there were many research studies conducted in to understand changing practices and need of the investor for saving and investment. But such study was not conducted particularly in this region. Many other related financial decisions and preferences are studied in this research. As demographic, psychographic and geographic factors affects saving and investment preference so this study is conducted in Nasik and Jalgaon district to understand impact of inflation on retirement planning and saving & investment decision.

OBJECTIVE

- To find out current status of income and other income preferences in demographics
- To find out the existing investment in to retirement and medical insurance products
- To find out sufficiency of investment and retirement age preference

RESEARCH METHODOLOGY

The Study was conducted on the basis of Primary data. More than 130 responses were collected from respondents of Nasik District. A well-structured questionnaire was prepared and administered to collect required data from respondents. Secondary data was also collected from various sources to get more clarity on designing questionnaire, framing objectives and other work.

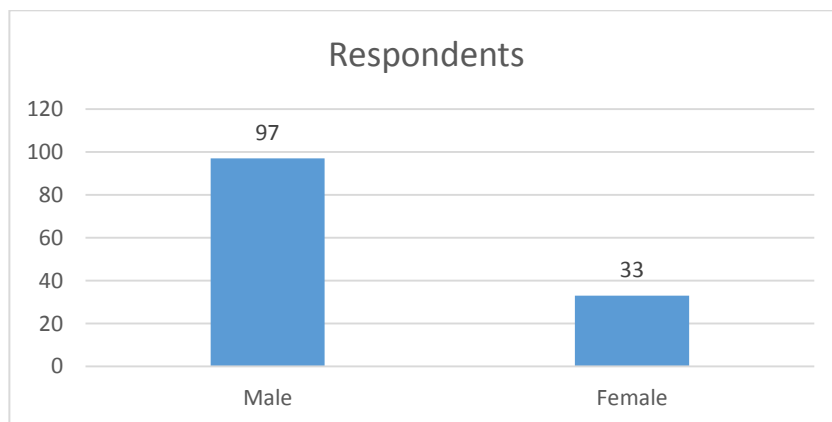
PLANNING OF RESEARCH METHODOLOGY

Literature Review – Statement of problem –Objective –Data collection through questionnaire-Data analysis - Data presentation – Finding & Conclusion

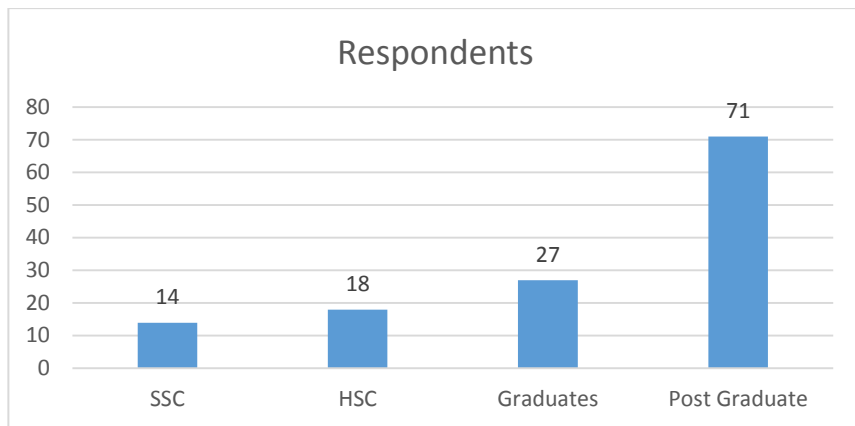
DATA ANALYSIS

Data analysis done with help of data collected from questionnaire collected from respondents of Nasik and Jalgaon district. The graphical presentation of data analysis gives detail idea about research outcomes. Following is data visualization of estimated research study.

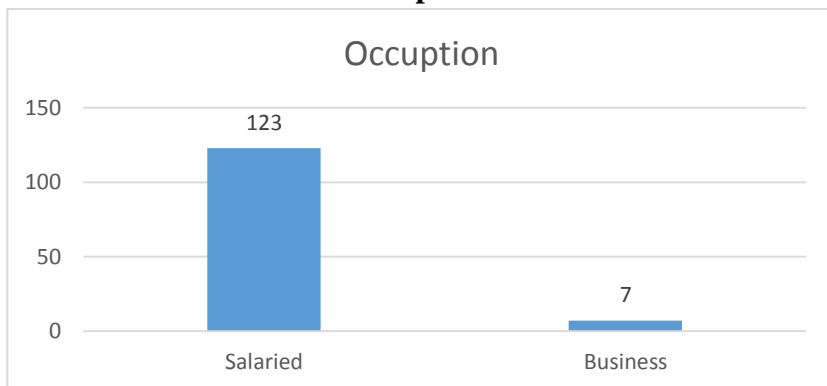
Gender



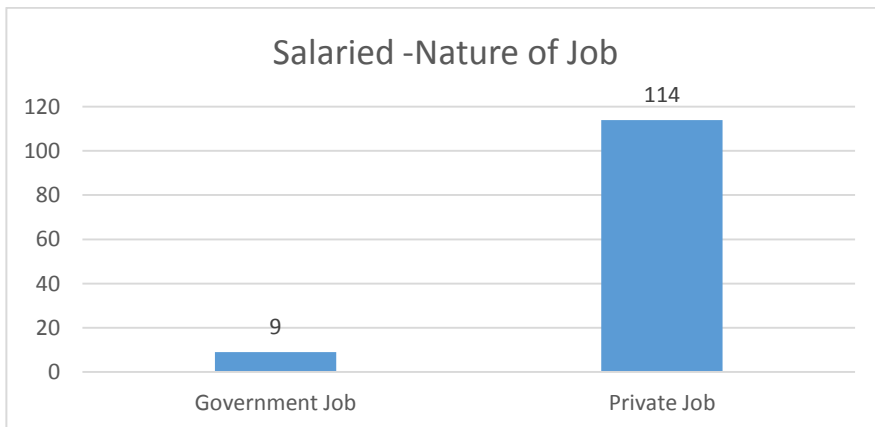
Education



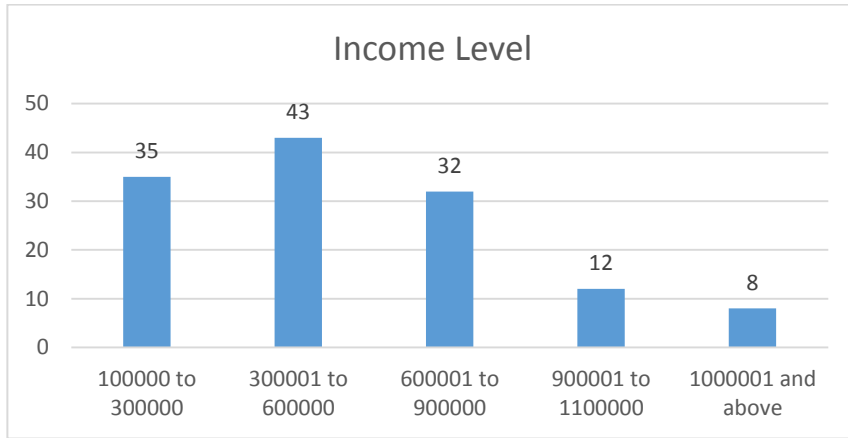
Occupation



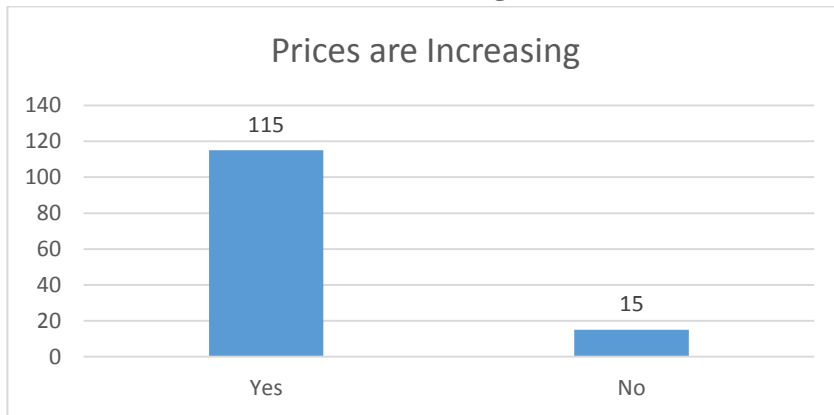
Salaried- Government and Private



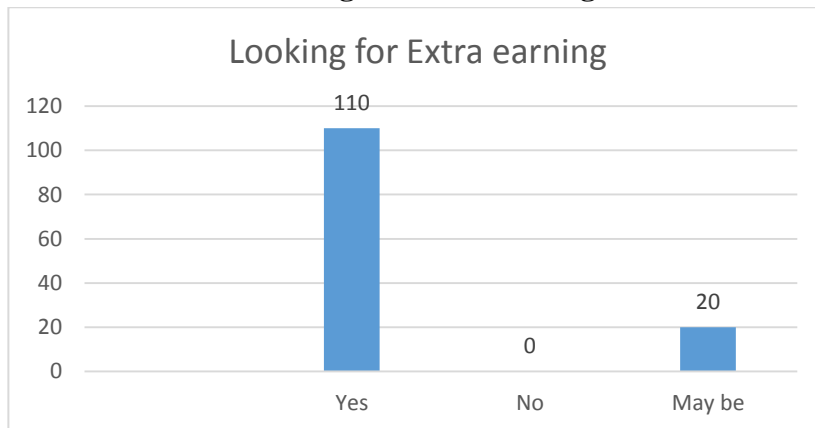
Income Level



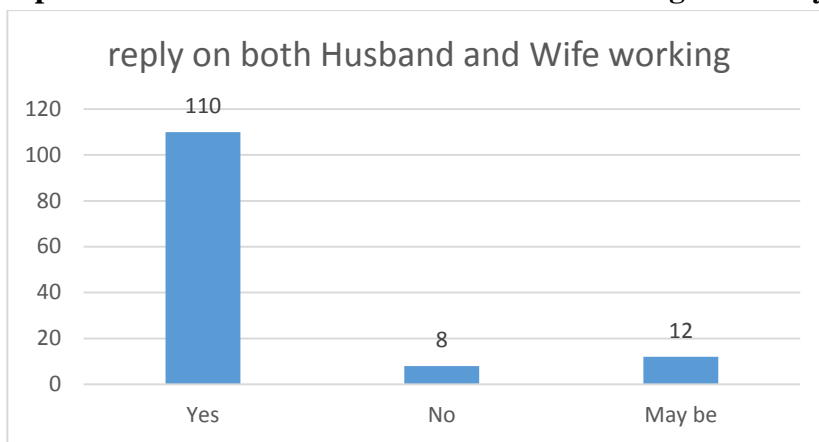
Prices are Increasing: Yes/NO



Looking for extra earning



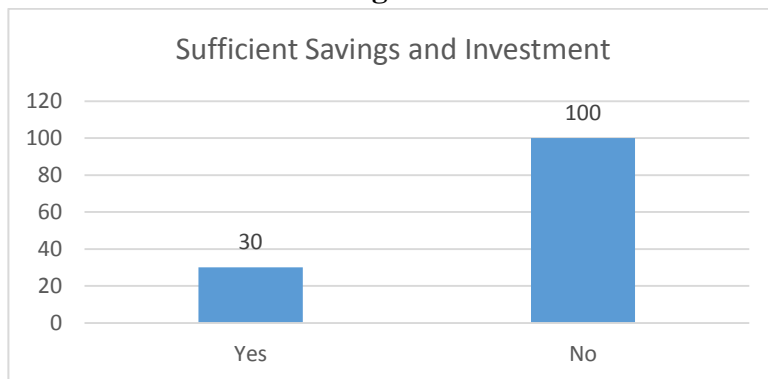
Opinion about – Both Husband and Wife earning for family



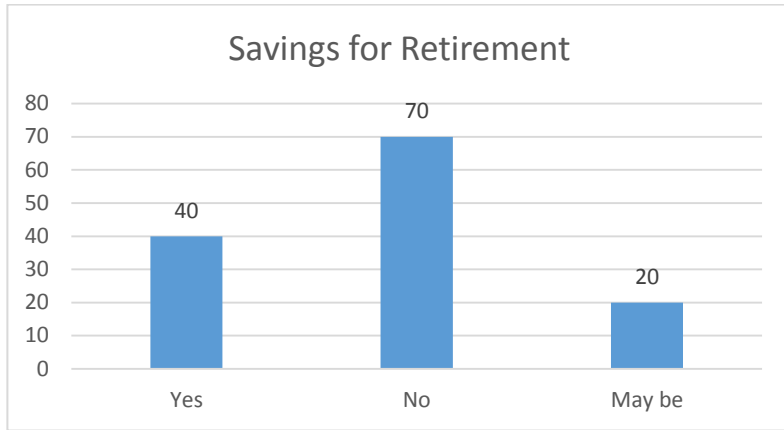
Retirement Age



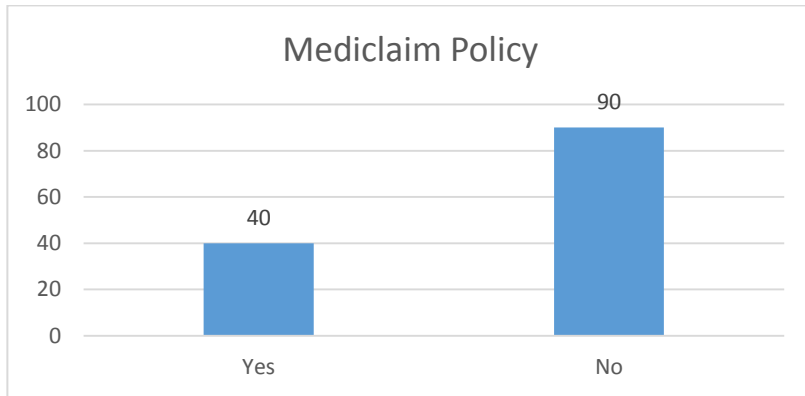
Sufficient Savings and Investments



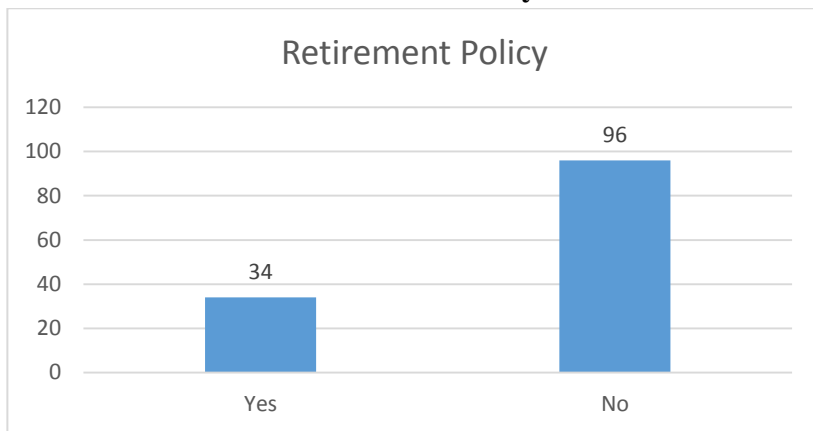
Savings for Retirement



Medical claim Policy



Retirement Policy



FINDING

It is observed that major respondents are male and less female. Category of Post Graduate respondents are maximum followed by Under Graduate, HSC and SSC. Maximum respondents are salaried and few of them are businessmen. Out of salaried respondents, maximum respondents are working in private job and very few are working in government job. Major respondents are below income of 6 lakh and few have in between 6 to 9 lakh and followed by 9 to 11 lakh and 11 lakh above are rare, this results in – maximum respondents are looking for extra earning and they have positive opinion about both Husband and Wife working. Maximum respondents preferred retirement age is between 59 to 60 and some are ready to work even after 65 years. Majority of respondents saving is not sufficient for investment. Many of the respondents say their retirement saving is not sufficient few are saying they have sufficient savings for retirement. Maximum respondents neither have medical insurance policy nor do they have retirement policy.

CONCLUSION

From above research study it is concluded that inflation is affecting the savings and investments decisions of the people. Many people are looking for extra earning, ready for both husband and wife earning for family and even ready to extend their retirement age to achieve their savings, investment and retirement planning. Many of them even don't have medical insurance policy and retirement policy.

REFERENCES

Agnieszka K. Konicz Bell Optimization-Based Guidelines to Retirement Planning and Pension Product Design

J. Turner, Saisai Zhang Optimization-Based Guidelines to Retirement Planning and Pension Product Design. Irrational Expectations, Future Social Security Benefits, and Life Cycle Planning, published in The Journal of Retirement 9 Feb 2019

M.V. Rooli Financial Literacy, Retirement Planning, and Household Portfolio Behavior: Four Empirical Contributions.

Tee Peck Ling, Ng Kean Kok Comparison of Returns between Unit Trusts and Savings Products: Evidence from Malaysia Basics of Personal Financial Planning Insurance Education Series by NIA, K C Mishra, Steward Doss, Cengage Delmar Learning India Pvt. Ltd. Personal Financial Planning, Benedict KohWaiMun Fong, Pearson

<https://www.rbi.org.in/>

<https://www.rbi.org.in/FinancialEducation/fame.aspx>

Information Communication Technology Values and Cyber law Practices in Education

Dr .Nikam V B

Vice Principal, Assistant Professor, Department of Commerce and Management , SSGM College
Kopargaon.

nikamvb23382@gmail.com

Abstract:-

As a researcher I agree the crime rate has reduced as people are remain in greart to use digital services, but online frauds have seen an expansion. Separately from being (ICT) Information Communication Technology, interaction/communication interfaces, sometimes these also help as platforms for criminal fundamentals and ultimately end up being immeasurable security concerns. This work from home has now become apro spect for cyber criminals to exploit the individuals through he-mail scams ,hacking passwords, phishing, ransc n attacks, financial frauds, online sexual harassment, etc. The research paper focuses on the prospects and constraints to ICT being used as a facilitator of change for Institutions in India. This paper focuses on ICT application in Indian Universities/ Colleges/ schools. It particularly settles on the importance of ICT values and the causes of low levels of ICT values application in Indian institutes. The paper posits that the world of ICT has been developing very speedily wherein there is a dire need to stabilize it, for which the entire educational structure should be transformed and ICT should be merged into educational activities, the reason being the overwhelming influence of ICT which cannot be neglected in the student's lives. The paper concludes that teaching and learning activities prescribed by the Universities/ colleges/ schools need to be reformulated and comprehensive strategies developed

Keywords:-ICT crime, cyber Crime, ICT values , individual Cyberspace

Introduction

Today's world has become global village through the World Wide Web and ICT practices. All the school, College students, employees and housewife's became global Internet village citizens. If we look out for one country as per the civilization, we found strict rules of constitution and Indian Law practices. The constitution of India stated all the do's and don'ts to Indian people. It's called the value system and it's implemented effectively in our country before thousands of year. As a results of these law, constitution implementation perfectly help to govern and administer people management to the governments. The final outcome of that is all governments can perform their duties very well. But, the development through technology they doing their duties. Now, the dependability on technology , internet , GPS Online banking, Work from Home , Online teaching platform , Social sites, entertainment platform , Ecommerce . E transactions Online banking is become our part of body. In the daily schedule all boys, men,women, girls, female, house wife's, you thand children using smartphones. During this pandemic the users are increased drastically. School and college students had opened their social media accounts and video conferencing platform. Due to pandemic covid 19 everybody using online transaction, online banking e commerce, and online working platform is used for earning money. Physically activity stopped and online dependency is increased.

People of every age group is spending time on social medias like Instagram, Facebook, what's app , YouTube , skype , and they exposed to internet village citizens which is globally connected .the privacy and security of people is finished due to this online connectivity . Self-discipline is finished. People know about the cyber law rules and regulation but the tolerance level of people is minimized. So many psychological issues came up in this lockdown period of covid19. Extra use of e commerce forshopping, banking trading stress has gone up and earning gone down . Lots of people lost their jobs in pandemic, these people violating others in family and their surroundings. Youth is trying to earn money, they are ready to work but jobs are not available. Due to unemployment family head and his dependent is overstress and they trying to do frauds, violence, teasing on online platform. In India now a days this is become a biggest challenge for government to maintain discipline and Peace.Always there is a control of central government to simplifying the life of citizens and provide them security. Government is having the responsibility to provide mental, financial, physical growth to citizen. However, in this digital civilization, have follow values. But, the awareness about these values can be taught to the students in school and colleges .Cyber law is made to implement these values among citizen in each country. This cyber law is based on cybercrimes. ICT is the part of cyber law. If citizens not follow cyber law and ICT values crime will become a criminal offence. Police complaint will register against digital citizen.

VOLUME 8 (SPECIAL ISSUE) 2022

ISSN 2454-3055

Manuscripts under Special issue are published with the Theme
"Modern Perspectives of Biological Sciences"

Guest Editor: Dr. S. Mohanasundaram
Assistant Guest Editor: Dr. S.S. Syed Abuthahir

**INTERNATIONAL
JOURNAL OF
ZOOLOGICAL
INVESTIGATIONS**

*Forum for Biological and
Environmental Sciences*

Published by Saran Publications, India



International Journal of Zoological Investigations

Contents available at Journals Home Page: www.ijzi.net
Editor-in-Chief: Prof. Ajai Kumar Srivastav
Published by: Saran Publications, Gorakhpur, India



ISSN: 2454-3055

Green Synthesis of Silver Oxide Nanoparticles by using *Clerodendrum bracteatum* Leaf Extract and Their Antibacterial Activity

Shinde Sagar I^{*1}, Kshirsagar Santosh R.¹, Gondake Sandip P.¹ and Patil Swapna S.²

¹Department of Chemistry, Dada Patil Mahavidyalaya, Karjat, Ahmednagar, Maharashtra, India

²Department of Zoology, Annasaheb Awate College, Manchar, Maharashtra, India

*Corresponding Author: Shinde Sagar I & sagarshinde7559@gmail.com

Received: 4th August, 2022; Accepted: 20th August, 2022; Published online: 28th August, 2022

<https://doi.org/10.33745/ijzi.2022.v08i0s.006>

Abstract: Plant-mediated nanoparticle production is fast, simple, environmentally friendly, and inexpensive. This study synthesised silver nanoparticles using *Clerodendrum bracteatum* leaf extract. FT-IR, SEM, XRD, and Zeta potential were used to characterise silver nanoparticles. FT-IR was utilised to determine the functional groups responsible for reducing silver nitrate and capping agents in the leaf extract. Using Zeta potential, silver nanoparticles' stability was measured. Silver nanoparticles' 18.3 mV negative Zeta potential showed durability. Silver nanoparticles show antibacterial action against *Staphylococcus aureus*, *Micrococcus luteus*, *Escherichia coli*, and *Pseudomonas aeruginosa*, which might help create novel antibacterial medicines.

Keywords: *Clerodendrum bracteatum*, Silver nanoparticles, FT-IR, SEM, XRD, Zeta potential, Antibacterial, Flavonoids, Alkaloids

Citation: Shinde Sagar I., Kshirsagar Santosh R., Gondake Sandip P. and Patil Swapna S: Green synthesis of silver oxide nanoparticles by using *Clerodendrum bracteatum* leaf extract and their antibacterial activity. Intern. J. Zool. Invest. 8(Special Issue): 00-00, 2022.

<https://doi.org/10.33745/ijzi.2022.v08i0s.006>



This is an Open Access Article licensed under a Creative Commons License: Attribution 4.0 International (CC-BY). It allows unrestricted use of articles in any medium, reproduction and distribution by providing adequate credit to the author (s) and the source of publication.

Introduction

Green chemicals have been used to synthesise metallic nanoparticles without contaminating the environment (Amin *et al.*, 2012). As a reducing and capping agent in green route-mediated metallic nanoparticle synthesis, plant extracts are used. Noble metal silver maintains a major place in nanomaterial research owing to its diverse characteristics (Dong *et al.*, 2017). Nanotechnology helps understand molecular, supramole-

cular, and atomic properties. Chemical approaches to generate nanoparticles are costly, time-consuming, and toxic (Ahmad *et al.*, 2011). Nanoparticle manufacturing must be quick, cheap, and environmentally friendly. Earlier studies focused on simple synthesis, not production. In this investigation, we made silver nanoparticles from *Clerodendrum bracteatum* leaf extract (Lee *et al.*, 2013).

Clerodendrum is a genus of small tropical trees, shrubs, and perennial plants found in Africa and southern Asia. South America, northern Australia, and eastern Asia have some species (Patel *et al.*, 2015). Traditional uses include treating bleeding, rheumatism, haemorrhoids, and lung cancer. Previous phytochemical studies on this genus isolated flavonoid compounds, phenylpropanoid glycosides, sesquiterpenoids, diterpenoids, triterpenoids, alkaloids, and others with antioxidant, antitumor, antibacterial, and anti-inflammatory properties (Zhang *et al.*, 2018; Hu *et al.*, 2018). This study synthesised silver nanoparticles using *Clerodendrum bracteatum* leaf extract. FT-IR, SEM, XRD, and Zeta potential were used to characterise silver nanoparticles. FT-IR was utilised to determine the functional groups responsible for reducing silver nitrate and capping agents in the leaf extract. Using Zeta potential, silver nanoparticles' stability was measured.

Materials and Methods

Clerodendrum bracteatum leaf extract synthesises of Ag₂O NPs:

30 g of *Clerodendrum bracteatum* leaves were extracted with 70% ethanol. 10 ml of extract and 90 ml of 1 mM silver nitrate solution were mixed in 250 ml Erlenmeyer flasks. The extract produced Ag₂O NPs. The reaction mixture turns from yellow to brown, indicating silver nanoparticle production. Then it was stirred for 5 h at 36°C. The precipitate was rinsed with deionized water and ethanol before drying for 5 h at 80°C. *Clerodendrum bracteatum*-assisted Ag₂O NPs were generated by calcining dried samples at 350°C for 3 h.

Characterization:

Functional groups in 4000-400 cm⁻¹ were determined using Perkin-Elmer FTIR spectra. XRD (Philips X'pert diffractometer with Cu K) was utilised to determine the Ag₂O NPs' crystal structure. Zeta potential measured particle sizes. High resolution scanning electron microscopy (HR-SEM) images were taken using a Philips XL30 ESEM with energy dispersive X-ray spectroscopy

to examine surface morphology and chemical analysis.

Antimicrobial activity:

Staphylococcus aureus, *Micrococcus luteus*, *Escherichia coli*, and *Pseudomonas aeruginosa* were cultivated on nutritional agar. Bacteria were cultured overnight in nutritious broth at 37 °C, then centrifuged for 5 min at 10,000 rpm and suspended in double distilled water. Cell density (A₆₁₀ nm) was standardised Spectrophotometrically. Pure Ag₂O NPs were tested using the well diffusion technique following reconstitution with saline (Haq *et al.*, 2021; Aravind *et al.*, 2021; Sounder *et al.*, 2018). Hi-Media ruler was used to measure the inhibitory zone in millimetres. Three sets per test were examined.

Results and Discussion

FT-IR studies:

Figure 1 shows Ag₂O nanoparticle FT-IR spectra. The 3405 and 2924 cm⁻¹ peaks are due to H₂O's OH stretching vibration in Ag-O-Ag. AgO's 610 cm⁻¹ peak (Chuntonov *et al.*, 2014).

XRD Analysis:

Figure 2 shows the XRD pattern of Ag₂O with *Clerodendrum bracteatum* leaf extracts, confirming NPS. XRD spectra were compared to Ag₂O (JCPDS no. 00-012-0793). Sharp and strong diffraction peaks indicated good crystallisation. Debye-Scherrer formula computed average crystallite size. Ag₂O crystallites average 25 and 20 nm. Ag₂O's XRD structure is wurtzite. Bragg reflection peaks were detected at 32.06°, 40.03°, 65.03°, and 79.84°, corresponding to the 111, 200, 220, and 311 planes of pure Ag₂O NPs. Using PANalytical X'Pert High Score Plus, Version 3.0.3, XRD confirmed biosynthesized Ag₂O NPs' FCC shape.

Sizing Particles:

DLS measurements were utilised to calculate SNP size. Figure 3 shows the SNPs' particle size dispersion. Particle diameters were 100.12 nm. Size difference between biggest and smallest

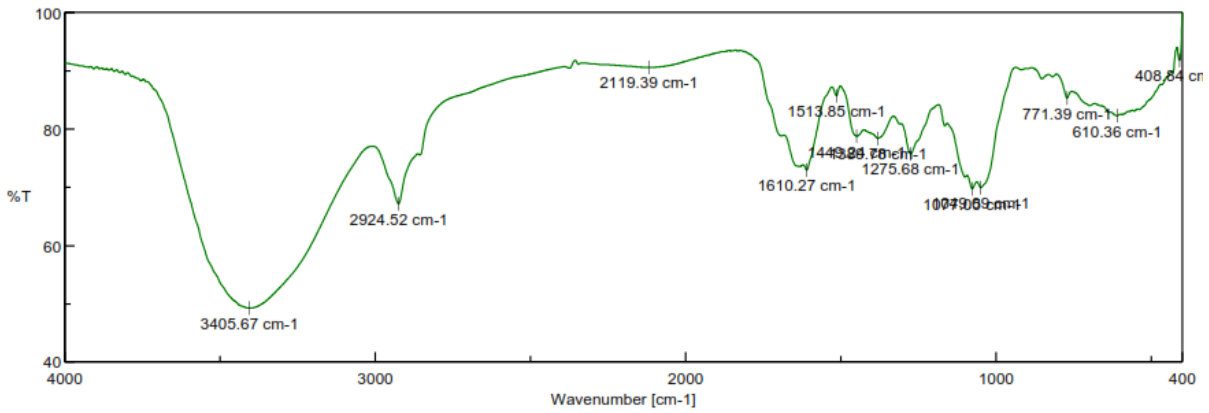


Fig. 1: FT-IR data of Ag₂O NPs with *Clerodendrum bracteatum* leaves extracts.

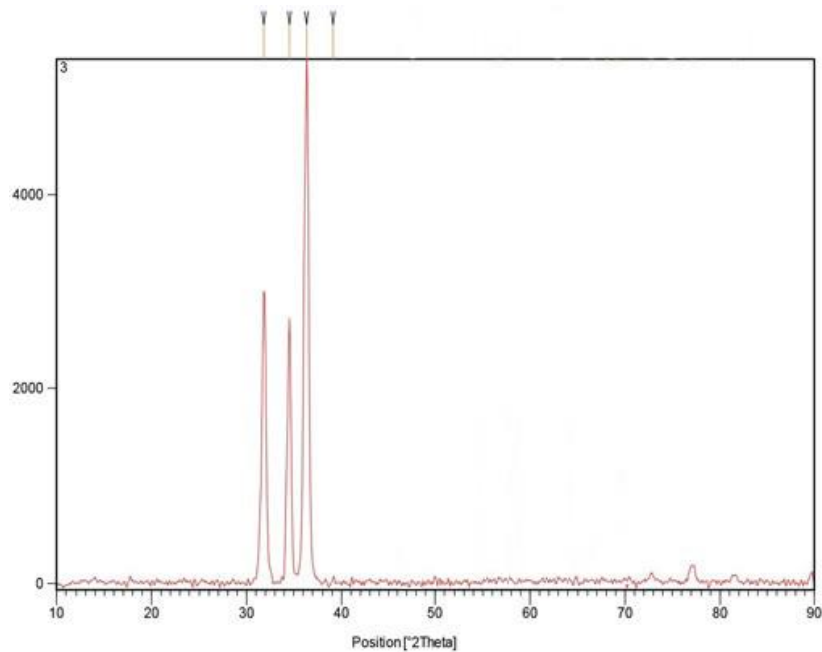


Fig. 2: XRD pattern of Ag₂O NPs with *Clerodendrum bracteatum* leaves extracts.

nanoparticles showed limited SNP dispersion. The nanoparticle zeta potential was 18.3 mV.

SEM Exam:

SEM examination revealed Ag₂O NPs' shape. Figure 4 shows Ag₂O SEM micrographs. Spherical, evenly-distributed particles were found. Ag₂O NPs featured grainy nanosheets stacked vertically. All samples averaged 50-65 nm particle size. Increased Ag₂O NPs matrix reduced average particle size. Formation of Ag-O-Ag on doped nanoparticle surfaces prevented crystal grain growth and particle separation, reducing particle

size (Jaishetty *et al.*, 2016; Nagadeep *et al.*, 2019; Jaishetty *et al.*, 2019).

Antibacterial:

We employed good diffusion to compare Ag₂O NPs with *Clerodendrum bracteatum* leaf extracts (Fig 5). *S. aureus*, *M. luteus*, *E. coli*, and *P. aeruginosa* were investigated for antibacterial efficacy against Ag₂O NPs. At 100 µl, the zone of inhibition (mm) was measured three times. The Ag₂O NPs improvement % was obvious. Ag₂O NPs inhibited *S. aureus*, *M. luteus*, *E. coli*, and *P. aeruginosa*. The inhibitory zone (%) was found at

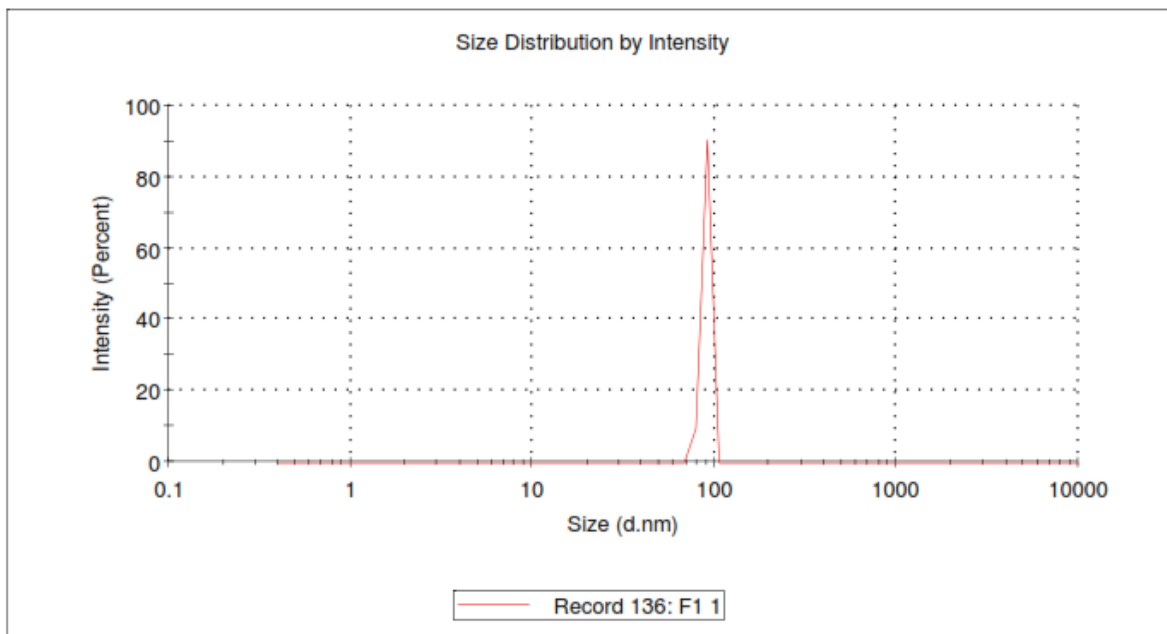


Fig. 3: Particle size analysis of the Ag₂O NPs with *Clerodendrum bracteatum* leaves extracts.

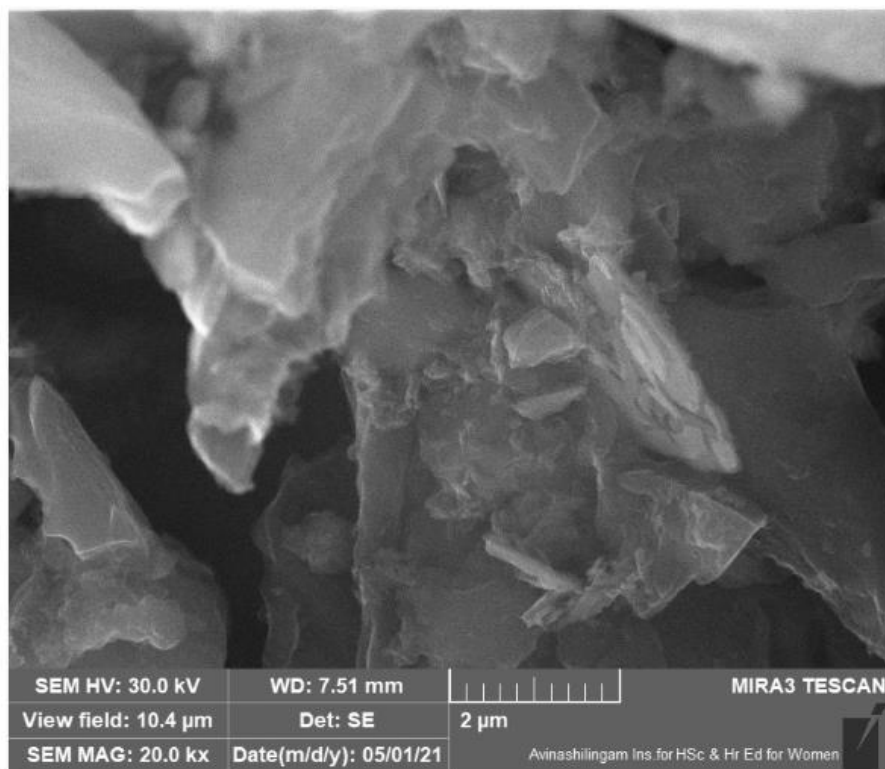


Fig. 4: SEM images of Ag₂O NPs with *Clerodendrum bracteatum* leaves extracts.

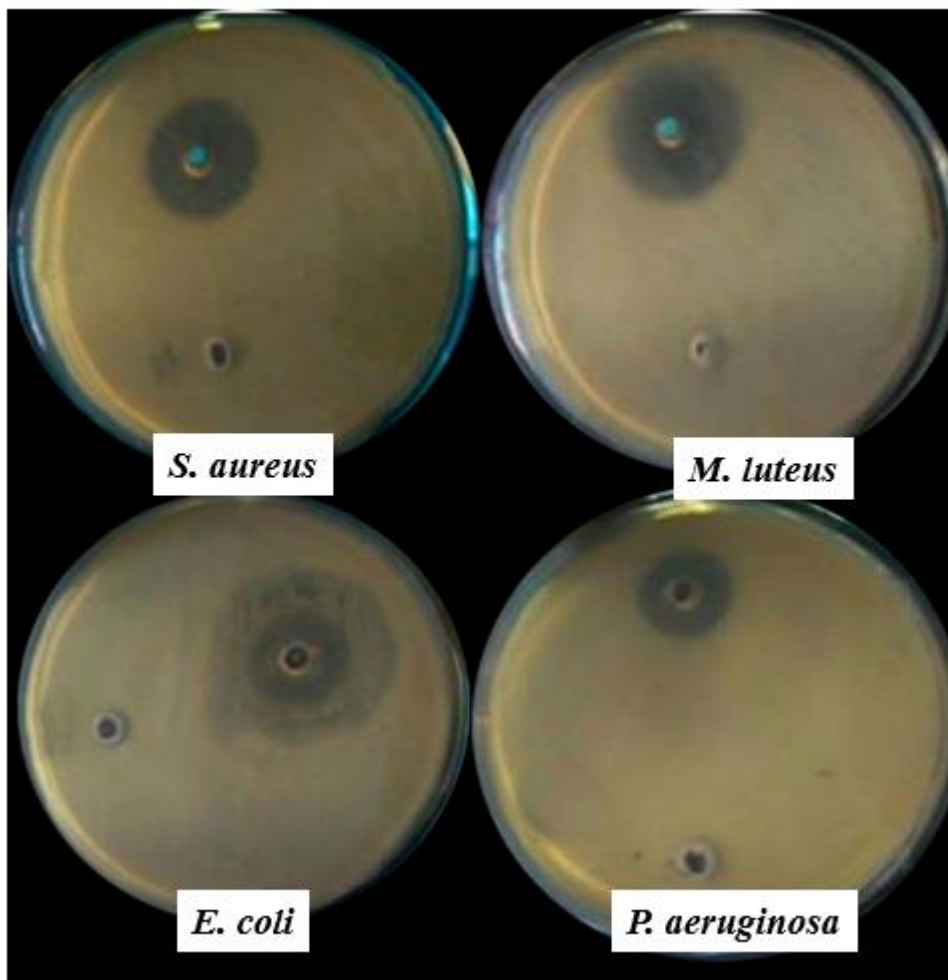


Fig. 5: Antimicrobial efficacy of Ag₂O NPs with *Clerodendrum bracteatum* leaves extracts.

100 μ l. Antimicrobial effectiveness of Ag₂O NPs with *Clerodendrum bracteatum* leaves was noticed.

Conclusion

We synthesised Ag₂O NPs from *Clerodendrum bracteatum* leaf extracts. It is an easy, green way to create safe nanoparticles. The nanoparticles' sizes were 100.12 nm. Nanoparticles were bigger because they were surrounded by a thin layer of proteins and metabolites such as terpenoids with functional groups of amines, alcohols, ketones, aldehydes, and other amines, alcohols, ketones, and aldehydes were identified using SEM, XRD, and FT-IR methods. All of these theories say that the ratio of plant extract to metal ion determines nanoparticle shape. Nanoparticles at higher concentrations appeared sheet-like, whereas those in lower concentrations were spherical. 100 μ l

Ag₂O NPs were bactericidal against *S. aureus*, *M. luteus*, *E. coli*, and *P. aeruginosa*. The investigations found that employing plant extracts to synthesise Ag₂O NPs is more cost-effective, energy-efficient, low-cost, and ecologically benign than using biohazardous chemicals.

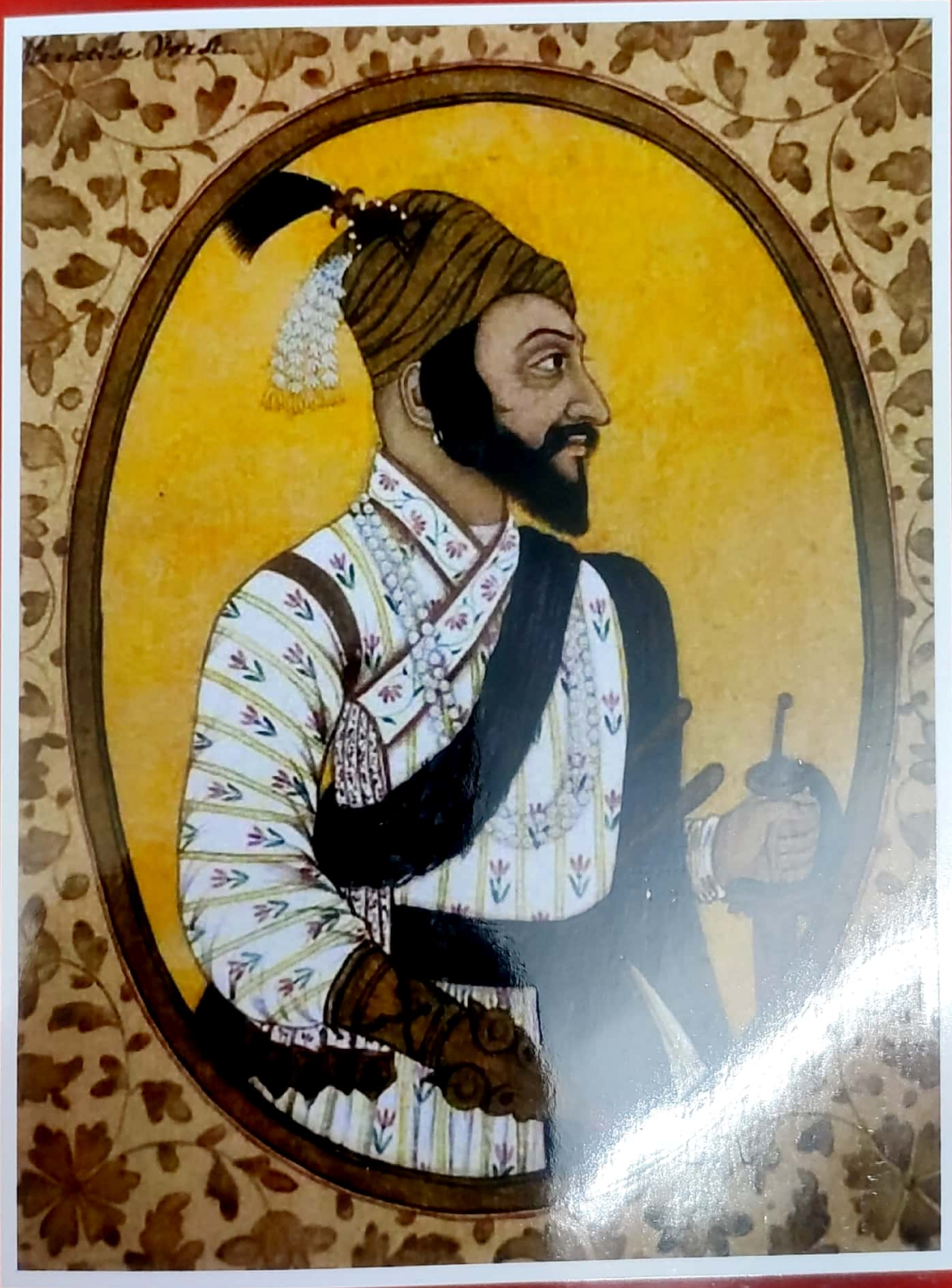
References

- Ahmad S, Rao H, Akhtar M, Ahmad I, Hayat MM and Iqbal Z. (2011) Phytochemical composition and pharmacological prospectus of *Ficus bengalensis* Linn. (Moraceae)-A review. J Med Plants Res. 5:6393-6400.
- Amin M, Anwar F, Janjua MR, Iqbal MA and Rashid U. (2012) Green synthesis of silver nanoparticles through reduction with *Solanum xanthocarpum* L. berry extract: characterization, antimicrobial and urease inhibitory activities against *Helicobacter pylori*. Int J Mol Sci. 13: 9923-9941.

- Aravind M, Ahmad A, Ahmad I, Amalanathan M, Naseem K and Mary SMM. (2021) Critical green routing synthesis of silver NPs using jasmine flower extract for biological activities and photo-catalytic degradation of methylene blue. *J Environ Chem Eng.* 9: 104877.
- Chuntonov L, Kumar R and Kuroda DG. (2014) Non-linear infrared spectroscopy of the water bending mode: direct experimental evidence of hydration shell reorganization. *Physical Chem Chemical Phys.* 16: 13172-13181.
- Dong C, Cao C, Zhang X, Zhan Y, Wang X, Yang X, Zhou K, Xiao X and Yuan B. (2017) Wolfberry fruit (*Lycium barbarum*) extract mediated novel route for the green synthesis of silver nanoparticles. *Optik* 130: 162-170.
- Haq S, Yasin KA, Rehman W, Waseem M, Ahmed MN and Shahzad MI. (2021) Green synthesis of silver oxide nanostructures and investigation of their synergistic effect with moxifloxacin against selected microorganisms. *J Inorg Organomet Polym Mater.* 31: 1134-1142.
- Hu HJ, Zhou Y, Han ZZ, Shi YH, Zhang SS, Wang ZT and Yang L. (2018) Abietane diterpenoids from the roots of *Clerodendrum trichotomum* and their nitric oxide inhibitory activities. *J Nat Prod.* 81: 1508-1516.
- Jaishetty N, Palanisamy K and Maruthapillai A. (2019) Enantiometric separation of sitagliptin in a fixed dose combination formula of sitagliptin and metformin by a chiral liquid chromatographic method. *Int J Pharma Pharmaceut Sci.* 11(6): 66-71.
- Jaishetty N, Palanisamy K, Maruthapillai A and Jaishetty R. (2016) Trace level quantification of the (-) 2-(2-amino-5-chlorophenyl)-4-cyclopropyl-1, 1, 1-trifluoro-3-butyn-2-ol genotoxic impurity in efavirenz drug substance and drug product using LC-MS/MS. *Scientia Pharmaceu.* 84: 456-466.
- Lee HJ, Song JY and Kim BS. (2013) Biological synthesis of copper nanoparticles using *Magnolia kobus* leaf extract and their antibacterial activity. *J Chem Technol Biotechnol.* 88: 1971-1977.
- Sounder L, Doss VA and Mohanasundaram S. (2018) Analysis of hydroethanolic leaf extract of *Aerva lanata* (L) in screening antioxidant activity and invitro antibacterial efficacy. *Int. J. Res. Pharm. Sci.* 9(3): 911-915.
- Nagadeep J, Kamaraj P and Arthanareeswari M. (2019) Gradient RP-HPLC method for the determination of potential impurities in dabigatran etexilate in bulk drug and capsule formulations. *Arabian J Chem.* 8: 3431-3443.
- Patel JJ, Acharya SR and Acharya NS. (2014) *Clerodendrum serratum* (L.) Moon - A review on traditional uses, phytochemistry and pharmacological activities. *J Ethnopharmacol.* 154: 268-285.
- Zhang SL, Huang RZ, Liao HB, Wang S, Chen ZF and Liang D. (2018) Cyclic pentapeptide type compounds from *Clerodendrum japonicum* (Thunb.) Sweet. *Tetrahedron Lett.* 59: 3481-3484.

तिफुण

वर्ष : १३ वे । अंक १ला । एप्रिल-मे-जून - २०२२



कुळवाडीभूषण
छत्रपती शिवाजी महाराज
विशेषांक

साहित्य, कला आणि लोकसंस्कृतीला वाहिलेले त्रैमासिक

तिफण

वर्ष १३ वे, अंक - पहिला; एप्रिल-मे-जून २०२२

UGC Care Listed Journal

ISSN 2231 - 573X

● संपादक ●

डॉ. शिवाजी हुसे

पत्ता : संपादक, तिफण, 'शिवार', श्रीराम कॉलनी, हिवरखेडा रोड,
कन्नड, जि. औरंगाबाद - ४३११०३, मो. ९९०४००३९९८



छत्रपती शिवाजी महाराज यांचे 'आरमार'विषयक धोरण - आज्ञापत्रकृत

- प्रा. राधाकिसन पांडुरंग मुठे

अण्णासाहेब आवटे कॉलेज, मंचर, ता. आंबेगाव, जि. पुणे
मोबाइल-८४८४०३६७५०, ई-मेल-radhakisanmuthe05@gmail.com

मध्ययुगीन कालखंडातील रामचंद्रपंत अमात्यकृत मराठेशाहीतील राजनीती अर्थात 'आज्ञापत्र' या ग्रंथामध्ये आरमार या प्रकरणात छत्रपती शिवाजी महाराजांचे आरमारविषयक धोरण यासंदर्भात माहिती दिली आहे. त्यातून त्यांची आरमारविषयक दूरदृष्टी स्पष्ट होते व आताच्या कालखंडातसुद्धा देशाच्या, राज्याच्या संरक्षणासाठी आरमार व्यवस्था कशी सक्षम असली पाहिजे हे राज्यकर्त्यांना सूचित करते; परंतु मध्ययुगीन कालखंडात आरमाराचे महत्त्व छत्रपती शिवाजी महाराजांनी जाणले आणि आपल्या स्वराज्यात प्रथम आरमार स्थापन केले. विशेषतः भारतीय आरमाराचा जनक म्हणून त्यांना ओळखले जाते. छत्रपती शिवाजी महाराज यांनी गड, कोट, दुर्ग, सैन्य व आरमार यांना अधिक महत्त्व दिले; कारण संरक्षणाच्या दृष्टीने या घटकांना अधिक महत्त्व होते, असा दूरदृष्टी असलेले राजा छत्रपती शिवाजी महाराज यांच्या रामचंद्रपंत अमात्य यांनी 'आज्ञापत्र' या ग्रंथात महाराजांचा आरमारविषयक दृष्टिकोन व धोरण यासंदर्भात अत्यंत मौलिक अशी मांडणी केली आहे, तसेच छ. शिवाजी महाराज एक राज्यकर्ते, राजा म्हणून आपल्या स्वराज्याचा रक्षणासाठी भविष्यात समुद्रातील किल्ले व समुद्र यावर ज्यांना सत्ता स्थापन करता येईल तो राजा आपले राज्य राखू शकेल याची जाणीव महाराजांना होती; कारण त्या कालखंडात, फिरंगी, यवन, इंग्रज यांच्यापासून समुद्रमार्गे स्वराज्यास धोका आहे, हे त्यांनी ओळखले होते. त्यामुळे छ. शिवाजी महाराजांनी आरमार उभारणीसाठी आपली योजना आखली. त्या अनुषंगाने रामचंद्रपंत अमात्य यांनी आपल्या आज्ञापत्र ग्रंथात छत्रपती शिवाजी महाराज यांचे आरमारविषयक विचार, धोरण व

महाराजांचे राजनीतिविषयक धोरण यासंदर्भात आपले विचार मांडले आहेत.

आरमार -

जगाच्या इतिहासात नोंद व्हावी इतके असामान्य नेतृत्व व कर्तृत्व छत्रपती शिवाजी महाराज यांच्या ठिकाणी होते. त्यामुळे त्या कालखंडात आरमार उभारणे छ. शिवाजी महाराजांच्या दूरदृष्टीचे द्योतक म्हणता येईल. मध्ययुगात त्यांनी आरमाराचे महत्त्व ओळखले. छत्रपती शिवाजी महाराजांनी आपल्या आरमाराच्या बळावर तत्कालीन कालखंडात शत्रूपक्ष इंग्रज आणि पोर्तुगिजांना नियंत्रणात ठेवले होते. महाराजांच्या या कार्याचे यथार्थ चित्रण सभासदाच्या बाखरीमध्येसुद्धा आलेले आहे. आरमाराची बांधणी व सुसज्जता या अनुषंगाने रामचंद्रपंत अमात्य यांनी 'आज्ञापत्र' या ग्रंथात छत्रपती शिवाजी महाराज यांचे आरमारविषयक धोरण, विचार यांचा अतिशय सखोल अशी मांडणी केलेली दिसते. ते म्हणतात, आरमार हे एक स्वतंत्र राज्यांगच आहे. ज्याप्रमाणे ज्याचे अश्वबल त्याची सर्व प्रजा असते, त्याप्रमाणेच ज्याच्याजवळ आरमार त्याचा समुद्र. यासाठी राजाकडे आरमाराची सिद्धता असली पाहिजे, असे विधान आरमार प्रकरणाच्या सुरुवातीला येते. यावरून आपणास छ. शिवाजी महाराज यांच्या आरमारविषयक दूरदृष्टी व धोरण या बाबतीत रामचंद्रपंत अमात्य आपल्या ग्रंथात उल्लेख करतात. त्याचबरोबर आरमाराची बांधणी कशी असावी आणि आरमार सुसज्ज कसे ठेवावे, याबाबतचा विचारही आज्ञापत्रात येतो. तो असा - जहाज, चालीचा गुराबा म्हणजे वापरात असलेले जहाज फार मोठे किंवा फार लहान नसावे तर ते मध्यम आकाराचे करून

तिफण : कुळवाडीभूषण छत्रपती शिवाजी महाराज विशेषांक

सजवावे. याठिकाणी गुराबा या शब्दाबरोबर गलबत, जहाज असा शब्द रामचंद्रपंत, आज्ञापत्रकार वापरताना दिसतात. मोठे व्यापारी गलबते, फरगात म्हणजे मोठी लढाऊ जहाजे जी वाऱ्याशिवाय हालू शकत नाहीत, ती उपयोगाची नाहीत. अशा गलबतावर लढवण्या शिपाई, तोफा, दारूगोळा, बंदुका, सुकंग इत्यादी साहित्य आरमाराला आवश्यक सज्ज ठेवावे. यातून आज्ञापत्रकार यांनी शिवाजी महाराजांच्या आरमारविषयक धोरणासंदर्भात अत्यंत समर्पक मांडणी केलेली दिसते. आरमार व्यवस्था कशी असावी किंवा करावी यासंदर्भात शिवाजी महाराजांचे धोरण आज्ञापत्रकार मांडतात की, आरमारचे वेगवेगळे सुभे (सरदार) करावेत. प्रत्येक सुभ्यात पाच गुरावे व पंधरा गलबते असावीत. त्यांच्यावर एक सरमुभा (मुख्य सरदार) असावा व त्याच्या आज्ञेत सर्वांनी राहावे, तसेच आरमारावरील सैनिकांचा पगार मुलकात म्हणजे जो वसूल येतो त्यातून द्यावा. जकातांचे उत्पन्न (पैदास्तीवरील) नेमणूक करू नये. पैदास्तीवरील नेमणूक केल्यास सावकारी (व्यापारी) बुडून जाईल, सावकारी वाढवावी. कारण सावकारीमुळे जकातीचे उत्पन्न वाढेल. आरमारावरील सैनिकांनी समुद्रात संचार करून शत्रूला जवळ येऊ देऊ नये. जलदुर्गासाठी लागणारे साहित्य व दारूगोळा वरंचेवर पोहोचेल अशी व्यवस्था करावी. दर्यावर्दी शत्रूच्या समाचाराला सज्ज राहून शत्रूचा प्रदेश जिंकावा. शत्रूच्या प्रदेशातील बातम्या गुप्तहेराकडून जमा करून शत्रूच्या प्रदेशातून निघून यावे. अशाप्रकारे छ. शिवाजी महाराजांनी आरमार बांधणीसाठी कशाप्रकारे धोरण राबविले, याचा परामर्श या ग्रंथात अमात्य घेताना दिसतात.

व्यापारी जहाजासंबंधीचे धोरण -

आज्ञापत्रात अमात्यांनी छत्रपतींच्या आरमारविषयक धोरणाच्या अनुषंगाने उल्लेख करताना म्हटले आहे, समुद्रात सरकारी परवाना घेऊन संचार करणाऱ्या व्यापारी जहाजांना दळणवळणाची मुभा द्यावी, असे आज्ञापत्रात नमूद केले आहे. यातून शिवाजी महाराजांची व्यापाराला उत्तेजन देण्याची दृष्टी प्रत्यक्ष येते. याबाबत आज्ञापत्रात आणखी सखोलपणे विवेचन येते. ते म्हणजे परवानाधारक सावकाराच्या वाट्याला जाऊ नये, तसेच परवानाधारक सावकारांना उपद्रव होत असेल, तर त्याचा बंदोबस्त करावा, त्याचे निवारण करावे, तर शत्रूच्या

मुलखातील सावकारी जहाजे जर आपल्या परिसरात आली तर ती पकडून बंदरात आणावीत. सर्व माल जप्त करावा आणि राजाच्या आज्ञेनुसार त्यांच्याविषयी वर्तन करावे. यावरून छत्रपती शिवाजी महाराजांची आपल्या व परक्या मुलखातील सावकारी जहाजांबद्दलची स्पष्ट भूमिका समजून येते, तसेच इंग्रज, पोर्तुगीज यांना शिवाजी महाराजांच्या आरमाराचा किती धाक वाटत असेल, याचीही कल्पना येते. आरमारासंदर्भात छ. शिवाजी महाराजांचे धोरण आज्ञापत्रमधून अमात्यांनी अत्यंत स्पष्टपणे मांडलेले दिसते, तसेच या ग्रंथात आरमारी युद्ध व आरमारी छावणी या अनुषंगाने छत्रपतींचे धोरण अथवा भूमिका रामचंद्रपंत अमात्यांनी आज्ञापत्र ग्रंथातून मांडताना त्यांनी शिवाजी महाराजांची आरमाराबद्दलची नीती स्पष्ट केली आहे. ती अशी - आपल्या आरमाराची शत्रूच्या आरमाराबरोबर गाठ पडली आणि युद्ध सुरू झाले, तर सर्वांनी एकत्र येऊन कस्त करून शत्रूशी झुजावे. आपले गलबत वाऱ्यावर चालत नाही असे वाटले तर काहीही करून शत्रूच्या ताबडीत न सापडता आपल्या जंजिऱ्याच्या (जलदुर्गा) आश्रयाला यावे. आपल्या तरांड्याला (गलबत) अपाय होऊ देऊ नये, आपले संरक्षण करून शत्रू जिंकावा शत्रू दमगीर झाला (दंमला) अथवा शरण आला, तर तोफांचा मारा करत दुरूनच त्याच्या शरणागतीला मान्यता द्यावी, तसेच आरमाराची छावणी दर्याला उधाण येण्याच्या अगोदर पंधरा दिवस अगोदर करावी. तीसुद्धा एका बंदरात अथवा जलदुर्गाजवळ किंवा उघड्या ठिकाणी करू नये. प्रत्येक वर्षी एकाच बंदरात त्याच्याकडून आगी लावल्या जातील किंवा धोका होऊ शकतो. या प्रत्येक वर्षात नवीन बंदरात छावणी करावी. शत्रू सहजासहजी पोहोचणार नाही याची काळजी घ्यावी. सर्व आरमार एका जागी न ठेवता अंतराने छावणी करावी. रात्री गस्त घालावी. आरमाराच्या अधिकाऱ्यांनी आपले कुटुंब दोन महिने घरीच ठेवून आरमाराची रात्रदिवस चाकरी करावी. आरमारास बरेच लाकूड लागते. अशा वेळी राज्यातील लाकूड राजाच्या परवानगीने तोडावे. आंबा, फणस ही झाडे यास हात लावू नये. जीर्ण झाली असतील तरच उपयोगात आणावीत. प्रजेने ही झाडे लेकराप्रमाणे वाढवलेली असतात. या विचारातून छत्रपती शिवाजी महाराजांची पर्यावरण बाबतीतील नैतिक

भूमिका लक्षात येते. एकूणच छत्रपती शिवाजी महाराज यांच्या राजनीतीमध्ये आरमाराचे स्थान हे किती मौलिक होते ते आपणास आज्ञापत्र या ग्रंथात रामचंद्रपंत अमात्य यांनी आरमार प्रकरणाच्या अनुषंगाने अत्यंत सखोलपणे मांडलेले दिसून येते, तसेच छत्रपती शिवाजी महाराज राजनीती व युद्धनीतील एक द्रष्टा राजा होता, हे अधोरेखित केले आहे. त्याचबरोबर 'आज्ञापत्र' रामचंद्रपंतलिखित ग्रंथ शिवाजी महाराजांच्या राजनीतीपर कौशल्यावर प्रकाश टाकणारा एक महत्त्वाचा

दस्तऐवज ठरतो, असे म्हटले तर वावगे ठरणार नाही.

संदर्भ ग्रंथ -

१. 'आज्ञापत्र' - रामचंद्रपंत अमात्य
२. 'आज्ञापत्र' - संपादक - डॉ. प्र. न. देशपांडे, प्रथम आवृत्ती - २००५, स्नेहवर्धन प्रकाशन डॉ. विजया देशपांडे
३. 'छत्रपती शिवाजी महाराज' - कृष्णराव अर्जुन केळूसकर - सरस्वती पब्लिशिंग कंपनी, आवृत्ती, जानेवारी २०१८



**PREVALENCE OF RELATIVE ENERGY SYNDROME-SPORTS (RED-S) AMONGST
ADOLESCENT FEMALE BASKETBALL PLAYERS FROM PUNE**

Sunil P Pansare^{1*}, ¹Department of Physical Education, Annasaheb Awate College, Manchar, Tal: Ambegaon, Dist.: Pune - 410503., Maharashtra, India.

U. D. Patil², ²Department of Physics, Annasaheb Awate College, Manchar, Tal: Ambegaon, Dist.: Pune - 410503., Maharashtra, India.

Bhagyashree Patil^{3,3} Shree Goraksha, Ayurvedic Medical College Hospital and Research Centre
Khamgaon

*Corresponding Author E-mail:

Abstract

Relative energy deficiency in sports (RED-S) is a growing concern among adolescent female athletes, particularly in sports that place a high emphasis on leanness and weight management. Basketball is one such sport where RED-S may be prevalent due to the pressure to maintain a lean body type for optimal performance. This study aimed to investigate the prevalence of relative energy deficiency in sport (RED-S) syndrome amongst adolescent female basketball players from Pune. A questionnaire was administered to 35 participants and consisted of 30 questions related to disordered eating, amenorrhea, and osteoporosis. The questionnaire used a Likert 5-point scale for responses, and the percentage scores were calculated for each element and overall. The study discusses the methods used to collect data, including surveys and analyzes the results to identify common characteristics and experiences among adolescent female basketball players with RED-S. The paper concludes with recommendations for the prevention and management of RED-S in this population, such as education and counselling on proper nutrition and energy balance, and monitoring of body weight and body composition. The results of the study showed that none of the participants had moderate to severe symptoms of disordered eating, amenorrhea, or osteoporosis. Furthermore, none of the participants had moderate to severe symptoms overall. Therefore, it was concluded that the adolescent female basketball players from Pune do not suffer from RED-S syndrome.

Keywords: *Relative Energy Syndrome (RED-S), disordered eating, amenorrhea, and osteoporosis.*

1. Introduction

The body needs the energy to survive, develop, stay warm, and perform. Nutrition is an important aspect of athletic performance for athletes to ensure healthy growth and development. Macronutrients, micronutrients, and fluids in adequate levels are required to supply energy for development and activities. In order to perform at their best, athletes must grasp the significance of eating before, during, and after a game.

One of the sports with the highest level of physical strain is basketball. A player can expend up to 1500–2000 calories while engaging in an activity. Energy shortage has long been recorded among athletes, and it is especially common in weight-sensitive sports like gymnastics, wrestling, diving, weight lifting, etc. Energy insufficiency can be caused by a variety of circumstances, including an athlete consciously decreasing energy consumption to achieve a specific weight category or masculine physique, an eating disorder or poor eating habits, or inadvertently owing to a lack of nutritional education.

The 20th century saw a tremendous rise in female involvement and popularity in athletics, particularly in the last 25 years, which reflects developments in contemporary cultures that emphasize gender balance. Women's sports are now largely acknowledged across the world, although there are still significant regional and national differences in performance and participation. While an increase in female engagement in sports, there is still a significant discrepancy in participation statistics between men and women. These inequalities persist throughout the world and continue to impede sports equality. Numerous organizations and

initiatives continue to be patriarchal and do not support gender equality in sports. In the meantime, female athlete's dietary needs, deficits, and associated studies have piqued the interest of researchers.

Based on the initial scientific data of Drinkwater et al., the Female Athlete Triad (Triad) was characterized in the 2005 IOC Consensus Statement as "the combination of disordered eating (DE) and menstrual irregularities, eventually leading to a drop in endogenous estrogen and other hormones, culminating in low bone mineral density" (BMD). The phrase "Female Athlete Triad" was used to characterize female athletes who had one or more of the triad's components, which included disordered eating, amenorrhea, and osteoporosis. The phrase "Female Athlete Triad" was once used to characterize female athletes who had one or more of the triad's components. Following advances in scientific understanding, the American College of Sports Medicine described the Triad as a clinical entity referring to the "connection among three inter-related aspects: energy availability (EA), menstrual function, and bone health" in 2007. Knowledge of pathophysiology describing the notion that the athlete evolves along a continuous spectrum over time ranging from the healthy athlete with optimal EA, regular menses, and healthy bones to the other end of the spectrum typified by amenorrhoea, low EA, and osteoporosis. The term "Relative Energy Deficiency in Sport" (RED-S), which the International Olympic Committee (IOC) established in 2014 to replace the phrase "Female Athlete Triad," now refers to a wider spectrum of health issues and their effects. The IOC discovered that the Female Athlete Triad had limitations in that it included all people who showed symptoms of energy deficiency, as well as restricting the impacts of eating an energy-deficient diet to three classes. For both male and female athletes, RED-S contains a greater spectrum of potential health and performance effects.

The need for addressing Relative Energy Syndrome-Sports (RED-S) amongst adolescent female basketball players from Pune is crucial for their overall health and well-being. RED-S is a condition that occurs when an individual's energy intake is not sufficient to meet their energy expenditure, leading to a disruption of normal physiological functions such as growth, menstruation, and bone health.

Adolescent female basketball players in Pune are at high risk of developing RED-S due to the intense physical demands of the sport. The combination of high-intensity training, competition, and travel can lead to an increase in energy expenditure, making it difficult for these athletes to consume enough energy to meet their needs. Additionally, societal pressures and unrealistic body ideals can lead to disordered eating patterns, further exacerbating the risk of RED-S.

The consequences of RED-S can be severe and long-lasting, including delayed growth and maturation, amenorrhea, osteoporosis, and increased risk of injury. Coaches, athletic trainers, and healthcare professionals in Pune must be aware of the risks and signs of RED-S and are equipped to provide appropriate support and guidance to adolescent female basketball players. This includes educating players on healthy nutrition, promoting a healthy body image and providing regular monitoring of growth and menstrual status.

Overall, addressing the need for RED-S prevention and management amongst adolescent female basketball players in Pune is crucial for their health and well-being, as well as their ability to perform and compete at a high level. In this work, we presented a case study of adolescent female basketball players from Pune city who administered a teacher-made questionnaire and its analysis which reflects the fingerprints of RED-S Syndrome.

2. Methodology

This article reflects "The Study of RED-S Syndrome Amongst Adolescent Female Basketball Players of Pune City". We conducted physical assessments such as body composition measurements and menstrual status evaluations to further understand the impact of energy imbalance on the players' physical health.

To ensure the reliability and validity of the questionnaire, it was reviewed and approved by a panel of experts in the field of sports nutrition and RED-S. The questionnaire was designed to assess participants' dietary intake, physical activity levels, and menstrual status.

We also conducted interviews with coaches and athletic trainers to gain insight into their understanding and management of RED-S within the team. This qualitative data helped to provide a more comprehensive understanding of the issue and the potential barriers to addressing it.

The data was collected through a combination of self-reported questionnaires, and personal interviews. Data analysis was performed using Excel and SPSS software, and the results were presented in the form of descriptive and inferential statistics, as well as the chi-square test.

The methodology of this research was designed to provide a comprehensive understanding of the prevalence, risk factors, and consequences of RED-S amongst adolescent female basketball players in Pune City, as well as to provide recommendations for future research and practice.

Variables of the Research

- Dependent: - RED-S Syndrome
- Independent: - Questionnaire
- Controlling Variables: -
- Extraneous: - Training type (hard training, irregular training); Practice or coaching time; Diet.

3. Data Analysis

Analysis of demographic information

Table 1 Demographic information of the participants in the study

Age	14 to 20 years
Playing since	2 to 5 years
Registered clubs	PDFA
Gender	Female
Total Participants	35

Descriptive analysis

The median values for each question on the questionnaire are displayed in the table. The median is the middle value of a dataset, and it can provide a better understanding of the distribution of scores when there are outliers or extreme values. For example, the median value for DE is 21.4, which indicates that half of the participants scored 21.4 or lower on the DE scale, while the other half scored higher. Similarly, the median values for AM and OP are 23.05 and 17.88 respectively, indicating that half of the participants scored 23.05 or lower on the AM scale and 17.88 or lower on the OP scale.

It's worth noting that the standard deviation of a dataset represents the degree of variation in the scores. A low standard deviation indicates that the scores are relatively close to the mean, while a high standard deviation indicates that the scores are more spread out. In the table, the standard deviation for DE, AM, and OP are 5.88, 5.78, and 5.37 respectively. This means that the scores for DE are relatively close to the mean, while the scores for AM and OP are more spread out.

The table provides valuable information about the prevalence of disordered eating, amenorrhea, and osteoporosis among adolescent female basketball players in Pune. The data suggests that a significant proportion of participants are at risk of RED-S, and it highlights the need for further research and intervention to prevent and manage this condition among this population.

Table 2 the descriptive statistics of points scored by the participants (N=35)

	DE	AM	OP
--	----	----	----

No. of Questions	11	10	9
Mean	21.4	23.05	17.88
Median	21	23	17
Std. Deviation	5.88	5.78	5.37
Minimum	11	15	9
Maximum	44	34	30

4. Interpretation of data Disordered Eating (DE)

Based on the information provided, it appears that the participants in the study were assessed for disordered eating using an 11-question survey that used a Likert scale (with scores ranging from 1 to 5) to measure their responses. The lower the score, the less likely the participant is to be suffering from disordered eating. The average score for the participants was 2.56, which suggests that they rarely exhibited symptoms of disordered eating. However, it is important to note that an average score of 2.56 on this scale does not give a definite diagnosis of disordered eating.

However, It's crucial to remember that this is based on self-reported data and may not necessarily reflect the true prevalence of disordered eating in this population. It is also worth noting that disordered eating can manifest in different ways and may not always be easily identified through a questionnaire.

The results of this analysis can be used as a baseline to monitor the prevalence of disordered eating in adolescent female basketball players in Pune City over time. It is also important to note that while the average score per question may indicate a lower risk of disordered eating, it is still important to monitor the individual scores of participants, as some participants may have scored higher and may be at a higher risk for disordered eating.

The fact that these results are based on a sample of teenage girls who play basketball in Pune City and may not generalize to other communities should also be noted. Further research is needed to understand the prevalence of disordered eating in other populations of adolescent female athletes.

Table 3 The analysis of disordered eating amongst adolescent female basketball players from Pune City.

	Total Question	Max. Points	Min. Points	Ave. Points	Ave. Points per Question
DE	11	55	11	21.4	1.94

Amenorrhoea (AM)

Based on the information provided, it appears that the participants in the study were assessed for Amenorrhoea (absence of menstrual periods) using a 10-question survey that used a Likert scale (with scores ranging from 1 to 5) to measure their responses. The lower the score, the less likely the participant is to be suffering from Amenorrhoea. The average score for the participants was 1.94, which suggests that they rarely exhibited symptoms of Amenorrhoea. However, it is important to note that an average score of 1.94 on this scale does not give a definite diagnosis of Amenorrhoea.

This is based on self-reported data, therefore it's crucial to remember that it could not accurately represent the prevalence of amenorrhoea in this community. It is also worth noting that Amenorrhoea can manifest in different ways and may not always be easily identified through a questionnaire.

The results of this analysis can be used as a baseline to monitor the prevalence of Amenorrhoea in adolescent female basketball players in Pune City over time. It is also important to note that while the average score per question may indicate a lower risk of Amenorrhoea, it is still important to monitor the individual scores of participants, as some participants may have scored higher and may be at a higher risk for Amenorrhoea.

It's also worth noting that these findings are based on a small sample of adolescent female basketball players from Pune City and may not be applicable to other demographics. Further research is needed to understand the prevalence of Amenorrhoea in other populations of adolescent female athletes. A proper diagnosis should be made by a qualified professional using a comprehensive assessment including physical examination, hormonal testing, and clinical history. Additionally, Amenorrhea can have various causes, some are related to medical conditions and others to lifestyle factors, so a proper diagnosis would take into account all possible causes.

Overall, the results of this analysis provide valuable information on the prevalence of Amenorrhoea in adolescent female basketball players in Pune City. It can be used as a baseline for future research and to develop interventions and support for the players who are suffering from Amenorrhoea. These data should be taken with a grain of salt, it would be important to conduct a clinical examination and hormonal analysis to confirm the presence of Amenorrhea.

Table 4 The analysis of Amenorrhoea amongst adolescent female basketball players from Pune City.

	Total Question	Max. Points	Min. Points	Ave. Points	Ave. Points per Question
AM	10	50	10	23.05	2.30

Osteoporosis (OP)

A proper diagnosis should be made by a qualified professional using a comprehensive assessment including bone density testing, hormonal testing, and clinical history. Additionally, Osteoporosis does not typically show any symptoms until a fracture occurs, so a proper diagnosis would take into account all possible causes and risk factors.

The participants in the study were assessed for Osteoporosis (a condition where the bones become weak and brittle) using a 9 questions survey that used a Likert scale (with scores ranging from 1 to 5) to measure their responses. The lower the score, the less likely the participant is to be suffering from Osteoporosis. The average score for the participants was 1.98, which suggests that they rarely exhibited symptoms of Osteoporosis. However, it is important to note that an average score of 1.98 on this scale does not give a definite diagnosis of Osteoporosis. This suggests that the participants rarely showed symptoms of osteoporosis. However, it's important to note that this is not a definitive diagnosis of osteoporosis and a physician should be consulted for further examination and testing. A proper diagnosis should be made by a qualified professional using a comprehensive assessment including bone density testing, hormonal testing, and clinical history. Additionally, Osteoporosis does not typically show any symptoms until a fracture occurs, so a proper diagnosis would take into account all possible causes and risk factors.

Table 5 The analysis of Osteoporosis amongst adolescent female basketball players from Pune City.

	Total Question	Max. Points	Min. Points	Ave. Points	Ave. Points per Question
OS	09	45	09	17.88	1.98

5. Evaluation of the key observations

This study only represents a small sample of adolescent female basketball players in Pune city and may not be generalizable to the entire population. Additionally, it is also important to consider other

factors such as socio-economic status, cultural norms, and access to healthcare that may also impact the prevalence of RED-S syndrome.

Furthermore, this study only focused on three elements of RED-S syndrome and there may be other aspects of RED-S that were not assessed. Therefore, further research is needed to gain a more comprehensive understanding of the prevalence and impact of RED-S syndrome among adolescent female basketball players in Pune city and other regions.

In a nutshell, this study highlights the importance of continued monitoring and education about RED-S syndrome among adolescent female basketball players and other athletes. It also highlights the need for further research to better understand the prevalence and impact of RED-S syndrome among athletes and to develop effective prevention and intervention strategies.

Conclusion

It can be concluded that the adolescent female basketball players from Pune City do not seem to be affected by RED-S syndrome. However, it is important to note that this study was conducted on a small sample size and further research is needed to confirm these findings. Additionally, it is important for coaches, trainers, and healthcare professionals to continuously monitor the players' physical and emotional well-being to ensure their health and safety. Specifically, the study highlights the importance of addressing the issue of RED-S syndrome in female athletes, as it can have serious consequences on their physical and mental health.

References

1. Committee IP. Classification by sport Official Website of the Paralympic Movement: International Paralympic Committee; [Available from: <https://www.paralympic.org/classification-by-sport>].
2. Heikura IA, Uusitalo ALT, Stellingwerff T, Bergland D, Mero AA, Burke LM. Low Energy Availability Is Difficult to Assess but Outcomes Have Large Impact on Bone Injury Rates in Elite Distance Athletes. *International Journal of Sport Nutrition and Exercise Metabolism*. 2018;28(4):403
3. Lange D. Number of athletes participating in the Summer Paralympics 1960-2016 [Report]. *statista.com: Statista*; 2017 [updated 08.2017; cited 2021 01.05]. Available from: <https://www.statista.com/statistics/815903/paralympics-number-athletes/>.
4. Oslo Economics. Idrett for mennesker med en funksjonsnedsettelse [Report]. *idrettsforbundet.no: Oslo Economics*; 2020 [updated 21.10; cited 2021 01.05]. Available from <https://www.idrettsforbundet.no/contentassets/70ae151872224b9fad4d46a552a5b038/rapport-2020--idrett-for-mennesker-med-funksjonsnedsettelse.pdf>.
5. Fredheim GO. Tidens parasatsing i Norge- skal doble antall medaljekandidater [Website article]. *idrettsforbundet.no: Norges Idrettsforbund*; 2019 [updated 04.06.2019; cited 2021 12.05]. Available from: <https://www.idrettsforbundet.no/nyheter/2019/tidens-parasatsing-i-norge--skal-doble-antall-medaljekandidater/>.
6. Tweedy SM, Vanlandewijck YC. International Paralympic Committee position stand—background and scientific principles of classification in Paralympic sport. *Br J Sports Med*. 2011;45(4):259-69.
7. International Paralympic Committee. Paralympic Sports [Website]. *paralympic.org: International Paralympic Committee*; [cited 2021 01.05]. Available from: <https://www.paralympic.org/sports>.
8. Scaramella J, Kirihenedige N, Broad E. Key Nutritional Strategies to Optimize Performance in Para Athletes. *Physical Medicine & Rehabilitation Clinics of North America*. 2018;29(2):283-98.
9. Figel K, Pritchett K, Pritchett R, Broad E. Energy and Nutrient Issues in Athletes with Spinal Cord Injury: Are They at Risk for Low Energy Availability? *Nutrients*.

10. Mitchell LE, Adzick NS, Melchionne J, Pasquariello PS, Sutton LN, Whitehead AS. Spina bifida. *Lancet*. 2004;364(9448):1885-95.
11. Blauwet C, Brook E, Tenforde A, Broad E, Hu C, Abdu-Glass E, et al. Low Energy Availability, Menstrual Dysfunction, and Low Bone Mineral Density in Individuals with a Disability: Implications for the Para Athlete Population. *Sports Medicine*. 2017;47(9):1697-708.
12. Morse LR, Biering-Soerensen F, Carbone LD, Cervinka T, Ciriigliaro CM, Johnston TE, et al. Bone Mineral Density Testing in Spinal Cord Injury: 2019 ISCD Official Position. *J Clin Densitom*. 2019;22(4):554-66.
13. Goktepe AS, Yilmaz B, Alaca R, Yazicioglu K, Mohur H, Gunduz S. Bone density loss after spinal cord injury: elite paraplegic basketball players vs. paraplegic sedentary persons. *Am J Phys Med Rehabil*. 2004;83(4):279-83.
14. Otzel DM, Lee J, Ye F, Borst SE, Yarrow JF. Activity-Based Physical Rehabilitation with Adjuvant Testosterone to Promote Neuromuscular Recovery after Spinal Cord Injury. *Int J Mol Sci*. 2018;19(6).
15. Ainsworth et al. (2011) Ainsworth BE, Haskell WL, Herrmann SD, Meckes N, Bassett Jr DR, Tudor-Locke C, Greer JL, Vezina J, Whitt-Glover MC, Leon AS. 2011 compendium of physical activities: a second update of codes and MET values. *Medicine & Science in Sports & Exercise*. 2011;43:1575–1581. doi: 10.1249/MSS.0b013e31821ece12.
16. Guthold et al. (2018) Guthold R, Stevens GA, Riley LM, Bull C. Worldwide trends in insufficient physical activity from 2001 to 2016: a pooled analysis of 358 population-based surveys with 1.9 million participants. *The Lancet*. 2018;6:e1077–e1138. doi: 10.1016/S2214-109X(18)30357-7.
17. Zahradnik et al. (2017) Zahradnik D, Jandacka D, Holcapek M, Farana R, Uchytíl J, Hamill J. Blocking landing techniques in volleyball and the possible association with anterior cruciate ligament injury. *Journal of Sports Sciences*. 2017;36:955–961. doi: 10.1080/02640414.2017.1346817.

See discussions, stats, and author profiles for this publication at: <https://www.researchgate.net/publication/366001227>

Fungal Spore Diversity over Garbage Depot of Pimpri Chinchwad, Pune, M.S., India

Article in Ecology Environment and Conservation · November 2022

DOI: 10.53550/EEC.2022.v28i07s.010

CITATIONS

0

READS

26

2 authors, including:



Abhishek Bhor

Savitribai Phule Pune University

7 PUBLICATIONS 22 CITATIONS

SEE PROFILE

Fungal Spore Diversity over Garbage Depot of Pimpri Chinchwad, Pune, M.S., India

Abhishek K. Bhor*¹ and Pravin B. Cholke²

¹*Department of Botany, Prof. Ramkrishna More Arts Commerce and Science College Akurdi, Pune, M.S., India*

²*Department of Botany, Anantrao Pawar College, Pirangut, Pune, M.S., India*

(Received 23 February, 2022; Accepted 12 April, 2022)

ABSTRACT

Aerobiology deals with the airborne particles of biological origin and their effect on living organisms. The atmosphere of the big city including Pimpri Chinchwad is dominated by biopollutants such as grain pollen, fungal grains and piles of dust particles. These days garbage disposal is a major problem in various cities. Many nearby villages are experiencing serious health problems due to elevated levels of aerobiopollutants. Air monitoring within garbage depot has been very rare. Therefore, it was felt that if a continuous survey of aerobiocomponents is conducted, it may be helpful in solving or suggesting a suitable solution. The present study deals with the assessment of aeromicrobiota over the garbage depot of Moshi, Pune for a year (Jan 2019 to Dec 2019). The study aimed to monitor the concentration of various biocomponents in the atmosphere over garbage depot. While scanning the prepared slides of the garbage depot for a year, fungal spores, pollen, hyphal fragments, insect parts, etc. were observed. However, during the present investigation, more emphasis has been given to the fungal components of airspora. The outcome of the present study would ultimately help allergy clinicians in the treatment of allergies and to the Municipal Corporation for designing the dumping site for garbage and developing better garbage disposal mechanisms ultimately bringing comfort to the population of the adjoining area.

Key words : Allergy, Garbage Depot, Fungal Diversity, Biocomponents, Airspora.

Introduction

Aerobiology deals with the airborne particles of biological origin and their effect on living organisms. Jacobs (1951) reported that aerobiology involves the dispersal of a number of insects, fungal spores, bacteria, viruses, pollen etc. and in fact all forms of life that are virtually borne aloft and transported partially or wholly by air currents. He also emphasised the importance of aerobiological surveys in connection to meteorological conditions.

The atmosphere of the big city including Pimpri Chinchwad is dominated by biopollutants such as grain pollen, fungal grains and piles of dust par-

ticles. These days garbage disposal is a major problem in various cities. Many nearby villages are experiencing serious health problems due to elevated levels of aerobiopollutants. The lives and productivity of plants, animals, and humans are all threatened by airborne infections and the resulting diseases in the areas where garbage depots are located.

The Moshi Garbage Depot is a site 12 km from Pimpri Chinchwad. Daily huge garbage dumps in the area by Pimpri Chinchwad Municipal Corporation (PCMC). There is growing pressure from locals on Pimpri Chinchwad Municipal Corporation officials to suspend the project and relocate the garbage depot. The fact is that there is no scientific method

available with the Municipal Council and the local people to assess the microbial flora in the air and its effects on human health. The Several fungal spores play a significant role in inducing illnesses in humans, which is a growing issue of human health hazards.

A regular monitoring network has to be established to predict changes in the environment of study area induced by bio pollutants and meteorological factors. Air monitoring within garbage depot has been very rare. Therefore, it was felt that if a continuous survey of aerobic components is conducted, it may be helpful in solving or suggesting the suitable solution. No systematic studies on fungal spore concentration and its effect on normal everyday activities and human population living around the garbage disposal plant have been reported. However, such information is needed to assess the importance of fungal spore concentrations and to understand the quality and quantity of the fungal spores over garbage depot. The present study deals with the assessment of aeromicrobiota over garbage depot of Moshi, Pune for a year (Jan 2019 to Dec 2019). The study aimed to monitor concentration of various fungal biocomponents in the atmosphere over garbage depot. An attempt was made to correlate the fungal spores in the air with existing meteorological conditions during the period of investigation.

Material and Methods

The present extramural aerobiological investigations were carried out over the Garbage Depot at Moshi, Pune from 1st January 2019 to 31st December 2019. It includes the qualitative and quantitative analysis of airspora for a year over Garbage depot using Tilak air sampler.

Composition and Identification of the Catches

Visual identifications under the microscope and comparisons with reference slides were used to identify the spores captured.

Most of the fungal spores have been recognized upto generic level. For confirmation of identification, reference slides of parasitic and saprophytic forms were prepared from adjoining area where sampling was carried out. Various types of biocomponents were trapped on the sampler's exposed cellophane tape during the investigation. In the present study the main importance was given on

the study of fungal spore types trapped as a component of airspora and their identification with percentage contribution to the total airspora.

Results and Discussion

Composition and Components of airspora over Garbage Depot

While scanning the prepared slides of Garbage Depot for a year, fungal spores, pollen, hyphal fragments, insect parts, etc. were observed. However, during the present investigation, more emphasis has been given on the fungal components of the airspora.

During the period of air sampling over the Garbage Depot for a period of 1 year, in all 24 fungal spore types were recorded. The fungal spores have been identified up to generic level as listed in Table 1.

Table 1 fungal spore types.

Table 1. Fungal Spore Types.

Ascomycotina	<i>Chaetomium</i> Kunz ex. Fr. <i>Cucurbitaria</i> Gray. Ex Grev. <i>Didymosphaeria</i> Fuck. <i>Hypoxyton</i> Bull ex Fr. <i>Leptosphaeria</i> Ces & de Not. <i>Melanospora</i> Corda. <i>Pleospora</i> Rabh. <i>Pringsheimia</i> Schultz.
Basidiomycotina	Basidiospores. Smut spores
Deuteromycotina	<i>Alternaria</i> Nees. <i>Bispora</i> Corda. <i>Cercospora</i> Fr. <i>Cladosporium</i> Link. <i>Curvularia</i> Boed <i>Diplodia</i> Fr. <i>Fusarium</i> Link. <i>Helminthosporium</i> Link. <i>Nigrospora</i> Zimm. <i>Pithomyces</i> Berk and Br. <i>Tetraploa</i> Berk and Br. <i>Torula</i> (Pers.) Link.
Zygomycotina	<i>Mucor</i> Micheli ex Fr. <i>Rhizopus</i> Ehrenberg.

Leptosphaeria, *Pleospora*, *Pringshemia*, *Alternaria*, *Cladosporium*, *Curvularia*, *Nigrospora*, *Helminthosporium*, *Tetraploa* found maximum during monsoon season. Their abundance were found to be influenced by the occurrence and amount of rainfall.

During the study the maximum spore concentration appeared in the period from June to October months of year 2019. Minimum number occurred in the months from March to May of year 2019. Seasonal changes were observed in different spore categories throughout the year. Out of the 24 fungal spore types, 12 belong to Deuteromycotina, 08 to Ascomycotina, 02 to Zygomycotina, and 02 to Basidiomycotina. Group Deuteromycotina was found dominant with 50.00% contribution. It was followed by Ascomycotina (33.34%), Zygomycotina (14.06%) and Basidiomycotina (2.60%) contribution.

Table 2 presents weather variables and monthly rational average percentage contribution of airspora. The highest airspora reported in July and September. In May, minimum percentage contribution of airspora was observed.

Month wise highest percentage contribution of Zygomycotina, Ascomycotina and Deuteromycotina was observed in July. Group Basidiomycotina showed its supremacy in November. Utmost percentage contribution of another group was also recorded in October. The pathogenic spore type smut was observed maximum in the month of June to

October. Other Pathogenic spore types like *Alternaria*, *Helminthosporium*, *Curvularia*, *Cercospora*, *Nigrospora* and *Fusarium* showed their presence throughout the investigation period with maximum event in August. Similar findings were recorded by Bharti (1998). This spore type was also reported to be allergenic. Spore types like *Tetraploa* were observed with low percentage contribution in April.

Cladosporium, *Alternaria*, *Nigrospora*, *Curvularia*, *Periconia* and *Helminthosporium* were the largest contributors to the airspora in each month of the study.

Average % of air spora during Jan 2019 to Dec 2019 over Garbage Depot

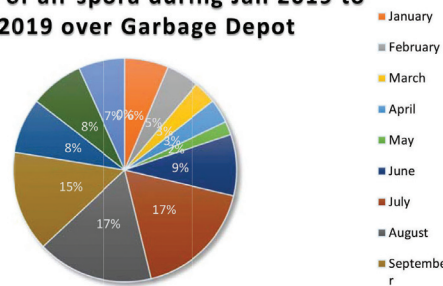


Fig. 1. Average % of air spora during Jan 2019 to Dec 2019 over Garbage Depot.

Table 2. Weather variables and % contribution of airspora in different months during Jan 2019 to Dec 2019 over Garbage Depot

Sr. No.	Month	Average % of air spora	Average Temperature (°C)	Average Rainfall in mm	Relative Humidity (%)	Wind Velocity km/hr.
1	January	6.32	25.83	00	36.66	08
2	February	4.75	29.89	00	26	9.14
3	March	3.37	33.88	00	17.7	11.93
4	April	3.43	37.1	0.5	15.56	13.06
5	May	1.96	36.58	5.38	21.09	15.96
6	June	8.89	30.8	30.56	53.5	18.33
7	July	17.48	25.35	256.1	80.32	20.45
8	August	16.8	25.35	134.2	77.09	24.25
9	September	14.55	25.16	60.65	78.3	17.77
10	October	08	26.12	3.88	71.96	9.96
11	November	7.7	28.03	1.20	51.26	9.03
12	December	6.74	26.45	00	46.61	9.7

Table 3. The total airspora and % contribution of each group in Garbage Depot during Jan 2019 to Dec 2019

Sr. No	Spore Group	Total airspora /m ³	Percentage contribution
1	Zygomycotina	3524502	14.06
2	Ascomycotina	8349331	33.34
3	Basidiomycotina	651313	2.60
4	Deuteromycotina	12525354	50.00
	Total	25050500	100

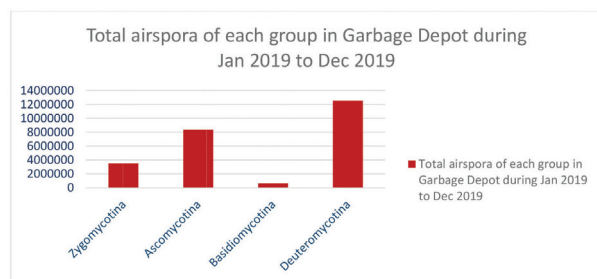


Fig. 2. Total airspora of each group in Garbage Depot during Jan 2019 to Dec 2019

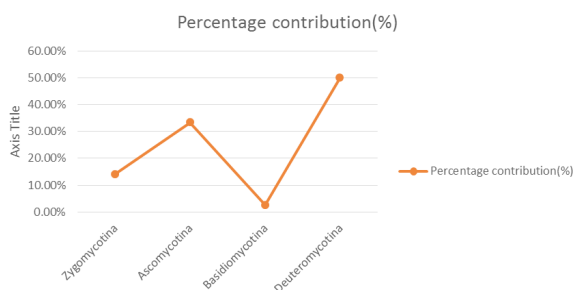


Fig. 3. Percentage contribution (%) each group in Garbage Depot during Jan 2019 to Dec 2019.

Table 3 shows the total airspora and percentages contribution of each class over Garbage Depot from January to December 2019. It shows the dominance of group Deuteromycotina followed by Ascomycotina and Zygomycotina.

Conclusion

The present research work was concerned with aeromycological sampling over garbage depot of Moshi. Air monitoring at Garbage depot has provided meaningful information of practical utility. A close relation between the source and release of allergic aerobiocomponents and its impact on the adjoining population may be clearly estimated. The air monitoring studies over garbage depot would serve as an important contribution to understand the airspora over garbage disposal plant. The outcome of present study would ultimately help allergy clini-

cians in treatment of allergy and to the Municipal Corporation for designing the dumping site for garbage and to develop better garbage disposal mechanism ultimately bringing comfort to the population of adjoining area.

Acknowledgement

The authors acknowledge with profound gratitude, the facilities provided by Principal, Prof. Ramkrishna More College, Akurdi, and Principal, Annasaheb Awate Arts, Commerce and Hutatma Babu Genu Science College Manchar for the completion of the present study. The authors are also thankful to the UGC for providing financial assistance for the research work.

References

- Adams, K. F. 1964. Year to year variation in fungus spore contents of the atmosphere. *Acta Allergol.* 19: 11-50.
- Barnett, H.L. and Hunter, B.B. 1972. *Illustrated Genera of Imperfect Fungi*. Burgess Publishing Company, Minnesota.
- Bharati, S.K. *Aerobiological investigation over garbage Depot*. Ph.D. thesis, Dr. Babasaheb Ambedkar Marathwada University, Aurangabad. 1998.
- Deshmukh, V. S. and Patel, S.I. 2019. Studies on allergenic airborne fungal spores from Satpur Industrial area Nashik. *IJRAR.* 6(2): 968-971.
- Ellis, M.B. 1971. *Dematioid Hyphomycetes*. CMI, Kew. 707.
- Gilman, J.C. 1957. *A Manual of Soil Fungi* (2nd Edition). The Iowa State College Press, Ames Iowa. 1957, 401.
- Jacobs, W.C. 1951. *Aerobiology In compendium of meteorology*. American Meteorological Society, Boston. 1103-1111.
- Patle, K. D. and Jadhav, S. K. 2012. Incidence of Airborne Fungal Spores at Raipur with Special Reference to Railway Station. *International Journal of Science and Research.* 3 (6): 1770-1776.
- Ritu Kunjam, Shriram Kunjam, V.K., Kanungo and Jadhav, S.K. 2021. Aeromycoflora of Phytopathogenic Fungal Spores at The Periphery of Raipur City. 34(1): 05-11.
- Tilak, S. T. and Kulkarni, R.L. 1970. A new air sampler. *Experimentia.* 26 : 443.